TARGETED NANOTHERAPY FOR PROSTATE CANCER: APPLICATIONS FOR CANCER THERAPEUTICS AND IMAGING

By

Seung Soo Lee

Division of Experimental Medicine, Faculty of Medicine, McGill University, Montreal, QC

A thesis submitted to McGill University in partial fulfillment of the requirements of the degree of Master of Science

TARGETED NANOTHERAPY FOR PROSTATE CANCER: APPLICATIONS FOR CANCER THERAPEUTICS AND IMAGING

Seung Soo Lee

Master of Science

Division of Experimental Medicine, Faculty of Medicine, McGill University, Montreal, QC

2017

ABSTRACT

Prostate cancer (CaP), like many cancers, evolves through the incursion of numerous somatic mutations and undergoes multiple selection processes, resulting in extensive genetic heterogeneity, ultimately leading to drug resistance. Many times, biological therapies lead to the selection of more aggressive cancers. Moreover, surgical or radiological treatments are also compounded by other physical side-effects. Therefore, a new generation of therapeutic approaches that would circumvent or overcome such limitations presented by current treatment options is essential. Recently, many types of nanoparticles have been applied broadly in the development of novel cancer therapies. Of the available nanoparticles, multi-walled carbon nanotubes (MWCNTs) offer unique properties such as chemical stability, efficient thermal and electrical energy absorption and conductivity, and extensive surface area availability. When combined together with a targeting moiety, MWCNTs may be used to deliver highly-localized "energy" (via a laser) in the immediate proximity to the cells and can cause significant cellular damage, thus making them an ideal physical therapeutic platform. Therefore, functionalizing the MWCNTs by conjugating antibody against prostate specific membrane antigen (PSMA), a marker for progressive CaP, on their surface would be an effective approach for active targeting. In the *in vitro* studies using PSMA positive LNCaP

prostate cancer cells, over 80% cell ablation was achieved within a 30 second exposure to low 2.7 W/cm^2 532nm wavelength laser. Furthermore, the specificity and selectivity of PSMA targeting was confirmed by assessing PSMA-null PC3 cell lines under the same conditions (<10% cell ablation), thereby overcoming some of limitations in the conventional photothermal therapy. Developing this new platform will undoubtedly bring a real change vs. current therapeutic modalities and will usher in a new age of effective cancer treatment, by squarely addressing tumoral heterogeneity.

RÉSUMÉ

Le cancer de la prostate (CaP), comme de nombreux cancers, évolue par l'incursion de nombreuses mutations somatiques et subit de multiples processus de sélection, aboutissant à une hétérogénéité génétique étendue résultant à une résistance aux médicaments. L'intervention thérapeutique biologique, le plus souvent par des médicaments ciblant des androgènes, peut conduire à la sélection de tumeurs plus agressives qui peuvent à terme se transformer en cancer résistant aux médicaments. De plus, les traitements chirurgicaux et/ou radiologiques peuvent également aggraver la situation par d'autres effets secondaires. Nous avons par conséquent développé une nouvelle approche thérapeutique en utilisant des nanoparticules ciblées qui agissent en photo-ablation physique qui contournerait et surmonterait les limites présentées par les options de traitements actuels. Récemment, des nanoparticules composées de différents matériaux ont été largement appliquées dans le développement de nouvelles thérapies contre le cancer. Parmi les nanoparticules disponibles, les nanotubes de carbone à parois multiples (MWCNTs) offrent des propriétés uniques telles qu'une stabilité chimique, une grande disponibilité en surface, ainsi qu'une absorption et une conductivité efficaces de l'énergie thermique et électrique. Lorsque ces nanoparticules sont combinées avec un fragment de ciblage, tel qu'un anticorps ou des molécules similaires, elles peuvent être utilisées pour distribuer une «énergie» hautement localisée à proximité immédiate des cellules et peuvent causer des dommages cellulaires importants. C'est pour ces différentes raisons que nous avons utilisé les MWCNTs en conjugaison avec un anticorps contre l'antigène de membrane spécifique de la prostate (PSMA), un marqueur de surface cellulaire pour CaP progressif, pour le ciblage photo-ablatif actif. Dans nos études *in vitro*, en utilisant les cellules du cancer de la prostate LNCaP positives pour PSMA, nous avons pu obtenir plus de 80% d'ablation tumorale avec une exposition de 30 secondes en utilisant un

laser à longueur d'onde de 532 nm de 2.7 W/cm^2. En outre, la spécificité et la sélectivité du ciblage de PSMA ont été confirmées en évaluant sous les mêmes conditions la lignée cellulaire PC3 qui n'expriment pas de PSMA. Ces résultats confirment également notre capacité à surmonter certaines limites présentées par la photo-thermothérapie traditionnelle. Le développement de cette nouvelle technique apportera sans aucun doute un véritable changement dans l'approche des modalités thérapeutiques actuelles et ouvrira une nouvelle ère de traitement efficace contre le cancer, en s'attaquant directement à l'hétérogénéité tumorale. Finalement, une revue de la littérature a été réalisée pour générer une liste des nanoparticules actuellement disponibles en nanomédecine, à la fois comme agent photothermique et comme vecteur de distribution du médicament. De ce fait, l'évaluation des différents nanomatériaux se fera en même temps que l'analyse du rôle émergent des nanoparticules dans l'environnement clinique potentiel.

ACKNOWLEDGEMENT

In this page, I would like to acknowledge and express my sincerest gratitude to everyone who had guided me through this inspiring journey of completing my MSc degree. Without them, completion of this project would not have been possible.

First of all, I would like to thank my supervisor and mentor Professor Miltiadis Paliouras for providing me with the opportunity to take part in this project. Not only had he provided exceptional supervision, which includes and is not limited to expertise in the field, scientific enthusiasm, patience and career mentorship, he was also a personal mentor, cultivating my growth not only as a researcher but as a person.

I would also like to express my gratitude to my academic advisor Professor Koren Mann and the committee members Professor Moulay Alaoui-Jamali and Professor Chen Liang for their constructive discussions, suggestions, and encouragements.

Next, I would like to thank other members in the lab and colleagues that I have worked with during completion of this project. I begin with Professor Mark Trifiro who, along with Professor Paliouras, has provided invaluable opinions regarding many aspects of the project. As a clinician and a biochemist, his opinions were especially critical in expanding my understanding about this project, and as a researcher in general. Furthermore, I was also very fortunate to work with Dr. Phil Roche, Paresa N. Giannopoulos, Carlos Alvarado, Alex Colarusso, Kamilia Daldoul, and others during my thesis for their expertise, support and feedback. In particular, I would like to thank Alex for his assistance in preparing the French abstract.

Lastly, but not least, I would like to express my love to my family. The first one goes to my younger brother June Soo, who came with me to Montreal to also pursue this Ph.D. in

marketing. His presence and support (both physically and mentally) was irreplaceable in this journey. Finally, I would like to thank my parents for their continuous support, encouragement and faith. I cannot imagine having come this far without their love.

TABLE OF CONTENTS

LIST OF FIGURES AND TABLES

Chapter 1

Chapter 2

Chapter 3

LIST OF ABBREVIATIONS

ADT	Androgen deprivation therapy
AR	Androgen receptor
AREs	Androgen response element
Arg	Arginine
Asp	Aspartic acid
BMI	Body mass index
BPH	Benign prostatic hyperplasia
CaP	Prostate cancer
COOH	Carboxylic group
CRPC	Castrate-resistant prostate cancer
CTAB	Cetyl trimethylammonium bromide
Cy5	Cyanine 6
DAPI	4',6-diamidino-2-phenylindole
DNA	Deoxyribonucleic acid
DHT	Dihydrotestosterone
DPSS	Diode-pumped solid-state
DRE	Digital rectal examination
EBRT	External beam radiotherapy
EDC	1-Ethyl-3-(3-dimethylaminopropyl)carbodiimide
EDTA	Ethylenediaminetetraacetic acid
EPR	Enhanced permeability and retention effect
FBS	Fetal bovine serum
Gly	Glycine

GnRH	Gonadotropin-releasing hormone
GNC	Gold nanocage
GNR	Gold nanorod
GNS	Gold nanoshell
GO	Graphene oxide
GTP	Guanine triphosphates
Gy	Gray
HDR	High dose-rate
HEK293	Human embryonic kidney cells 293
HIFU	High-intensity focused ultrasound
HRP	Horseradish peroxidase
IgG	Immunoglobulin G
IGRT	Image-guided radiation therapy
IMRT	Intensity-modulated radiation therapy
IONP	Iron oxide nanoparticle
Laser	Light amplification by stimulated emission of radiation
LSPR	Localized surface plasmon resonance
LDR	Low dose-rate
LHRH	Luteinizing hormone–releasing hormone
Mal	Maleimide
MWCNT	Multiwalled carbon nanotube
NHS	N-Hydroxysuccinimide
NIR	Near infrared
NP	Nanoparticle
nRGO	Reduced nano-graphene oxide

OPSS	Ortho-pyridyl disulfide
PBS	Phosphate buffered saline
PCA3	Prostate cancer antigen 3
PCR	Polymerase chain reaction
PEG	Polyethylene glycol
PET	Positron emission tomography
PIN	Prostatic intraepithelial neoplasia
PSA	Prostate specific antigen
PSMA	Prostate specific membrane antigen
RES	Reticuloendothelial system
RNA	Ribonucleic acid
RPMI	Roswell Park Memorial Institute
RT-PCR	Reverse transcription polymerase chain reaction
SBRT	Stereotactic body radiation therapy
SDS-PAGE	Sodium dodecyl sulfate-Polyacrylamide gel electrophoresis
SPR	Surface plasmon resonance
SWCNT	Singlewalled carbon nanotube
TWEEN20	Polysorbate 20

Chapter 1: Prostate Cancer - An Introduction and Literature Review

1.1 Introduction

Prostate cancer (CaP) was first described in 1853 by Dr. J. Adams, a surgeon at the London Hospital (1). In his report, Adams had included a histological assessment of CaP, for which he described the occurrence of the disease as very rare (2, 3). Ironically, contrary to the initial descriptions, the occurrence of CaP is quite prevalent in today's world. According to the American Cancer Society, an estimated 180,890 men in the United States will be newly diagnosed with CaP in 2016, and approximately 26,120 men will die from it (4). Of all new cancer diagnoses, the rate of CaP incident is the highest in males (second only to lung cancer when both sexes are accounted for), and CaP-related deaths in males are also second only to lung cancer; and fifth behind lung, colon/rectal, pancreatic, and liver cancers when including both sexes (4). The high incident of CaP is also observed in other Western countries, such as Canada (top incident rate among men in 2015) (5) and United Kingdom (the most common in cancer in males and second most common cancer in 2014 when including both sex, accounting for 13.4% of all new cancer cases) (6). Contrary to the high incident rate in the Western society, the incidents of CaP in Asian countries, while becoming an emerging concern with increased screening, are not as high as those observed in Western countries (7, 8) (**Figure 1.1A**).

According to multiple epidemiological studies, African nations have the highest rate of mortality, followed by Europe and the American continent and lowest in Asia (7, 9, 10) (**Figure 1.1B**). Nevertheless, these statistics do not fully represent the full scope of the disease, as CaP incidents among Asian-American populations are more than three times higher than that of the Asian population (11) (**Figure 1.1C**). Therefore, numerous factors, including socioeconomic, cultural, and genetic factors could contribute to variations among inter- and intra-racial populations.

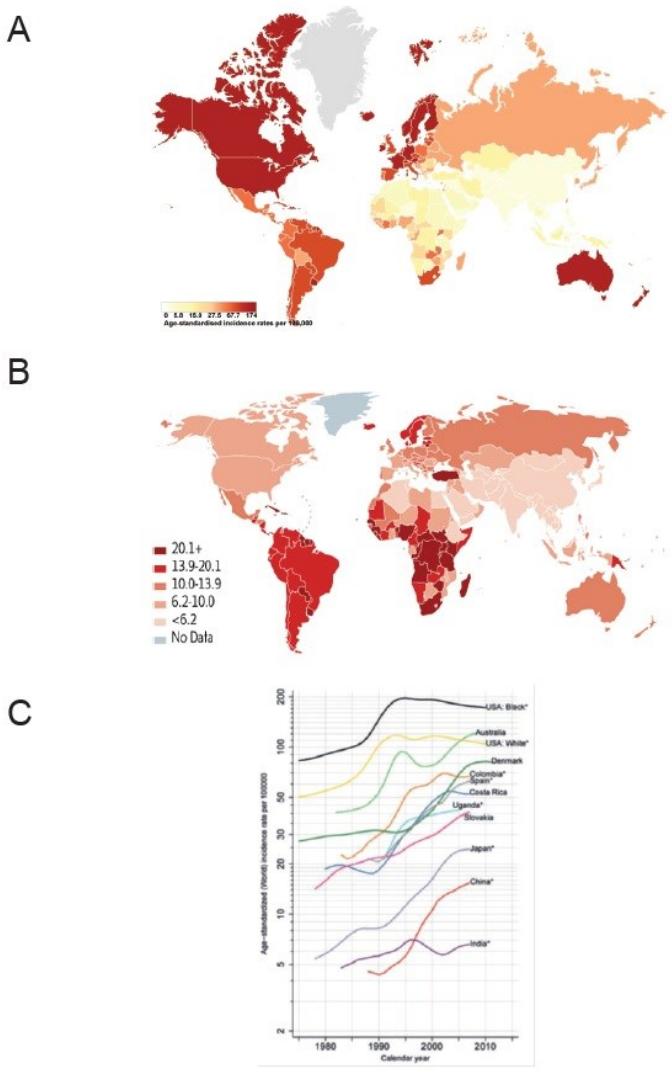

Figure 1.1 Worldwide prostate cancer statistics in 2012. 1.1A shows the rate of prostate cancer incidents per 100,000 people worldwide, clearing showing higher incidents in Western worlds. 1.1B shows the mortality rate per 100,000. While 1.1A showed significantly higher prevalence of prostate cancer in Western society, the rate of mortality is much higher in the less developed regions. Lastly, 1.1C shows the incident rates of prostate cancer per 100,000 in selected populations according to the racial background.

The figure is adopted from World Cancer Report 2014, International Agency for Research on Cancer, World Health Organization (12).

The exact etiology for CaP is still indistinct (13-15). The only established risk factor for CaP is a family history of the disease; compared to the general population, the risk of CaP development in those that have first-degree relatives with CaP is twice as high (16, 17). Although no single gene has yet been identified as the cause of this neoplastic growth, a number of genes have so far been proposed as potential drivers, including mutations in *BRCA1, BRCA2*, *HPC1 (*also known as *RNASEL)*, and *PTEN* (18-21). In addition, a number of other potential risk factors have also been identified including, age, dietary patterns, ethnicity, and environmental factors; with studies being performed to investigate how these factors may influence normal prostate cells to develop into adenocarcinoma (11, 22, 23). In fact, the ethnic background of patients continues to be recognized as a key component in the different CaP incident rate among various populations. Particularly, the variation of CAG/polyglutamine tract length in androgen receptor protein influences its activity. Androgen receptor (AR) is a key protein critical in CaP pathogenesis (24), with an association of CAG/polyglutamine tract length variation with race and with incidents of CaP. Longer polyglutamine tract repeats have been associated with lower CaP incidents (25), and often found in Asian populations. Caucasians have slightly shorter polyglutamine tracts and Black/African populations have the shortest tract.

CaP is universally multifocal (26-28) and is uniformly associated with hyperplasia or hypertrophy (14, 26), with multiple lesions coexisting in the gland. These characteristics are used as a metric by pathologists to assess the overall staging of the tumor via Gleason scoring (29). While socioeconomical and cultural aspects cannot be disregarded, multifocal cancers such as CaP are heavily linked to genetic changes.

1.2 Prostate and Cancer Development

The prostate gland is a unique structure present in male reproductive system. Located directly below the bladder and above the muscles of the pelvic floor, the main role of the prostate is to secrete alkaline prostatic fluid rich in proteins and minerals that protects and nourishes the sperm (30, 31). When the prostatic fluid is combined with sperm, it forms semen, which is sequentially ejaculated via urethra during sexually stimulation. The gland is divided into four regions, including the three zones (peripheral, transitional, and central) and the anterior fibromuscular stroma forming the entire anterior surface of the prostate (13, 32, 33). Studies have shown that compared to other regions, CaP is most likely to occur and advance in the peripheral zone (up to 75%), the largest zone of the gland. In addition, CaP development may also be observed in other zones (up to 20% of CaP in the transitional zone and about 2.5% in the central zone) (34).

Often, men between the ages of 55-65 may have symptoms associated with prostate enlargement. These symptoms often cause the gland to exert pressure against urethra and bladder, possibly causing pain and discomfort (35). These enlargements are categorized into several classes. The benign growth of the gland, in which the enlargement occurs within the prostatic stromal and epithelial cells in the transitional zone, is known as benign prostatic hyperplasia (BPH) (36, 37). BPH is relatively common and may not need to be addressed medically. While BPH normally does not develop into malignant forms of tumor, it remains unclear whether there may be a causal association between BPH and CaP (37, 38). In some cases, the enlargement may become malignant. These types of growths in prostate cells are defined as prostatic intraepithelial neoplasia (PIN). Unlike prostate adenocarcinoma, the neoplastic transformation of prostatic cells is still local and confined within the peripheral zone of the epithelium (39, 40). PIN has been associated with the earliest development of CaP, yet whether PIN originates directly from normal prostate cells or from abnormal dysplastic

cell types has not been clarified (41). Because of the slow growth rate of tumorigenic cells in the prostate gland (39, 42, 43), not all patients undergo immediate treatment with the diagnosis of PIN. Moreover, it is also unclear how exactly PIN develops into full adenocarcinoma, with investigations currently underway to clarify the relationship (13, 44).

Most cases of CaP are first diagnosed by physicians by prostate-specific antigen (PSA) screening. PSA screening is a routine test in the diagnosis of CaP for men over the age of 40 (45). PSA is a protein produced and secreted by the prostate gland. In PSA screening, most physicians consider blood PSA levels of 4.0 ng/mL as normal. Above this level, physicians will recommend a prostate biopsy to determine the presence of CaP. Depending on the characteristics and appearance of the biopsy at the time of the diagnosis, a patient may be recommended for immediate therapy which includes a partial or a full prostatectomy, radiotherapy, or a combination of both, or the patient may also be recommended for active surveillance that does not involve direct intervention. Generally, after the initial therapy, the tumor burden is decreased significantly, which indicated by the dramatic decrease in PSA level **(Figure 1.2)**. Androgen hormones play and important role in CaP progression as they stimulate prostate cells to grow and proliferate, and are linked to the expression of PSA. When dihydrotestosterone (DHT) or testosterone is present, they bind to the AR, which causes a conformational change and the subsequent release from HSP90 inhibition, leading to AR's translocation to the nucleus. In the nucleus, AR forms a homodimer, binds to androgen response elements (AREs) DNA *cis*-elements, and acts as a transcription factor regulating the expression of AR target genes to maintain prostate function and homeostasis (46). PSA is one gene whose expression is directly regulated by AR activity.

Initial biological therapy is almost always androgen- or AR-directed and could include the prescription of AR antagonists (anti-androgens) or 5α-reductase inhibitors (that blocks conversion of testosterone to DHT). Nevertheless, patients that were given the initial

therapy face disease recurrence with new lesions appearing, with even the possibility of the disease invading beyond the gland (47, 48). Subsequently, serum PSA levels increase to pre-treatment levels, an indicator of disease recurrence (49). At this stage, patients would proceed to androgen deprivation therapy (ADT). ADT therapy consists of either surgical or chemical castration, in combination with continued anti-androgens, to remove the major source of androgen hormone production in the testes. Chemical castration is achieved with the use of luteinizing hormone-releasing hormone (LHRH) agonists or gonadotropin-releasing hormone (GnRH) antagonists which serves to reduce serum testosterone levels under 0.5 ng/mL, so that there are not enough androgens to activate AR signaling. 5α-reductase inhibitors can also be used, in order to further inhibit production of DHT production in the prostate (46, 50-52). By restraining androgen production and circulation, ADT aims to accomplish the therapeutic effect of limiting the proliferation of both the normal and neoplastic cells. Therefore, targeting the androgen signaling axis by either the ligand or the AR has become a widely used non-surgical method of treatment for CaP (53, 54). Similarly, ADT provides initial promise in the treatment of advanced CaP by lowering the serum PSA level and regression of tumor mass, yet eventually a proportion of cells acquire resistance via unique mechanisms of its independent reliance on androgen hormone for cell maintenance and proliferation. By this stage, CaP is referred to as in a state of hormone-refractory or castrate-resistant (CRPC). To overcome these challenges, more potent next-generation androgen directed therapies have been developed, such as such as enzalutamide and abiraterone acetate, that target the androgen signaling pathway. However, their clinical effectiveness has been limited, with the 5-year relative survival rate of 29.3% among those with metastatic CRPC (55).

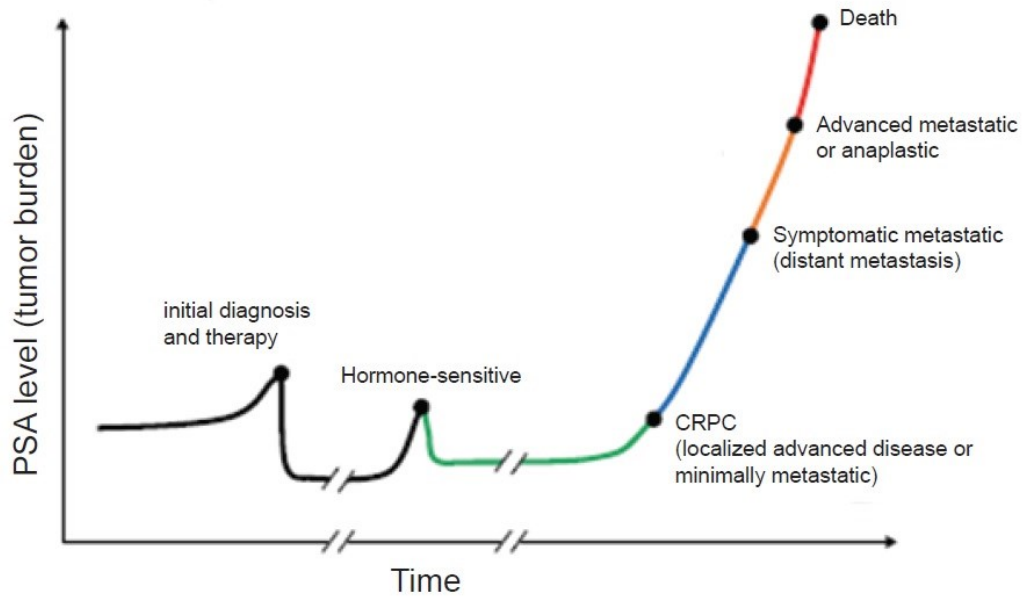

Figure 1.2 Prostate cancer development from local to advanced stage. The different stages of prostate cancer are evaluated according to the blood PSA level. Higher levels of blood PSA correlates to increased tumor burden. Based on the stage of tumor development at the time of initial diagnosis, patients are given the option of active surveillance/watchful waiting versus local treatments which may include surgery or radiation therapy. If the tumor persists or recurs after the initial treatment, the patients then undergo systemic treatments to ensure that the therapeutics can reach the individual tumor cells. At this stage, hormone-sensitive treatments such as ADT are often provided. Nonetheless, prostate cancer ultimately becomes nonresponsive to these ADT, by which the tumor is then recognized as CRPC. Chemotherapy and second-generation drugs are available, yet by this stage the outcome is not promising and patients often results in death.

The figure is adopted from "The current evidence on statin use and prostate cancer prevention: are we there yet?" (56)

1.3 CaP Screening and Diagnosis

Early CaP usually does not cause any physical symptoms. Therefore, the diagnosis of CaP is often made by routine PSA screening. On the other hand, when a patient reports certain symptoms that are specific for CaP such as urinary incompetence, hematuria, erectile dysfunction, pain in the hips, back, or chest, or signs of weakness in the lower body, it may signify the need for additional examinations to evaluate whether the symptoms are due to BPH or due to actual growth of prostatic neoplasm (57). In such examinations, multiple inspections using different methods are performed.

1.3.1 Digital Rectal Examination

Digital rectal examination (DRE) is one of the first physical exams performed by an urologist when checking the patient's prostate gland. During the procedure, a physician examines the patient's prostate gland with her finger to check for nodules, gland asymmetry and hardening, all of which may hint at inflammation or hyperplasia of the gland (58). The examination itself does not guarantee accurate diagnosis and often, DREs may not be sensitive enough for physicians to differentiate between hyperplasia and the very early stages of the CaP. Furthermore, the tumor lesions may originate from inaccessible regions of the gland (59). For accurate diagnosis, blood PSA levels are simultaneously evaluated to ensure that any tumor is identified as early as possible.

1.3.2 Transrectal Ultrasonography

While DREs are widely used as an initial tool to identify potential patients, it is limited in that the information obtained from such screening is obtained only through the palpable means. Further physical examination may be done using instrumentations such as transrectal ultrasonography, which allows physicians to visualize the gland and the

surrounding tissues. Furthermore, transrectal ultrasonography may also be used for biopsy acquisition, where a small sample of prostate tissue (including tissues that appear normal and the abnormal) is collected using a thin biopsy needle and analyzed under a microscope.

1.3.3 Prostate Biomarkers

In 2000, Hanahan and Weinberg suggested that numerous changes occur in cellular pathophysiology as cells become tumorous. Known as hallmarks of cancer, such changes include self-sufficiency in growth signals, insensitivity to anti-growth signals, evasion of apoptosis, limitless replicative potential, sustained angiogenesis, tissue invasion and metastatic properties, deregulated metabolism, evasion of the immune system, genome instability, and inflammation (60). During these changes, neoplastic cells may develop unique characteristics, allowing them to be discriminated from the benign cells. Once these characteristics are established, they may be exploited in the search for tumor in their earliest stages of development. These characteristics may be objectively measured and evaluated as indicators of biological and pathogenic processes, or even pharmacologic responses to a therapeutic intervention are defined as biomarkers (61). These biomarkers may allow early diagnosis, which greatly enhances the chance of successful treatment and survival for cancer patients. A few biomarkers have been identified and evaluated for CaP with some currently being used for clinical diagnostics, screening, and treatment. These markers are categorized into serum, urinary, or tissue biomarkers.

1.3.3.1 Prostate Specific Antigen

Prostate specific antigen (PSA), also known as kallikrein-3 (KLK3), is a glycoprotein enzyme that belongs to the human kallikrein family. In humans, they are encoded by the *KLK3* gene and secreted primarily in the ductal and acinar cells of the prostate epithelium (58,

62, 63). Human PSA was first purified by Wang et al in 1979 (64), and it was first isolated from the prostate tissue by the same group in the following year (65). PSA is naturally produced by the prostate, as it is a target of AR-dependent gene activation, and is one of the main components of the seminal fluid. It is involved in the dissolution of the coagulum via proteolysis, allowing sperm to be liberated and become “active” (63). Naturally, circulation of PSA in blood is limited through leakages into the extracellular fluid (66). Nonetheless, during tumor development, normal glandular structure is altered, leading to increased leakage of PSA (66). In PSA screening, this increase in blood PSA concentration is measured using immunoassay; and as mentioned, serum PSA values of 4.0 ng/mL is recognized as a threshold value for further biopsy (67).

Although PSA is the most popular biomarker for CaP, it is also arguably the most controversial. The main controversies regarding PSA testing is focused in the accuracy and the reliability of the diagnosis. While elevation of blood PSA concentration is used as the criteria for CaP diagnosis, changes in the concentration is not tumor-specific and may also be associated with various other symptoms including benign prostate hyperplasia (68). Accordingly, current PSA screening methods has been associated with significant rates of false-positive, false-negative and over-diagnosis (69, 70). Initial studies have reported that blood PSA concentrations over the threshold have been associated with a positive predictive value of about 30% in men aged over 50 years old (71). Another study reported that the blood PSA threshold value has been associated with a negative predictive value of about 85% in men of median age of 69 years old at the time of biopsy (72). Due to the lack of specificity, associated risks in cancer therapy, and the fact that a significant percentage of CaP cases never actually become malignant, the benefits and harms in PSA screening is still under debate (73).

1.3.3.2 Prostate Cancer Antigen 3

First identified from mRNAs from urine samples using polymerase chain reaction (PCR) in 1999, prostate cancer antigen 3 (PCA3) has been emerging as a strong candidate to replace PSA screening (74, 75). It has been reported that *PCA3*, a prostate-specific gene, is present in 95% of all CaP cases, making it an ideal candidate for screening (75). *PCA3* is reported to be mapped in chromosome 9q21-22, where alternative polyadenylation and splicing produces multiple combinations of transcripts (74-76). These alternative *PCA*3 transcripts often contain high density of stop codons, thereby possibly functioning as a non-coding mRNA (68, 75). It has been proposed that PCA3 protein is involved in the survival of CaP cells by modulating the transcriptional activities of the androgen receptor target genes (77).

PCA3 as a biomarker has few advantages over conventional PSA screening. First, unlike PSA screening which is not tumor-specific and may be influenced by non-tumorigenic sources (BPH, age, etc.), PCA3 overexpression is restricted in prostate tumor tissues and not in BPH tissues and other organs of the body, including normal prostate, testicles, bladder, kidney, seminal vesicles, brain, and lungs (78). Furthermore, a meta-analysis published in 2010 reported that up to 3400 patients were evaluated with PCA3 levels, of which the overall sensitivity of the screening was up to 82.3% and the specificity up to 89%, further justifying the use of PCA3 as a potential biomarker (68).

1.3.3.3 TMPRSS2:ERG Gene Fusion

Gene fusions are defined as structural chromosomal aberrations (including translocations, deletions, and inversions) consisting of two chromosomal regions that changes position, resulting in a new gene with a unique and often deleterious functions (78, 79). Before 2005, gene fusions were not associated with the physiology of CaP (80). However,

this landscape had changed when a group from University of Michigan reported about a frequent chromosomal rearrangement on chromosome 21 featuring *TMPRSS2*, an androgen-regulated gene that encodes enzyme transmembrane protease, serine 2 and *ERG* gene that is regulated by estrogen and acts as a transcriptional regulator (81-83) (**Figure 1.3**). Transgenic mouse models have also demonstrated that ERG genes promoted tumor growth, especially mimicking early events in human CaP development (84). In addition, cohort studies of patients with localized CaP showed that TMPRSS2:ERG gene fusion was associated with Gleason score and cancer-specific deaths (85).

Therefore, its high specificity for CaP and the relatively simple accessibility in identifying gene fusions in serum, prostatic fluid or urine, makes TMPRSS2:ERG gene fusion a unique candidate for CaP screening. Nevertheless, TMPRSS2:ERG is by no means infallible. Studies have shown that compared to conventional PSA screening, TMPRSS2:ERG has lower sensitivity of diagnosing CaP (true positive rate; correctly identifying those with the disease) (68, 83, 86). Furthermore, the rate of fusion is variable according to the ethnic background, with lower prevalence in the Asian population. Moreover, this ethnic variability complicates the efforts of ensuring universality in TMPRSS2:ERG screening by making it difficult to identify a general cutoff value that would be applicable to all populations.

Recently, combining PCA3 screening with TMPRSS2:ERG gene fusion screening has been used in clinic. When applied together, the combination screening complements each other's weakness by improving on sensitivity of the screening, as TMPRSS2:ERG gene fusion screening corrects false-negative results obtained from PCA3 screening and vice versa (87, 88). This combination screening paves for a new era in CaP screening and diagnosis by providing an alternative panel against the heterogeneitic nature of the disease.

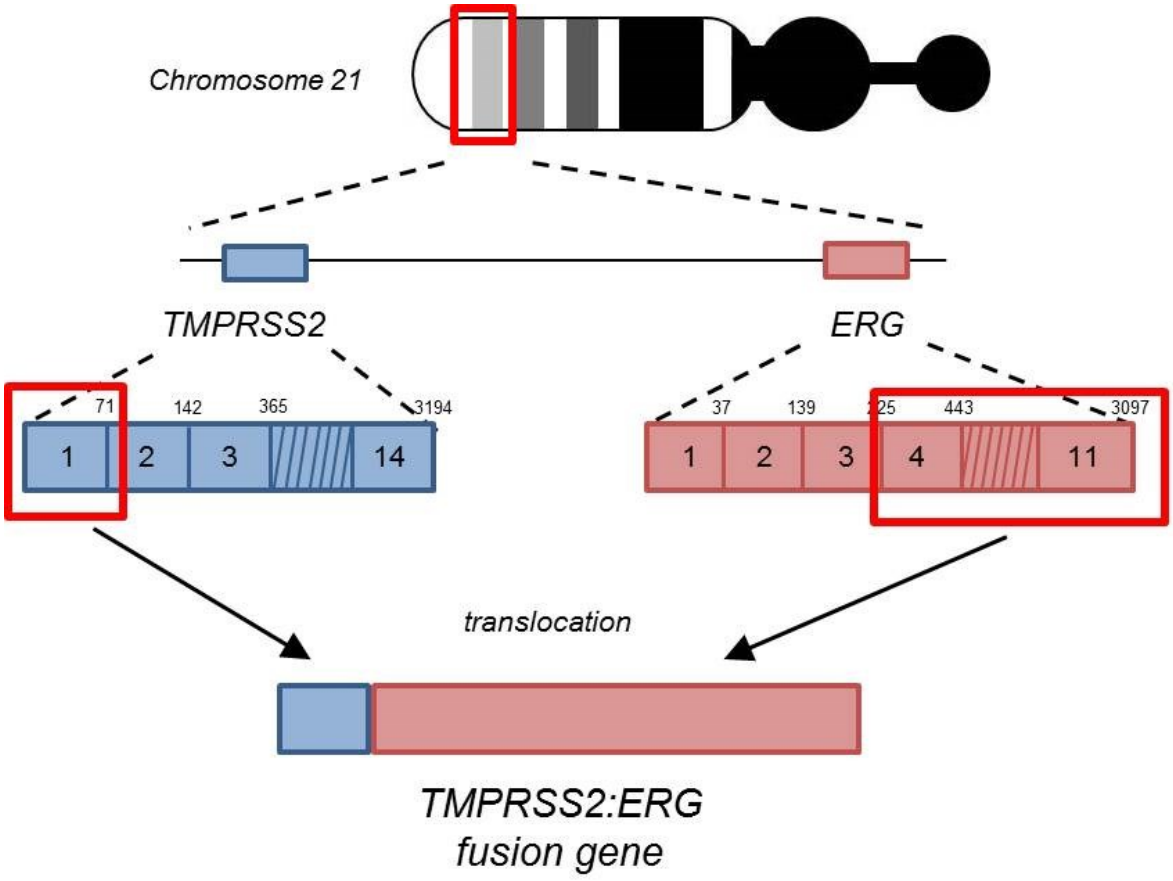

Figure 1.3 TMPRSS2:ERG gene fusion and its role in prostate cancer. Since the discovery, TMPRSS2:ERG gene fusion has been associated with the CRPC phenotype. Both *TMPRSS2* and *ERG* genes are located on chromosome 21. Mechanisms such as deletion of intervening genes between the two genes, or translocation (as shown in the figure) may lead to the formation of the fusion gene (89), resulting in formation of a new phenotype that may exacerbate the tumor development.

The figure is adopted from "ETS gene fusions in prostate cancer" (90).

1.3.3.4 Prostate Specific Membrane Antigen

Prostate specific membrane antigen (PSMA), also known as glutamate carboxypeptidase 2 or N-acetyl-L-aspartyl-L-glutamate peptidase 1, is a type II transmembrane protein that is highly expressed in the prostate compared to other organs in the body (91-93). The expression of PSMA increases as the tumor develops, and at the later stages in CaP PSMA is the second-most upregulated gene product in CaP (92, 94, 95). As the name suggests, PSMA has known enzymatic activities, acting as a glutamate-preferring carboxypeptidase (91).

PSMA is associated with unique characteristics that make them a great candidate as a target for screening and therapeutics. As mentioned previously, PSMA levels have been reported to be elevated in CaP, particularly in the poorly differentiated, metastatic, and hormone-refractory carcinomas (93, 96-98). This is unique because many of the screening methods cannot readily distinguish between the local and advanced/metastatic CaP. In addition, PSMA has a unique feature in that when its ligand is bound to PSMA, the ligand becomes internalized. This feature may be exploited in cancer therapeutics, where molecules of interest may be targeted directly against tumor cells.

In cancer diagnosis, PSMA may be utilized in multiple ways. PSMA activities are detected through reverse transcriptase polymerase chain reaction (RT-PCR) techniques, which could be highly specific and sensitive in detection if targeted against a proper marker. Studies demonstrated that performing RT-PCR screening using PSMA as the target led to low false-positive rate (0.8%), as well as high rate of detection of prostate cells in metastatic patients (up to 88%), signifying the possibility of PSMA as a valid target (96, 99). Furthermore, by combining radiolabeled isotope to anti-PSMA antibody, PSMA may be used as a probing target with position emission topography (PET) imaging to provide high resolution image of the prostate and the potential metastatic locations (95, 100).

1.4 Treatment Options

Not all cases of CaP require therapeutic intervention, and with the continuing debate between active surveillance versus therapeutic interventions, all CaP patients must be approached independently. Therefore, appropriate treatment plans need to be conceived according to the individual's current status of the disease development, even if the tumor is still localized within the gland. Furthermore, recurrence and metastasis of the cancer requires additional attention as they require altogether different approaches.

1.4.1 Active Surveillance (Watchful Waiting)

Like most other neoplasms, early detection and intervention of high-risk CaP may contribute to substantial reduction in mortality (101, 102). As the name suggests, in active surveillance, patients are continuously monitored by serial PSA testing, repeated biopsies, physical examination of the prostate such as DRE and more (16, 103), yet no active therapeutic actions are taken. However, according to randomized trials, those with favorable-risk (low-risk) CaP did not improve significantly from radical prostatectomy versus watchful waiting in terms of survival advantage, as 21 out of 364 (5.8%) men that underwent radical prostatectomy died from CaP or related treatment, while 31 out of 367 (8.4%) men in the observation group died (101, 104). Among the 52 patients that have died in the study, two thirds of all deaths (34 deaths) were considered to be CaP-specific, of which there was no significant difference in the prostatectomy vs. observational group (16 vs 18 deaths, respectively). Therefore, while current available screening options may benefit high-risk groups with diagnosis and treatment, these options may also be prone to over-diagnosis and treatment for low-risk groups (101). Accordingly, there has been a shift from active treatment to watchful waiting/active surveillance in the past decade.

Despite the benefits of active surveillance, persistence or recurrence of CaP is often

reported based on multiple mechanisms (49) **(Figure 1.4)**. Once the disease recurs, the tumor may have metastasized into other parts of the body. Due to the reliance on androgen for growth in CaP, the treatment plan aims to manage the level of androgen at this stage. This could be done chemically via ADT or surgically via orchiectomy. Orchiectomy is a surgical procedure in which the patient's testes are partially or completely removed. Testicles are the major source of testosterone, thus by undergoing orchiectomy patients are expected to see a reduction in tumor proliferation.

1.4.2 Radiotherapy

Along with radical prostatectomy, applying radiotherapy has been the traditional approach in treating low- and intermediate-risk CaP (105). In the course of treatment plans, about one fourth of all CaP patients have received or will undergo some form of radiotherapy (106). Similar to the surgical approach, radiotherapy in CaP is generally performed for patients with localized tumors. Generally, radiotherapies are categorized into two types – external beam radiation therapy and brachytherapy.

1.4.3 External Beam Radiation Therapy

External beam radiation therapy (EBRT) is one of the most widely used forms of radiation therapy. As the name suggests, during EBRT, an external source of ionizing radiation (normally between 65~80 Gy) (107) is directed at the location of the tumor over multiple 2 to 4 Gy fractions. While the delivery of radiation at the site is effective in destroying localized tumor, the main drawbacks of EBRT has been the non-targeted damage induced on normal cells.

Nevertheless, technological advances in image-guided radiotherapy (IGRT) and intensity modulated radiation therapy (IMRT) have revolutionized the way radiotherapy is

delivered to CaP patients. Physicians have been able to optimize treatment plans through precise locating of the tumor mass, modulating the amount of radiation to be delivered at each exposure and determining the frequency of delivery to be made (108-110). These advantages have allowed significant reduction of non-targeted damage in the adjacent area, thereby reducing post-therapy side effects by a considerable amount (111).

1.4.4 Brachytherapy

Another commonly used form of radiotherapy in CaP treatment is brachytherapy. In brachytherapy, seeds, which are small, sealed particles emitting radiation are placed next to the targeted tumor tissue (112, 113). Unlike EBRT where patients receive radiation from external sources, brachytherapy's energy sources are the inserted radioactive particles themselves. There are two types of brachytherapy in CaP depending on the dosage of the radiation being delivered: low (LDR) and high-dose rate (HDR). Often, LDR brachytherapy is applied for CaP treatment based on its reduced side effects, with HDR brachytherapy used to supplement EBRT. Due to low side-effect profiles, ease of implementation, highly favorable treatment outcome and quick recovery from the procedure, LDR brachytherapy is becoming popular as an alternate method in CaP treatment. However, similar to EBRT and surgical procedures, the current use of brachytherapy is limited to localized CaP. In addition, although the radioactivity of the seeds is carefully controlled, they may still cause side effects including erectile dysfunction and urinary incontinence (113, 114).

1.4.5 Surgery

Radical prostatectomy still remains to be the primary treatment option for localized CaP (105). Radical prostatectomy can be performed via the classical open approach in which a large surgical incision is made to access prostate, or it may be performed in the minimally

invasive approach in which lacroscopy is used to minimalize incision while gaining access to the gland. Both approaches aim to remove the prostate gland and some of the surrounding tissues from the body, thereby removing the tumor mass. Although significant improvements in radical prostatectomy have been made, it is still associated with considerable morbidity and post-operative complications including erectile dysfunction and urinary incompetence. While the definition of erectile dysfunction is variable according to different sources, the occurrence of erectile dysfunction following radical prostatectomy is reported has been reported in up to 70% of the patients (115, 116). This is directly related to quality of life and has placed post-operative recovery of erectile dysfunction in the list of primary attention, especially as there is an increase in diagnosis of CaP in younger men in recent years. While the exact etiology is yet unclear, post-operative erectile dysfunction is predominantly associated with intraoperative injury or postsurgical inflammation damaging the cavernosal neurovascular bundle (116, 117).

Urinary incompetence is another commonly reported post-surgical complication. The etiology of urinary incompetence after radical prostatectomy is multifactorial; in addition to surgical performances, the prospect of post-operative urinary incontinence also depends on the age of the patient, prostate volume, body mass index (BMI), and past history of lower urinary tract symptoms (118). It has been reported that an increase in patient's age is correlated with increased incidence of urinary incontinence, as aging weakens one's sphincter muscles and also may aggravate neural systems that controls urination. Despite the potential side effects caused by the surgical procedures, local prostatectomy still remains a very viable option due to its effectiveness.

1.4.6 Hormone Therapy

Growth of the tumor in the prostate gland is regulated by hormones, specifically by androgens. The potential of hormone-directed regulation in CaP treatment was first identified during early 1900s, when Dr. Charles Huggins from University of Chicago discovered the reversible relationship between androgen ablation and prostate glandular atrophy (119). Based on this relationship, a selected pool of patients with advanced CaP was therapeutically treated with ADT (either by methods of surgical castration or by using estrogen therapy), which led to a significant reduction in the tumor size. Since then, many CaP therapeutics have been focused on refining hormone treatment.

Once the initial, local tumor spreads beyond the prostate, surgical and radiotherapeutic options become limited. In such cases, hormone therapy is recommended. Among different options in hormone therapy, ADT is accepted as the non-surgical standard of care in CaP treatment. Circulation of excess androgens has been associated with malignant growth of the prostate by activating a positive feedback mechanism, subsequently causing an increase of *AR* transcription in CaP cells (120, 121). Many prostatic tumors also have a genomic duplication and amplification of the AR gene (122, 123), resulting in increased AR activity with low circulating androgen levels as a consequence of ADT (121).

Hormone therapies interfere by targeting the AR pathway, either at the level of androgen production or at the level of AR activity. Currently available drugs include enzalutamide, a potent next-generation androgen receptor signaling inhibitor (anti-androgen drug), and abiraterone acetate, a CYP17A1 steroidogenesis inhibitor (124, 125). Both interfere with the regular androgen signaling pathway by reducing androgen availability, or competitively bind to the ligand binding domain of the androgen receptor and therefore preventing cancer progression and increasing progression-free survival (126-129). In addition, not only do these anti-androgen drugs compete with androgens to interfere with the signaling

pathway, they have also been reported to prevent nuclear translocation of the *AR* and the subsequent cascade of downstream activation of genes targeted by *AR* (130, 131).

Despite these promising results from next-generation androgen directed therapeutics, they are not without their limitations. Already, mutations in AR have resulted in development of resistance to these second-generation drugs (132-135), with the first somatic mutation in the AR to enzalutamide having been identified 6 months after the initial clinical use (136, 137). Despite the imperative role of AR in CaP development, merely inhibiting its signaling pathway has prompted a selection mechanism allowing the tumor to become resistant (**Figure 1.4**). Combinations of multiple anti-androgen drugs are under trial, yet the results are not as promising as initially envisioned (138, 139).

1.4.7 Chemotherapy

Along with ADT, the use of chemotherapy against metastatic CRPC is also a widespread treatment option. However, because of relative toxicity associated with chemotherapy and ineffectiveness of the drugs themselves, use of chemotherapy in metastatic CRPC often fails to show a significant improvement in patient's survival (140, 141). The therapeutic effects and cytotoxicity of many chemotherapeutic drugs are attributed to their ability to interfere with cell division. The taxane family of drugs; docetaxel, cabazitaxel and paclitaxel, are most often used in advanced CaP, and work as mitotic inhibitors by targeting microtubules. During normal cell division, there is a dynamic equilibrium between free and polymerized subunits fueled by presence of guanine triphosphates (GTP) allowing for tubulin plasticity (142). Nonetheless, taxanes disrupt this dynamic equilibrium by preventing depolymerization of tubulins, thus interfering with the normal formation of microtubules and thereby blocking cell division. In addition, unlike previously available drugs in chemotherapy, reports have also suggested a role of microtubules in androgen signaling (143). Taking into

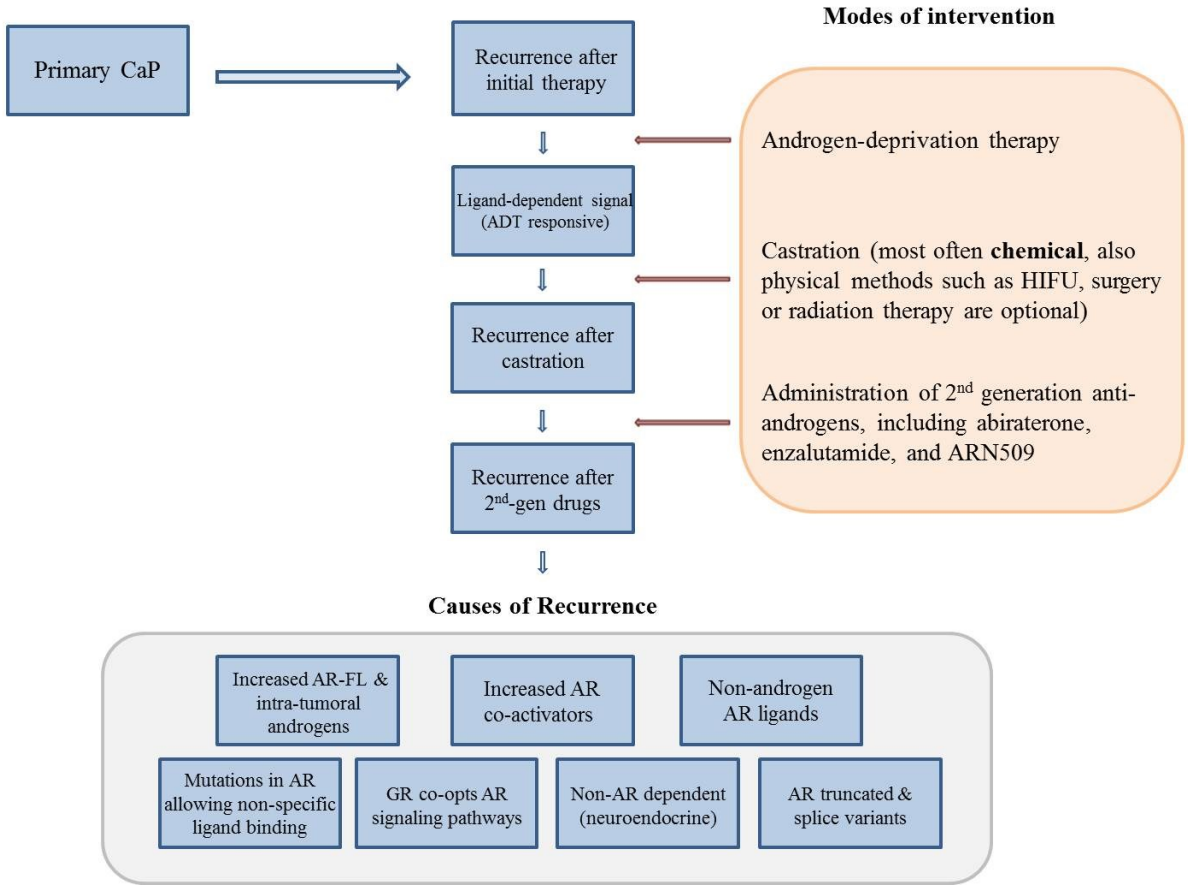

Figure 1.4 Emerging mechanisms of resistance in prostate cancer. Similar to other types of cancers, resistances to therapeutics are observed at multiple stages in prostate cancer development. It remains to be seen whether the tug-of-war between traditional therapeutics and tumor resistance can be won, yet it is clear that up to now, different forms of therapy have ultimately failed due to multiple molecular mechanisms, of which some are listed at the bottom of this figure.

account the fundamental role of AR in CaP progression, this may explain why compared to other chemotherapeutic drugs, taxanes have been successful in the treatment of CaP. Specifically, taxanes have been shown to inhibit the nuclear localization of AR by interfering with normal microtubule function (144). Nevertheless, the use of chemotherapeutic drugs is hampered with serious side effects as well as potential development of resistance mechanisms, limiting their long-term application.

1.4.8 Focal Ablation Therapies

Finally, the genetic heterogeneity and subsequent molecular diversity CaP has limited the long-term clinical success of conventional "biological therapies". These methods often enhance or inhibit certain pathways that are critical for tumor development. However, tumors in general have a strong propensity to develop resistance mechanisms as a result of prolonged and repeated use of these conventional treatment regimens. Therefore, focal ablative therapies have gained considerable attention as a potential method to complement or even replace current treatment regimes. Tumor ablation is a minimally invasive technique that is nowadays commonly used to treat multiple types of cancers by delivering energy directly to the targeted tissue and exert damage, causing cellular breakdown (145). These physical ablations, unlike the conventional biological therapy, bypass the risk of drug resistance and potentially recurrence by selectively damaging the tumor mass with external energy.

1.4.8.1 Stereotactic Body Radiotherapy

Radiotherapy such as EBRT and brachytherapy has been used to treat localized CaP in the last few decades. Nevertheless, the use of radiotherapy has been limited by the intensity of the radiation being delivered and their potential side effects. Stereotactic body radiotherapy (SBRT) has overcome these limitations by delivering lower doses of radiations

from multiple positions of the body (in the doses of >5 Gy per fraction), which are targeted at the tumor so that only the tumor receives high doses of radiation while the surrounding tissues receive minimal dose (146). In a 2013 phase 2 clinical study, the effectiveness of SBRT for localized prostate cancer demonstrated comparable results in terms of PSA relapse-free survival (93% for all patients), supporting the use of SBRT as an alternative, safer option (147).

1.4.8.2 Hyperthermia/Photothermal Therapy

High temperature impairs cellular activity. From the era of whole body hyperthermia, the concept of utilizing heat against malignant tissue has evolved to a level where specific and minimal delivery of heat against tumor using thermal agents is now possible. Although photothermal therapies using laser-stimulated nanoparticles are still under pre-clinical development, hyperthermia therapy using magnetic nanoparticles is already undergoing clinical trials, with superior complete response when combined with radiotherapy versus receiving radiotherapy alone (62.5% vs 39.6%) (148).

1.4.8.3 High Intensity Focused Ultrasound

As the name suggests, high intensity focused ultrasound (HIFU) utilizes focused ultrasound waves with power normally exceeding 5 W/cm^2 and frequencies within the range between 0.8-3.5 mHz to thermally ablate tumor cells (105). During HIFU therapy, an ultrasound probe is placed transrectally to deliver energy and simultaneously provide real time imaging. A 2015 clinical study with 918 patients undergoing HIFU therapy using Sonablate® probe resulted in cancer specific survival rate of 97.4% and ten year overall survival of 89.6% (149). Nevertheless, the current data on the safety and efficacy of HIFU therapy in CaP treatment remains incomplete, and further clinical trials are required.

1.4.8.4 Focal Cyroablation

While the other focal therapies for CaP have focused on delivering energy to raise the cellular temperature, focal cryoablation aims to stimulate tumor damage damaging cell membranes and organelles by exposing the targeted area to rapid freezing-thawing cycle (150). Systematic reviews suggest a biochemical disease-free survival rate between 71-93% at 9 to 70 months of follow-up (151).

Although these focal therapies are showing promises and are either already being utilized in clinic or undergoing clinical trials, most of them are limited to early, local CaP.

1.5 Conclusion

CaP is a complex disease. While the early, localized CaP may appear benign, the unique multifocality and the inherent heterogeneitic nature of the tumor eventually lead the tumor to become lethal as the cancer becomes metastatic, spreading beyond the initial gland. Multiple forms of therapy at all levels of CaP have been so far discussed, yet none of them are conclusive. Furthermore, while therapies to localized CaP are effective, treatments for late-state CaP are faced with incredible complexity and also with the resistance to the currently available therapeutics which spans ADT (including biological and hormonal therapies), chemotherapy, and more. Therefore, a novel method, which would circumvent the need of the therapeutic agents to elicit biological responses to promote tumor death, would be promising. Based on these principles, we have employed nanomaterials as a potential physical therapeutic platform in which direct damage against tumor may be induced.

Chapter 2: Prostate Specific Membrane Antigen-Directed Carbon Nanotube for Targeted Extreme Nearfield Ablation of Prostate Cancer Cells: An *in vitro* study

PREFACE TO MANUSCRIPT

The manuscript was accepted for publication by Tumor Biology, December 2016. Its assigned DOI is 10.1177/1010428317695943.

Prostate cancer is one of the most diagnosed cancers amongst men. Although reasonable surgical and medical treatments exist, there are many side effects that compromise patients' quality of life. Moreover, recurrence rates are not negligible, exposing the patients to additional morbidity and even death. All of the above emphasize the need for a new technology to treat local recurrence and metastatic disease, with the potential of fewer side effects, and minimal compromise to quality of life.

The use of multi-walled carbon nanotubes (MWCNT) is an innovative approach that may have therapeutic potential for recurrent or metastatic disease. By using the prostate specific membrane antigen as a cell surface target, that is expressed in LNCaP prostate cancer cells, we propose that it will be possible for the MWCNT to exert their action by destroying both cancer and adjacent unwanted prostate tissue via a targeted photothermal ablative approach without significant bulk heating; thus protecting cells surrounding the prostate gland not expressing the targeted receptor.

We have identified the following objectives:

1) By utilizing nanomaterials that readily convert light into thermal energy, adopt a photo-thermal method in cancer ablation where a local, selective physical damage upon the targeted tumor tissue may be achieved
2) In addition to generating abovementioned therapeutic effects, manipulate the nanomaterials in a way so that they may also serve as a platform for diagnostic purposes (i.e. theranostic).

CONTRIBUTION OF AUTHORS

Seung Soo Lee

1) Cell culture maintenance
2) Preparation of the nanomaterials, including conjugation and handling
3) Image acquisition with spinning-disk confocal microscopy
4) Performed all cell ablation studies
5) Designing of the thermal camera and acquisition of temperature data
6) Analyzed all resulting data and created figures accordingly
7) Wrote and edited the manuscript

Philip J. R. Roche

1) Designing of the laser device
2) Assistance in nanoparticle chemistry and preparation

Paresa N. Giannopoulos

1) Performed western blots
2) Assistance with cell culture maintenance

Elliot J. Mitmaker

1) Participated in editing of the manuscript

Michael Tamilia

1) Participated in editing of the manuscript

Miltiadis Paliouras

1) Supervision of the project
2) Image acquisition with spinning-disk confocal microscopy
3) Editing/modifications of the figures
4) Participated in writing and editing of the manuscript

Mark. A. Trifiro

1) Supervision of the project
2) Participated in editing of the manuscript

2.1 Abstract

Almost all biological therapeutic interventions cannot overcome neoplastic heterogeneity. Physical ablation therapy is immune to tumor heterogeneity but nearby tissue damage is the limiting factor in delivering lethal doses. Multi-walled carbon nanotubes (MWCNTs) offer a number of unique properties; chemical stability, photonic properties including efficient light absorption, thermal conductivity, and extensive surface area availability for covalent chemical ligation. When combined together with a targeting moiety such as an antibody or small molecule, one can deliver highly localized temperature increases and cause extensive cellular damage. We have functionalized MWCNTs by conjugating an antibody against prostate specific membrane antigen (PSMA). In our *in vitro* studies using PSMA positive LNCaP prostate cancer cells, we have effectively demonstrated cell ablation of >80% with a single 30 second exposure to a 2.7W, 532 nm laser and for the first time without bulk heating. We also confirmed the specificity and selectivity of PSMA targeting by assessing PSMA-null PC3 cell lines under the same conditions (<10% cell ablation). This suggests that we can achieve an extreme nearfield cell ablation effect thus restricting potential tissue damage when transferred to *in vivo* clinical applications. Developing this new platform will introduce novel approaches towards current therapeutic modalities and will usher in a new age of effective cancer treatment squarely addressing tumoral heterogeneity.

2.2 Introduction

Prostate cancer (CaP) is the most common neoplastic disorder in men, but only a fraction of those affected, whom cannot yet be identified, will develop more significant advanced disease. As a consequence, initial localized disease is difficult to address and is prone to over-diagnosis and over-treatment. In early disease, passive active surveillance is most likely practiced. Later stage disease is associated with a transition of the tumor(s) towards an androgen-independent state, a fatal prognostic sign (152). Surgery is clearly curative in early disease, but the complications are still very substantial.

Early cancers evolve through many somatic mutations (153-157) and undergo many selection processes, and many times induced by classical drug therapies themselves initiating drug resistance. CaP studies have shown extensive genetic alterations exemplified by single missense mutations, copy number variation, splicing variants, genetic rearrangements and short DNA alterations in a large number of genes (154, 158-163). However, physical agent therapies are immune to genetic alterations, as they are more likely to deliver damaging entities to a targeted “area” or “field”, and as such are lethal to tumor cells irrespective of their genetic background, as long as they are present within the targeted area.

Thus, physical agents could circumvent many of the concerns of treating advanced localized disease and would be curative, where surgical options may be unavailable. Therefore, agents that manipulate temperature, light, or radioactivity should be considered. Though used in the past they are limited by possible nearby tissue damage. There has never been an attempt to devise an adequate systematic effective targeted nearfield delivery of physical agents. These modalities, in addition to classical radiotherapy and brachytherapy, usually lack sufficient cell destruction or cause significant damage to critical nearby tissues. For example, a limitation of high-intensity focused ultrasound (HIFU) is the potential damage to nearby tissues and therefore lacks high precision, and thereby limited to CaP *in situ* (164).

A superior targeting approach for cancer cells would require a mechanism by which a highly-localized physical agent is in immediate proximity to the cells, ideally at the cell surface, causing significant cellular/intracellular damage with extreme efficiency deferring nearby tissue effect. To do so we employed functionalized multi-walled carbon nanotubes (MWCNTs), which are engineered soluble colloidal suspensions possessing tunable thermal, magnetic, and electromagnetic wave interaction properties.

Several groups have used nanoparticles for ablative therapy (many without targeting it to the tumor, or using direct injection (165-168)) which was very effective yet introduced excessive bulk heating ($t > 50$ °C). However, bulk heating of a treated region can cause serious nearby damage in the clinical setting. Other nanoparticles require large light fluxes/ultra-short light pulse modulations (169) with prolonged exposure of 5 to 15 minutes (170) even for moderate temperature increases of only few degrees, which can be detrimental and inefficient with lower rates of cell ablation.

Presently, a high-level of biological and chemical functionalization potential is available for binding of targeting ligands to MWCNT nanoparticles, thus mediating cancer cell recognition and subsequent nearfield cell ablation. Expanding on our previous study (171) of MWCNT nanoparticle-mediated targeting strategy, here we specifically target prostate specific membrane antigen (PSMA) expressed in prostate cancer cells by optimizing the nanoparticle functionalization and antibody conjugation chemistry. We also aimed to show that highly efficient targeting should place a sufficient number of nanoparticles directly on the surface of cells so as to deliver exquisite extreme nearfield heat energy sufficient for cell ablation without bulk heating. Bulk heating reflects misdirected energy and can have serious effects on nearby tissue if used *in vivo*. These MWCNTs have the added critical benefit of simultaneously providing a self-imaging platform, so as to document and quantitate successful targeting (i.e., theranostics).

2.3 Materials and Methods

2.3.1 Cell lines and culturing

LNCaP, PC3 and HEK293 cells lines were obtained from the American Type Culture Collection (ATCC, Rockville MD). LNCaP and PC3 cells were cultured in RPMI1640 media supplemented with 10% fetal bovine serum (FBS) and 1% penicillin/streptomycin. Cell lines were incubated at 37°C, 5% CO_2 humidified air in plastic culture flasks. Once confluent, cells were harvested by using Versene solution (0.48 mM EDTA in PBS) to maintain cell surface integrity and were suspended in chilled PBS in preparation for incubation with functionalized MWCNTs.

2.3.2 MWCNT particle functionalization and antibody conjugation chemistry

Multi-walled carbon nanotubes functionalized with carboxylic group on the surface (MWCNT-COOH) were purchased from Cheap Tubes Inc. (Cambridgeport, VT). In a stock MWCNT solution, 15 mg of MWCNTs and 200 µL of polysorbate 20 solutions (TWEEN20) were suspended in d_2H_2O to obtain final concentration of 60 mg/L. The MWCNT solution was sonicated 7 times each for 20 minute durations at 4°C. During each interval, 1 mL aliquots of the stock solution were prepared to assess the solubility and dispersion of MWCNTs. To evaluate the solubility and dispersion, the aliquots were filtered with 0.45 µm Amicron filter, and the absorbance values (measured by NanoDrop UV-Vis spectrophotometer) of the filtrate was compared to the unfiltered, sonicated stock solution. The stock solution was sonicated until the absorbance values of the stock was equal to the absorbance values of the filtrate (172, 173). Size-modified MWCNT solution was mixed with 40 µL 1-Ethyl-3-(3-dimethylaminopropyl) carbodiimide (EDC) 20.9 mM, 40 µL N-Hydroxysuccinimide (NHS) 34.8 mM, and 20 µL 0.2 mM heterobifunctional maleimide-PEG_{5000}-NH_2 crosslinker (Mal-PEG_{5000}-NH_2) (Nanocs, New York, NY) in a final volume of

300 μL. The mixture was allowed to react in 25°C for thirty minutes to ensure that the coupling reaction at the amine side of the PEG crosslinker is completed with EDC-NHS activated COOH groups of MWCNTs. Once the reaction was completed, the protein or antibody of interest containing functional groups (sulfhydryl groups) was added to the mix and was incubated at 4°C overnight to allow the maleimide side of the crosslinker to fully react with the functional SH-groups on the protein. The final product was centrifuged at 12,000g at 4°C for 30 minutes, resuspended in PBS and was sonicated to ensure monodispersion of the antibody functionalized MWCNTs. UV-Vis measures of the final product were obtained to ensure that the solution's absorbance values were still larger than 0.03 units at 532nm wavelength. Conjugation of the targeting antibody to the maleimide-PEG_{5000}-NH_2 crosslinker is outlined in **Figure 2.1 and Supplemental Data S1.**

The same PEG functionalization protocol was performed using Cy5-PEG_{5000}-NH_2 dye (Nanocs, NY). The following PSMA antibodies (EPR6253 and EP3253) were tested (Abcam, Toronto, Canada). Other antibodies used included mouse IgG (Millipore, Billerica, MA) and α-mouse-linked-HRP (GE Healthcare, Baie-d'Urfé, Canada).

2.3.3 Western blot analysis

PC3 and LNCaP were collected using 0.05% trypsin and lysed using 1 X Reporter Lysis buffer. The samples were then precipitated overnight in room temperature before loading onto the gel. 20 μg of total-cleared cell lysate was loaded on an 8% SDS-PAGE gel. Primary PSMA (EPR6253) antibody was diluted to 1:1000 and used under manufacturer's instructions (Abcam, Toronto, Canada). Antibody against β-actin was used as a loading control.

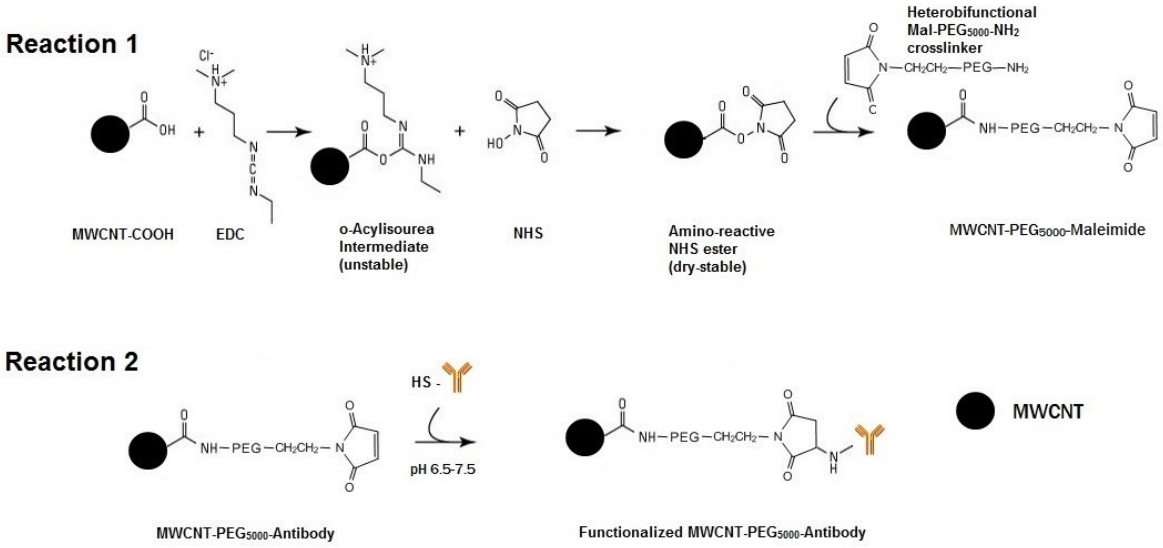

Figure 2.1 Conjugation Chemistry. Coupling chemistry used with Mal-PEG-CNTs to attach bio-affinity molecules. Initially EDC/NHS chemistry is used to link maleimide-PEG-amide to COOH-functionalized MWCNT in Reaction 1. Reaction 2 allows for the coupling of bio-affinity molecule to maleimide component of PEG.

2.3.4 Cell ablation studies

Using LNCaP, PC3 or HEK293 cell lines, ~300,000 cells suspended in 150 µL PBS was well-mixed with 75 µL of functionalized MWCNTs or α-PSMA-MWCNTs. A negative control with PBS was also prepared. Each experiment was performed ≥ 3 times. These mixtures were incubated for one hour at 37°C and 5% CO_2 on a rotator. After incubation, mixtures were centrifuged at 500g for five minutes, washed three times in PBS, and resuspended in 225 µL PBS. This washing step was repeated for a total of three times. The solution mixture was then aliquoted into 25 µL fractions in PCR tubes, which were then subjected under green diode-pumped solid-state laser (DPSS laser; power at 2.7W and laser emission at 532nm) for 30 seconds. Finally, cell counts for laser treated and untreated cells were obtained using trypan blue staining under a hemocytometer. Cell ablation was calculated as: % Cells Ablated = (number of live cells post laser treatment/number of live cells pre laser treatment) X 100.

2.3.5 Live cell imaging with Cy5-crosslinked MWCNT

For Cy5 tagging of the MWCNTs, our standard conjugation method was employed, except maleimide-PEG_{5000}-NH_2 crosslinker was mixed with Cy5-PEG_{5000}-NH_2 (Nanocs, New York, NY) solution (0.2 mM; 4:1 maleimide crosslinker to Cy5 dye ratio) in the dark to provide fluorescence. The conjugated products were washed three times with PBS to ensure unbound Cy5-PEG_{5000}-NH_2 dye was removed. Approximately 50,000 PSMA-positive LNCaP and PSMA-null PC3 cells were seeded onto LabTek II chamber slides (purchased from Thermo Fisher Scientific, Rochester, NY) in respective wells. The seeded cells were incubated overnight at 37°C and 5% CO_2. On the next day, α-PSMA-MWCNT conjugates with or without Cy5 and PBS control were incubated with the two cell lines for one hour in identical conditions. 138 µL of 300 nM stock of 4',6-Diamidino-2-Phenylindole,

Dihydrochloride (DAPI) solution was also added for nuclear staining. After incubation was completed, the wells were washed three times with RPMI medium to remove any unbound Cy5-tagged MWCNTs. The chamber was then visualized under Leica spinning disk confocal microscope (Wetzlar, Germany).

2.4 Results

2.4.1 Non-targeted cell ablation studies.

One of the major properties of nanoparticles including MWCNTs is the plasmonic generation of extreme heat at their surface upon exposure to light. Thus, we aimed to assess PEG functionalized MWCNTs and their ability to ablate cells, when solely mixed together with HEK293 cells without antibody conjugation and without washing in a non-targeted experiment. MWCNTs were mixed in a 1:2 volume ratio of particles to cells, and exposed to a 2.7W 532nm laser for 5, 10 or 20 seconds (**Figure 2.2A**). Cell death was visualized by a simple trypan blue staining, with cells counted on a hemocytometer. With increasing exposure to the laser, the number of live cells drops. By 20 seconds, not a single live (or white) cell could be counted. Moreover, the number of "blue" or dead cells is also dramatically reduced from the starting input cell numbers, indicating that the process has resulted in a physical disruption/destruction of the cells. The reduced presence of "blue" cells together with the reduced number of total cells after 20 second laser exposure suggests that the cells are not undergoing an apoptotic programmed or necrosis cell death, but rather a very physical ablative destruction by the generation of bulk heating (see below). After laser treatment, a portion of the cells were plated onto 6-well plates and assessed for survival and growth after 5 days **(Figure 2.2B)**. The 5 and 10 second laser exposure was not adequate to ablate all the cells and a confluent lawn of cells could be observed after reseeding. However, from the 20 second laser treatment we could not observe any cell growth after 5 days,

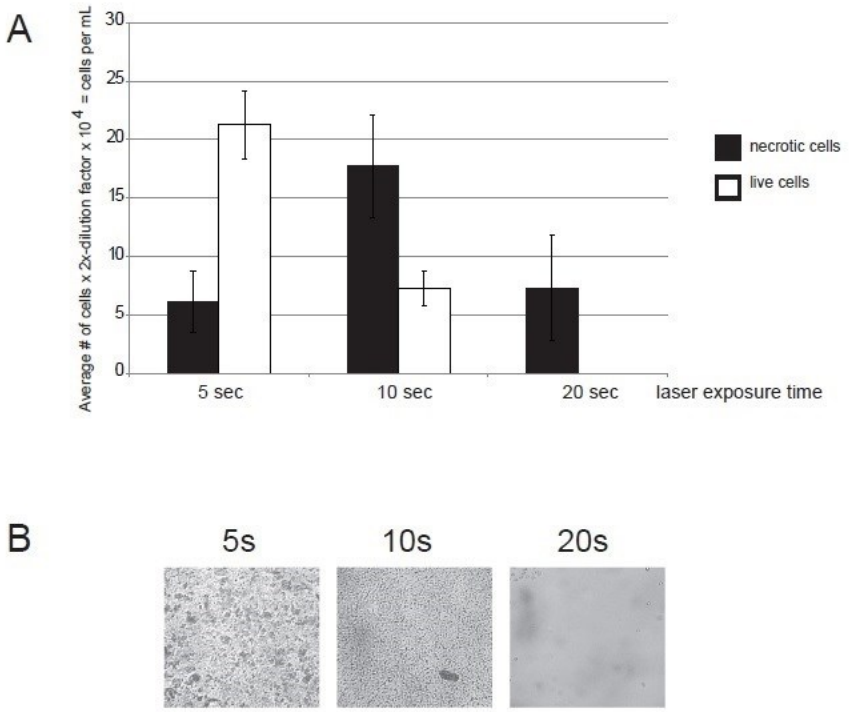

Figure 2

Figure 2.2 Non-targeted cell ablation studies. A. PEG-maleimide functionalized multi-walled carbon nanotubes (MWCNT) was used to test the potential to kill HEK293 cells by bulk heating of the solution mixture and shows the effects of 3 different exposure times (5, 10, 20 seconds) with a 2.7W, 532nm laser (n=5). Following laser treatment, cells death was assessed using Trypan blue staining. **B.** After laser treatment, portion of HEK293 cells were seeded into 6-well plates and grown for 5 days. Following 20 seconds of laser treatment, no cells could be discerned growing on the plates.

emphasizing complete ablation. It is also clear that for photothermal bulk heating of the MWCNTs at lower concentrations (mass per volume), carbon-based materials are more effective compared to alternatives such as silica particles, ferrous or gold particles (174-176).

2.4.2 PSMA antibody selection and near-field targeting of LNCaP cells.

To determine the effectiveness and extent of the antibody conjugation method using malemide-PEG_{5000}-NH_2 bifunctional crosslinkers, we have performed a semi-quantitative, dose-dependent chemiluminescent assay. Different amounts (2, 5, 8, 10, and 12 μg) of α-mouse HRP-IgG were conjugated onto MWCNTs as outlined in our protocol. A diluted (1:10) portion of each sample was loaded onto a microtiter plate and mixed with chemiluminescent solution. Similarly, as a standard we loaded different amounts (2, 5, 8, and 10 μg) of solely unconjugated α-HRP-IgG (diluted by a factor of 1:1000) onto to a microtiter plate. Intensity of the chemiluminescent reaction is shown in **Figure 2.3**. The results display a very linear relationship on the amount of α-HRP-IgG that can be conjugated to the nanoparticles; conjugation of 12 μg α-HRP-IgG did not reach a MWCNT saturation point.

The average molecular weight of MWCNT is in the order of 10^8 g/mol; thus there are approximately 10^3 less particles than antibodies; each particle has approximately 10^5 COOH groups, providing a very close equimolar ration of COOH groups and antibody used in these experiments. Increasing the amount of EDC and NHS for the carbodiimide reaction to increase functionalization of the carboxylic groups on MWCNTs, was ineffective, as only a marginal difference was observed, suggesting that we are employing enough carbodiimide for functionalization of the carboxylic groups (data not shown).

PSMA was selected as the target of choice for selectively targeting prostate cancer cells. The expression of PSMA is highly restricted to human prostate secretory epithelium; its level of expression is correlated with the tumor aggressiveness; and it is present in all stages

of the disease from early disease and especially elevated in advanced hormone refractory and metastatic disease (177-180). Furthermore, PSMA provides an excellent target for monoclonal antibody strategies because it is long-lived on cancer cells, and comprises a large extracellular domain. Therefore, we selected to test two different PSMA antibodies, 5 μg of EP3253 and EPR6253 antibodies by conjugating them onto MWCNTs and used for our targeted cell ablation studies of PSMA expressing LNCaP cells. EP3253 and EPR6253-MWCNT conjugates were prepared and incubated in a 1:2 MWCNT:cell ratio for 1 hour, washed thoroughly with PBS and exposed to laser treatment for 30 seconds. Both α-PSMA-MWCNT conjugates showed efficient targeted ablation of PSMA-expressing cells, with >60% of LNCaP ablated (**Figure 2.3C**), suggesting that the difference between the two antibodies were marginal (181).

We also assessed whether the targeting of PSMA to LNCaP is restricted to the exposed extracellular domain, and that the α-PSMA-MWCNT conjugates are not internalized. Therefore, we similarly conjugated 5 μg of the antibodies against intracellular androgen receptor (AR), which is known to be well expressed in LNCaP cells, and IgG (a non-specific targeted antibody) to MWCNTs and proceeded with cell ablation studies **(Figure 2.3D)**. The amount of cell ablation is very minimal and significant between the α-PSMA targeted vs. α-AR or IgG targeted cells (EPR6253, 5μg: α-AR p=0.00499, IgG p=0.00039; EP3253, 5μg: α-AR p=0.00419, IgG p=0.00016), and moreover, illustrates that the MWCNT are not internalized to target intracellular moieties such as the AR. This is in contrast to non-targeting MWCNTs shown with HEK293 cells where bulk heating is required to confer cell ablation; altogether we have shown that effective targeting of the MWCNTs now delivers highly efficient, highly localized cell ablation so much so as to avoid overall bulk heating (see below).

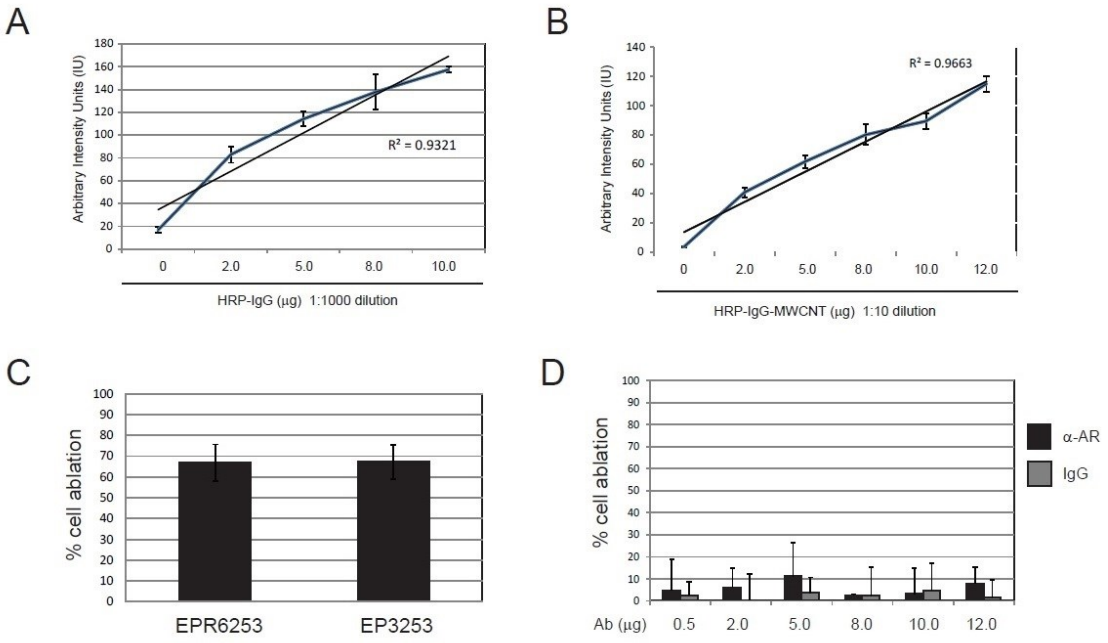

Figure 3

Figure 2.3 *α*-PSMA targeted cell ablation. A. Standard curve of HRP-IgG antibody diluted 1:1000, loaded onto a black clear bottom microplate and mixed with chemiluminescent solution (n=3). B. MWCNTs conjugated with different amounts of HRP-IgG, diluted 1:100 and loaded onto microplate and mixed with chemiluminescent solution (n=3). Images were captured with a Bio Rad gel imager and densitometry of signal intensity was measured by ImageJ. **C.** Two PSMA antibodies from Abcam [EPR6253 (n=3) and EP3253 (n=3)] conjugated to MWCNTs and used to ablate LNCaP cells. Both antibodies showed similar abilities to ablate cells. **D.** Androgen receptor (AR) (n=3) and IgG (n=3) antibodies were also conjugated onto MWCNTs and used as negative controls to ablate LNCaP cells.

2.4.3 Optimization of *in vitro* cell ablation studies

2.4.3.1 Working concentration of α-PSMA-MWCNT conjugates

Next, the working concentration of MWCNT-antibody conjugate was determined by preparing a dose-response curve. Six concentrations of α-PSMA ranging from 0.5 μg to 12 μg were conjugated to MWCNTs, to determine a working concentration of antibody that could be effectively used for further ablation studies. **Figure 2.4A** shows the increased efficiency in ablation of LNCaP cells with increasing amounts of α-PSMA conjugated onto MWCNTs. Initially, a linear increase in cell ablation efficiency was observed at lower concentrations. However, when more than 5 μg of α-PSMA was conjugated onto the MWCNTs, the efficiency of cell ablation decreases and begins to plateau, with no significant difference between 10 μg and 12 μg of antibody addition. Although, we have not saturated the amount of antibody on the MWCNT (**see Figure 2.3**), it appears that between 8 to 10 μg of antibody in the conjugation reactions confers sufficient binding to the PSMA targets on LNCaP cells. This suggests that a critical content of antibody per MWCNT is required for optimal targeting, and the more antibody-laden MWCNTs do not lead to more particles per cell surface. For all further experiments, 5 μg of α-PSMA was conjugated to MWCNTs.

2.4.3.2 Determination of Cell:MWCNT ratio

The ratio of LNCaP cells to α-PSMA-MWCNT conjugates was optimized by altering the ratio of cells to MWCNT conjugates. Four volumetric ratios of cells to α-PSMA-MWCNT conjugates (3:1, 2:1, 1:1 and 1:2 cell to conjugate) were examined, while other conditions were kept consistent. As the concentration of α-PSMA-MWCNT conjugates increased, higher cell ablation efficiency was observed **(Figure 2.4B)**. When increased α-PSMA-MWCNT conjugates are incubated with LNCaP, the cell ablation increases from 38.8% ± 4.3 at 3:1 cells:MWCNT conjugates ($p=2.61 \times 10^{-9}$, α-PSMA-MWCNT vs. MWCNT) to

71.2% ± 4.7 at 1:2 cells:MWCNT conjugates (p=0.266, α-PSMA-MWCNT vs. MWCNT).

Unconjugated MWCNTs did not demonstrate any cell ablation potential; however, when a 1:3 cells:unconjugated MWCNT ratio was used, we observed a significant increase in cell ablation. We observed a similar result in our previous assessment of α-TSHR-MWCNT targeting of papillary thyroid cancer cells (171). The washing of high MWCNT to cell mixture was insufficient to remove the excess concentration of nanoparticles and enough residue MWCNTs remained to confer some cell ablation. Lastly, we did not observe significant difference in PBS controls, with 5%, 8%, 5%, 9% cell loss in 3:1, 2:1, 1:1 and 1:2 cell to MWCNT mix, respectively; with laser exposure, suggesting that laser itself has no detrimental effects.

2.4.3.3 Length of exposure to laser

Finally, we evaluate the effects of laser exposure in cell ablation by lengthening the time of laser exposure. LNCaP cells incubated with α-PSMA-MWCNT were exposed to 2.7W laser for different lengths of time (20, 25, 30 and 35 seconds) (**Figure 2.4C**). Simultaneously, we also assessed unconjugated-MWCNT and PBS incubated with LNCaP as controls. With longer exposure, we observed an increase in cell ablation efficiency with α-PSMA-MWCNTs with; 49% ($p=2.05x10^{-8}$, α-PSMA-MWCNT vs. MWCNT, at 20 seconds), 54% ($p= 1.59x10^{-9}$, α-PSMA-MWCNT vs. MWCNT, at 25 seconds), 58% ($p=4.93x10^{-8}$, α-PSMA-MWCNT vs. MWCNT, at 30 seconds), and 63% ($3.23x10^{-10}$, α-PSMA-MWCNT vs. MWCNT, at 35 seconds). No specific cell ablation was also observed with either unconjugated-MWCNT or PBS. Thus, PSMA target-bound MWCNTs exposed to laser for a longer time periods results in higher cell ablation. When the temperature of the tube was monitored, we observe only small temperature changes between the different time points, with the highest bulk solution temperature observed was 41.2 ºC at 35 seconds.

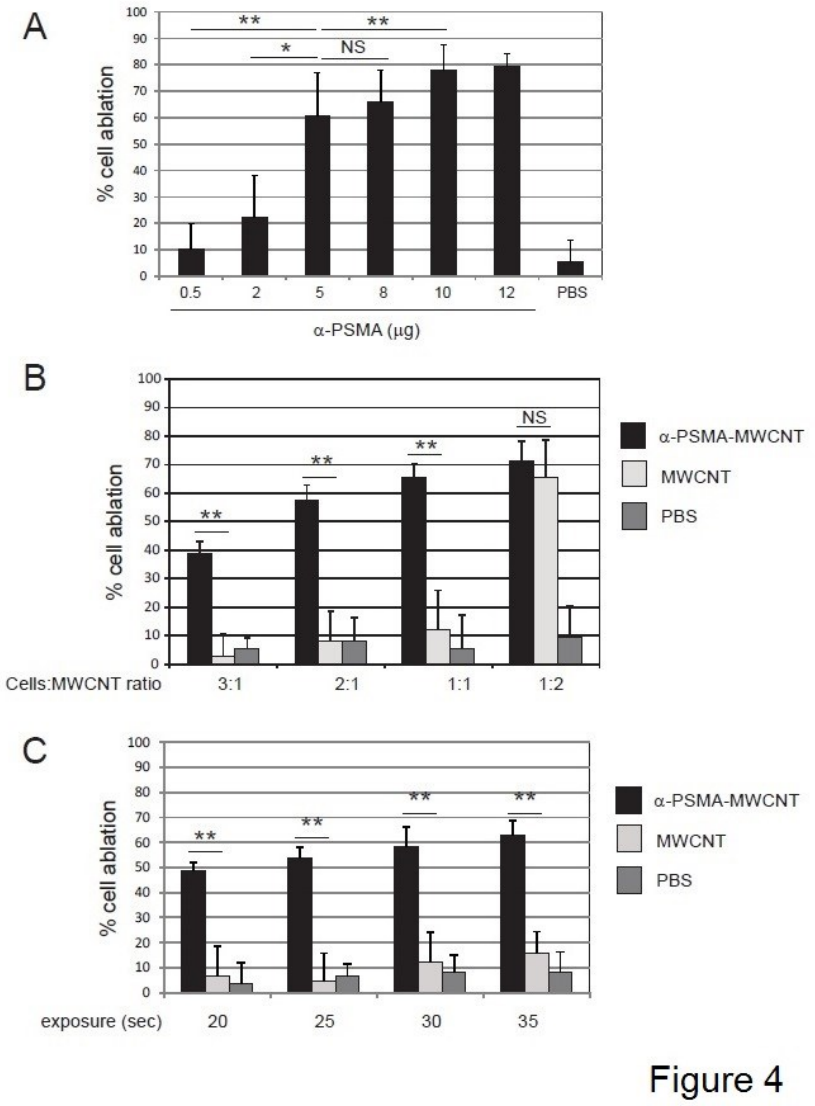

Figure 4

Figure 2.4 Optimizing targeted cell ablation of LNCaP cells. A. Different amounts of α-PSMA was conjugated to MWCNTs and used for cell ablation studies (n=5). **B.** Different volumetric ratios of cells to α-PSMA-MWCNT conjugates were assessed in cell ablation studies. It could be observed that at the 1:2 ratio, the MWCNT alone result in significant amount of cell killing, this is due to the inability to wash away the large amounts of nanoparticles (n=3). **C.** Using 2:1 ratio, cells-α-PSMA-MWCNT mixture was exposed to different lengths of time (n=3). Statistical significance was determined between the different concentrations (*, $p<0.05$; **, $p<0.005$; and NS, not significant).

2.4.4 Selective α-PSMA-MWCNT targeting of prostate cancer cells

To evaluate whether α-PSMA-MWCNTs could exhibit specific PSMA targeted cell ablation, we used PSMA-null PC3 cells (**Figure 2.5A**). In principle, each MWCNT molecule has multiple carboxylic groups that can serve as binding platforms for numerous moieties. Exploiting this property, we dual-functionalized MWCNTs with Cy5-PEG_{5000}-NH_2 and maleimide-PEG_{5000}-NH_2 (onto which α-PSMA was linked), thus allowing for selective fluorescent imaging of PSMA targeted cells (**Figure 2.5B**). We also prepared negative untargeted single conjugated Cy5-MWCNT and PBS controls to demonstrate non-selective interactions to the cells (data not shown). As expected, the dual labeled α-PSMA;Cy5-MWCNT conjugates only interacted with LNCaP and not PC3 cells. Finally, selective cell ablation of α-PSMA-MWCNT conjugates was evaluated between LNCaP and PC3 cells (**Figure 2.5C**). It was observed, and confirming, that only LNCaP cells were sensitive to α-PSMA-MWCNT with 63.0% ± 8.8 cell death; compared to 9.7% ± 7.2 with PSMA-null PC3 cells ($p=0.00011$).

2.4.5 α-PSMA-MWCNT targeting confers extreme nearfield cell ablation without bulk heating

Central to our approach of mediating extreme nearfield cell ablation we assessed bulk temperature of the media during our ablation experiments. In Figure 1, we demonstrated non-targeted cell ablation of HEK293 cells; the temperature of the media in our non-targeted experiments resulted in complete cell death in 20sec laser exposure, where the bulk temperature reached up to 60°C in approximately 19 seconds **(Figure 2.6A)**. 5 and 10 second exposures to the laser did not significantly increase the bulk temperature of the mixture, as the temperature was well below <50 °C, the tolerable temperature threshold for normal cells.

We further assessed the bulk temperature of α-PSMA-MWCNT targeting of LNCaP

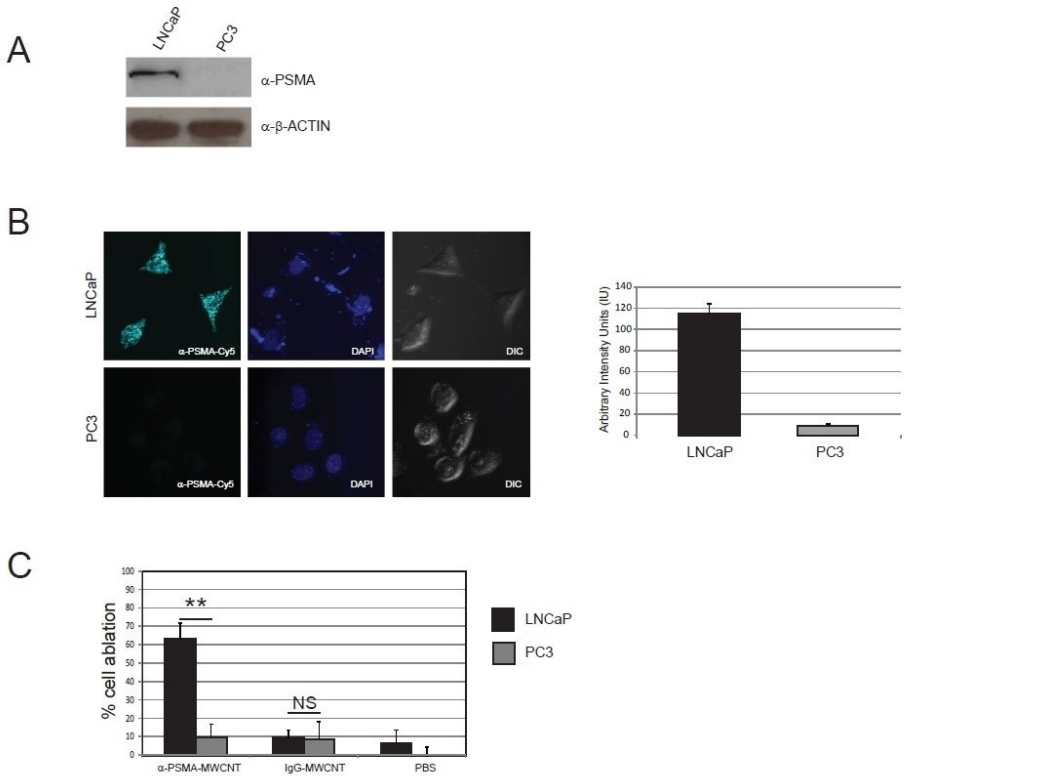

Figure 5

Figure 2.5 Selective PSMA targeting of LNCaP vs. PC3 cells. A. Western blot analysis of PSMA positive LNCaP cells vs. PSMA negative PC3 prostate cancer cells. **B.** Dual labelling of MWCNTs with α-PSMA and Cy5, for live imaging LNCaP and PC3 cells. Shown are stacked images from the spinning disk confocal microscope of LNCaP and PC3 cells labelled with Cy5, nuclear staining marker DAPI, and corresponding differential interference contrast (DIC) whole cell image. Intensity measurements were made for Cy5 staining using ImageJ software of numerous other slides and represented graphically next to the confocal images. A total of 20 cells were selected from images for which intensity analysis was performed. **C.** Cell ablation experiments using α-PSMA-MWCNT against LNCaP and PC3 cells. IgG-MWCNT conjugates and PBS were used as controls in these studies (n=5). Statistical significance was determined between the different concentrations (**, $p<0.005$; and NS, not significant).

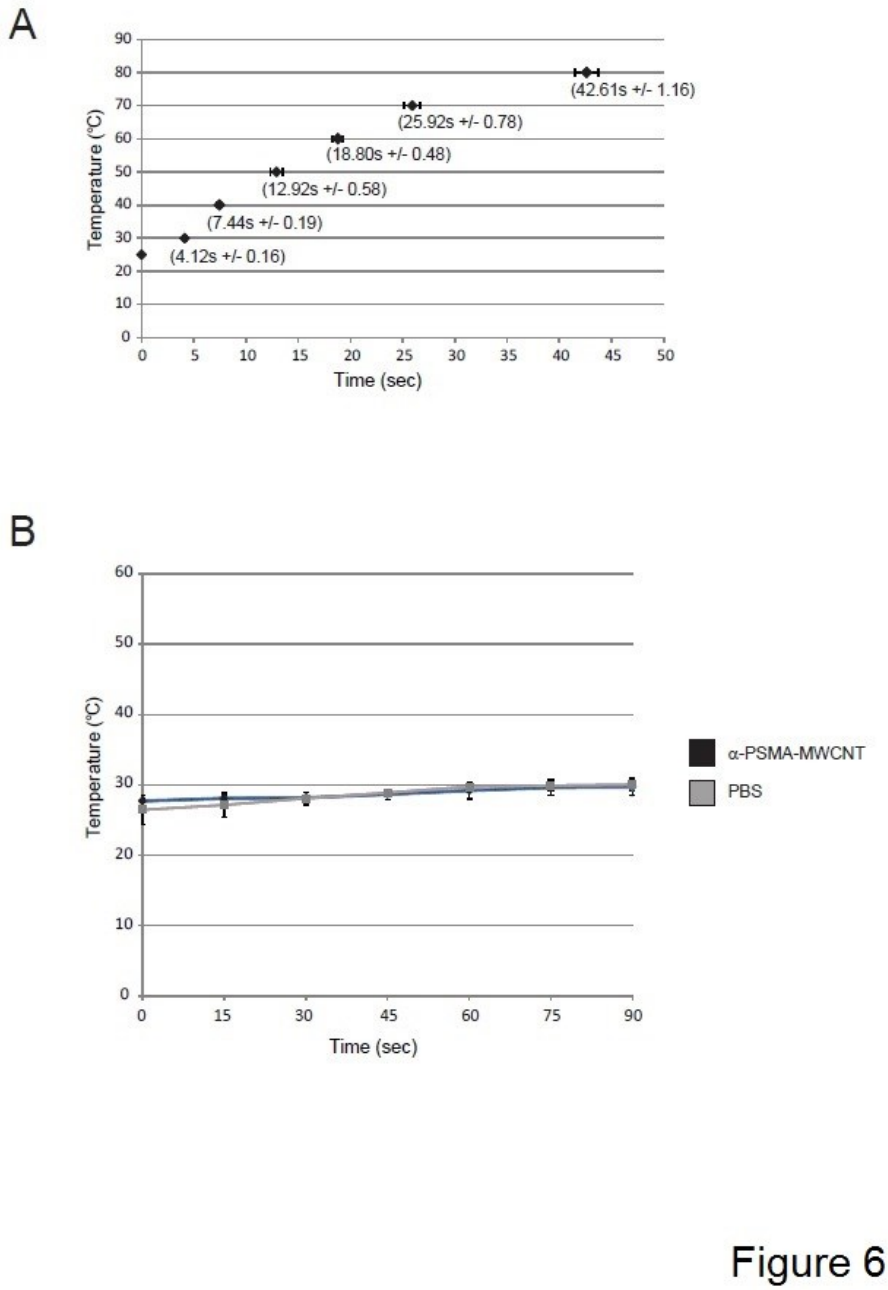

Figure 2.6 Bulk temperature analysis of cell-MWCNT mixtures. A. Temperature rate readings of LNCaP cells mixed with PEG-MWCNTs (2:1 ratio) (n=3). Graph shows the time taken to reach fixed temperatures (30, 40, 50, 60, 70, 80°C). B. Temperature monitoring of α-PSMA-MWCNT targeting experiment of LNCaP cells, over 90 seconds. Temperature readings were also performed with PBS control experiments (n=5).

cells (using 2:1 cells:MWCNT ratio) and found no significant increases in bulk temperature of the mixture **(Figure 2.6B)**. Even after prolonged exposure of up to 90 seconds, which is well beyond our 30 second laser exposure of targeted ablation experimental design, the bulk temperature of the cell-α-PSMA-MWCNT mixture remained essentially unchanged due to the minimal remaining concentration of non-bound MWCNTs after multiple washes.

This supports our assertions of a nearfield targeted photothermal ablative strategy as being extremely effective without bulk heating, and represents a significant departure from current focal methodologies. Significant tumor cell killing without a bulk heating in the clinical setting would greatly minimize extra-cellular and tissue structure damage of patients.

2.5 Discussion

There are a number of obstacles with the current treatment options for CaP. Surgical removal of the tumor and/or the prostate itself, as well as radiotherapy including external beam radiation therapy (EBRT) and brachytherapies are all limited to early, localized stages of CaP and are often associated with serious complications, including damage to surrounding tissues, erectile dysfunctions and urinary incontinence (182-184). Biological targeting using either hormone-directed anti-androgens or androgen deprivation and chemotherapies, while effective in earlier stages, eventually leads to therapeutic resistance. The process of drug resistance is a result of extensive genetic heterogeneity in advanced disease allowing for therapeutics to initiate selective pressures on the tumor cells, where cells will often incur mutations to the target protein and hence the evolution into drug resistance tumors (185). Therefore, there is a need for a novel and selective platform for circumventing some of the problems posed with traditional approaches regarding prostate cancer treatment.

One of the methods to evade current genetic heterogeneity in CaP treatment is to promote physical damage on tumors via a photothermal approach, either in combination with

surgery or by itself. Similar to radiotherapy, physical damages exerted by photothermal bulk-heating approach is effective in ablating tumor cells in that they cause irreversible damage onto the tumor, as shown in **Figure 2.2**. Nevertheless, significant damages to nearby, non-targeted tissues and structures upon treatment still remains a major challenge. Furthermore, to achieve desired effects, different groups have reported either use of prolonged exposure time with laser, extreme high laser power, or an excessive amount of nanoparticles making it a challenge for use *in vivo* and/or clinics (169, 170, 186-188). We have comparatively summarized the use of a number of different nanoparticles in targeted and untargeted *in vitro* experiments in **Table 2.1**.

To approach these difficulties, we have developed a targeted nanoparticle approach of using a tumor specific targeting moiety conjugated to PEG-functionalized MWCNTs. Other groups have found significant non-specific binding of nanoparticles, due to lack of PEGylation (addition of polyethylene glycol), allowing for misguided non-targeted cell killing (165, 166, 168, 189-194). Almost all have not included a negative relevant control cell line to ensure specificity (165-168, 189, 194-196). Therefore, by directing energy provided from laser sources to α-PSMA-conjugated PEG-functionalized MWCNTs placed in extreme proximity to the surface of tumor cells, we have demonstrated the capacity of this platform to exclusively damage and/or destroy targeted cells upon treatment without significant bulk heating. To achieve over 80% of targeted cell ablation (approximately 240,000 cells out of 300,000 cells), only 0.33 μg of functionalized MWCNTs, that would approximately equate to 100,000 particles per cell with cells expressing approximately 180,000 PSMA surface antigens (197), were needed to be exposed by a 2.7W laser for 30 seconds (**Figure 2.5A**) without significant increase in medium bulk temperature. MWCNTs have two distinct characteristics that would allow the achievement of such significant cell ablation; first, the high thermal conductivity of the particles to generate high localize heat , and second, the

motive force of the particles upon laser exposure into the cells; thereby causing significant cell damage (198). In this regard, our nanoparticle targeted cell ablation method greatly outperforms currently available nanoparticle-mediated photothermal methods, opening up possibilities to be used for rapid and efficient tumor cell ablation with minimal damage to critical nearby tissue in effect displaying extreme nearfield efficacy. Currently available nanoparticles, including carbon nanotubes, gold nanorods, nanospheres, and nanoshells, are potent enough to raise the temperature of the medium in a short period of time by magnitudes of tens of degrees via surface plasmon resonance when exposed to laser at their peak absorption range. Nevertheless, many of these models, even if they are targeted toward specific tumor mass, may face challenges in confining heat production at the very local levels; studies show that during the photothermal treatments of the cells using the nanoparticles, the temperature of the entire field is raised by a significant amount (199-202). This could raise serious concerns about damage upon nearby, non-targeted tissue as the entire field is being affected. Our method tries to overcome this drawback by promoting target-specific attachment of the nanoparticle products to the tumor: this had led to dramatic reduction in overall heat generation of the field (**Figure 2.6**), while producing enough thermal energy at proximity to the target to induce sufficient damage on the tumor while minimizing temperature change. Moreover, almost all have not included a negative relevant control cell line to ensure specificity. Therefore, by directing energy provided from laser sources to α-PSMA-conjugated PEG-functionalized MWCNTs placed in extreme proximity to the surface of tumor cells, we have demonstrated the capacity of this platform to damage and/or destroy only targeted cells upon treatment without significant bulk heating.

Following the accomplishments of our *in vitro* cell ablation studies, an *in vivo* study is the next step in assessing the use of targeted MWCNT in delivering near-field photo-thermal damage to tumor lesions. Although a pre-clinical animal model would recapitulate

some aspects of the extensive biological and anatomical nature of living organisms, there are some inherent challenges that would need to be addressed. First, unlike the *in vitro* experiments, in an in vivo environment the tumor would be surrounded by a number of layers of cells which the stimulating laser light would need to penetrate to activate the tumor-targeted MWCNT. However, previous studies have demonstrated that a continuous 1 W/cm^2 808 nm laser can penetrate up to 6.4 cm of bovine tissue sample (203). Pulsing of the laser would achieve deeper penetration of the light. Moreover, the use of fiber optics can bring the light source in closer proximity to the tumor. Secondly, *in vivo* stability of the nanoparticle conjugate and the efficiency in biodistribution throughout the circulation would need to be evaluated. Our experiments have shown that an intraperitoneally injected untargeted fluoro-labeled antibody-conjugated MWCNT spreads throughout their body cavity with loss of signal within 72 hours of injection (unpublished data). Localization and retention of the antibody conjugated MWCNT to the directed tumor would next need to be evaluated. Lastly, *in vivo* studies would also need to consider but not limited to, cellular interactions, systemic reactions, and whole body metabolism and physiological responses (204).

While we have extensively conjugated antibodies on the surface of MWCNTs for quantification and cell ablation purposes, in theory these nanoparticles may be used as a platform for any moiety, as long as the active groups on the moiety can be exploited by the conjugating chemistry. For example, we have dual-labeled the MWCNTs with a mixture of α-PSMA and Cy5 dye, which allowed us to visualize the actual localization of the nanoparticles on the targeted cell surface. Similarly, the potential for visualization of *in vivo* localization of dual-labeled MWCNTs cannot be ignored. Theoretically, with appropriate targeting system, this platform may be used to locate not only the primary tumor site, but can be also used to identify metastatic or recurrent disease. Moreover, specifically addressing tumor heterogeneity, the possibilities can be considered that our platform has the ability to carry

multiple number of targeting molecules and pro-drugs to tumor cells. Coupling a pro-drug to the platform can limit systemic toxicities of current therapies.

Supplemental Data S1 – Expanded protocol of conjugation methodology

1. 15 mg of carboxylic group (COOH) functionalized multi-walled carbon nanotubes (MWCNT) are mixed with 240 mL of autoclaved d_2H_2O. 200 µL of polysorbate 20 (Tween-20) solution is also added as a surfactant, and the solution is topped up to 250 mL with d_2H_2O to obtain the final concentration of 60 mg of carbon nanotubes per liter. The solution is then repeatedly sonicated 7 times, in 20 minute intervals at 4°C. During each interval, 1 mL aliquots of the solution was filtered with 0.45 µm Amicron filter, and the absorbance values (measured by NanoDrop UV-Vis spectrophotometer) of filtrate was compared to the unfiltered stock solution. Finally, the MWCNT solution was filtered using a Grade 1 Whatmann paper and aliquoted into smaller fractions. .

2. 200 µL of functionalized, sonicated MWCNT-COOH (12 µg/ 0.12 pmol) are mixed with 40 µL of 20.9 mM 1-Ethyl-3-(3-dimethylaminopropyl)carbodiimide (EDC) solution in phosphate buffered saline (PBS, pH : 7.4) and 40 µL of 34.8 mM N-Hydroxysuccinimide (NHS) solution in PBS (total volume: 280 µL) and vortexed briefly. EDC reacts with the carboxylic acid groups, and NHS is added to improve the efficiency of the reaction by creating a dry-stable NHS ester that is amine-reactive at physiological pH. This linkage is zero-length, and the bond-forming reaction occurs immediately. There is sufficient EDC/NHC to activate all accessible COOH groups (there are approximately 10^5 COOH groups/ MWCNT)

3. Once NHS ester forms (MWCNT-NHS ester), 20 µL of 0.2 mM maleimide-polyethylene $glycol_{5000}$-amine crosslinker solution in PBS (Mal-PEG_{5000}-NH_2,

molecular weight 5000 g/mol) is added (4 nM) (total final volume, 300 μL). The amine side of the Mal-PEG_{5000}-NH_2 crosslinker is expected to attack the NHS ester, forming a stable, amide-bond based conjugates (MWCNT-PEG_{5000}-Mal). This reaction is given 30 minutes in room temperature to ensure completeness.

4. Antibodies of interest (that contain sulfhydryl groups –SH) are added to the solution at desired amount. The maleimide group that extends out of the activated MWCNTs specifically react with sulfhydryl groups when the pH of the reaction mixture is between 6.5~7.5, forming a stable, nonreversible thioester linkage (MWCNT-PEG_{5000}-Antibody). This reaction is left overnight in 4°C to ensure completeness. Roughly using of 10 μg of Antibody will yield 2000 antibodies per MWCNT.

5. Next day, the solution is then centrifuged at 12000g for 30 minutes and is resuspended in 300 μL PBS. The pellet is then sonicated at minimum power to ensure that the linkage does not break. Once sonicated, the solution is checked for absorbance values using UV-Vis spectroscopy. Resuspension volume is adjusted until the absorbance value is 0.03 absorbance units at wavelength of 532 nm.

Table 2.1 – Comparative table of nanoparticles for cell photo-ablation (Supplemental Data S2)

Study	Cell line	Negative Control Included?	Type of nanoparticles	Targeted ablation (moiety)	PEGylation	Type of laser (nm)	Laser power (W/cm^2)	Exposure time	Cell ablation (%)	Comments
Our current study	LNCaP	Yes	MWCNTs	Yes (PSMA)	Yes	532	2.7	30 sec	>65	Increased antibody loading onto the nanoparticle improves cell ablation efficiency.
Our previous study (205)	BCPAP	Yes	MWCNTs	Yes (TSHR)	Yes	532	2.7	30 sec	>65	Targeting antibody linked to MWCNT by thiol linkage.
Chakravarty et al, 2008 (190)	Daudi	Yes	SWCNTs	Yes (CD22)	Yes	805-811	5	7 min	~90	Cell ablation percent is approximated from graph.
Marches et el, 2009 (191)	Daudi	Yes	SWCNTs	Yes (CD22)	No	808	9.5	4 min	~90	Cell ablation percent is approximated from graph.
Shi Kam et al, 2005 (206)	FR+ HeLa cells*	Yes	SWCNTs	Yes (folate)	Yes	806-810	1.4	2 min	N/A	Numerical value of cell ablation is not included; "extensive" cell ablation observed via cell morphology changes.
Burke et al, 2009 (167)	RENCA	No	MWCNTs	No	No	1064	3	45 sec	Up to 100	No colonies formed from cells treated with MWCNTs and 45 sec of 3W laser exposure.
Hashida et al, 2014 (207)	Colon 26 Hep G2	No	SWCNTs	No	No	808	6	3 min	55.8 86.7	Concentration of 0.75 µg/mL of SWCNTs was used for Colon 26 cells, 2.5 µg/mL for Hep G2 cells.
Burlaka et al, 2010 (208)	EAC	No	MWCNTs	No	No	780-1400	3.5	1.5 min	95.2	MWCNT concentration was 0.1 mg/mL.
Mendoza-Nava et al,	HeLa	No	Gold nanospheres	Unclear (synthetic	No	532	0.65	6 min	~95	Cell ablation percent is approximated from graph;

2013 (189)				peptide)						Synthetic peptide (octreotide) used, but targeting molecule unknown.
El-Sayed et al, 2006 (209)	HSC 313, HOC 3	Yes	Gold nanoparticles	Yes (EGFR)	Yes	514	13~64	4 min	N/A	Only pictures are included, no percent cell ablation.
Boca et al, 2011 (195)	NCI-H460	No	Triangular AgNP	No	Chitosan-coated **	800	12~54	10 min	0~90	Cell mortality (%) is dependent upon the power of the laser source for a number of at least 600 cells in the irradiation spot.
Lapotko et al, 2006 (193)	K562	Yes	AuNP	Yes (CD15, glycophorin-A)	No	532	5 J/cm^2	7 min	100	Individual cells (total of 150), from a monolayer of cells incubated with gold NPs, were irradiated; W = J/s.
Xiao et al, 2009 (192)	SK-BR-3	Yes	SWCNTs	Yes (HER2)	No	808	5	2 min	~100	Cell ablation percent is approximated from graph.
Shao et al, 2007 (210)	BT474 MCF-7	No	SWCNTs	Yes (IGF1R, HER2)	Yes	808	0.8	3 min	~100	Cell ablation percent is approximated from graph.
Melancon et al, 2008 (194)	A431	No	Hollow gold nanoshells	Yes (EGFR)	No	808±10	40	5 min	~70	Cell lysis was observed via staining.
Abo-Elfadl et al, 2016 (211)	Sk-Mel-28	No	Gold nanosemicube	No	Yes	700	0.4	5 min	<60	IC_{50} in presence of laser exposure was 3.41 μg/ml.
Chen et al, 2007 (212)	SK-BR-3	No	Gold nanocage	Yes (EGFR)	Yes	810	0~1.5	5 min	~100	With increased power density, increased cell ablation (20% cell ablation at 0.9 W/cm^2 to close to 100% by 1.5 W/cm^2).
Liang et al, 2016 (213)	MCF-7	No	SWCNTs	No	Yes	808	1~2	4 min	<80	~50% cell ablation when the concentration of nanoparticle used was 50 μg/mL; ~80% when

										concentration was 400 µg/mL.
Song et al , 2016 (214)	U87MG	No	Gold nanoshell	No	Yes	808	0.125~0.5	200 sec	<90	50% cell ablation when laser power was 0.125 W/cm^2; up to 90% when power was 0.5 W/cm^2.
Liu et al, 2016 (215)	A375 HeLa	Yes	Chitosan-modified Cu_2Se	No	Chitosan-coated **	808	3	5 min	<65 <90	30% cell ablation when suggested concentration (6.25 µg/mL) was used; Maximum effects were achieved when 50 µg/mL was used.
Paholak et al, 2016 (216)	SUM159	No	Iron oxide nanoparticles	No	Polymer-coated ***	885	<0.5	10~20 min	20~95	Cell ablation efficiency dependent on length of laser irradiation.
Zhao et al, 2016 (217)	4T1 murine BC cells	No	Iron doped copper sulfide	No	Yes	1064	0.5 (Up to 1 W)	5 min	<90	At 0.5 W 5 minutes exposure, cell ablation was only around 20%.
Chen et al, 2016 (218)	HeLa	No	Graphitic carbon nanotubes	No	No	808	9	3 min	<95	Concentration of NP from 0~100 µg/mL; at 25 µg/mL killing = 45%, at 50/100 µg/mL killing up to 95%
Wu et al, 2016 (219)	4T1	No	Iron oxide nanoparticles	No	No	808	2	5 min	< 80	Concentration of NP from 0.05~0.8 mg/mL; at 0.05 killing = 30%, at 0.2 killing = 45%, at 0.8 killing = 80%
Jørgensen et al, 2016 (220)	H727	No	Silica gold nanoshell	No	Yes	807	0.58	5 min	N/A	*In vitro* cell killing not shown – *in vivo* pictures.
Li et al, 2016 (221)	CT26 TRAMP-C1 (both murine)	No	Copper nanowire	No	Yes	808	1.5	6 min	< 70	Cell ablation effective in concentrations >0.01mg/mL; 15% death at 2.5mg/mL.

Kalluru et al, 2016 (222)	B16F0	No	Graphene oxide (carbon)	Yes (folate)	Yes	808 980	0.32	15~18 min	<60 <85,	Cell killing experiments performed in two different background temperatures (37 vs 4°C), with 37°C generating stronger results.
Biffi et al, 2016 (223)	MDA-MB-231	No	Core-shell silica PEG	No	Yes	808	36	1 min	~43	
Fekrazad et al, 2011 (175)	KB cell	Yes	Au-Silica nanoshell	Yes (HER2)	Yes	820	4	2 min	>69.4	Gold-silica hybrid

* HeLa cells overexpressing Folate Receptor (FR)

** Chitosan-coated consists of chitosan (a cationic polysaccharide with low toxicity, high biodegradability and biocompatibility) flakes mixed with the nanoparticle of interest (195, 215).

*** Polymer-coated consists of diblock copolymer poly(ethylene oxide)-b-poly(γ-methacryloxypropyl trimethoxysilane), providing a core-shell structure to stabilize nanoparticles while providing platform for biomarker conjugation (216, 224).

Chapter 3: Nanomaterials in Medical Settings - A Brief Review

3.1 A Short History

Three scientists can be credited with the conceptual origin of nanotechnology. The concept nanotechnology actually goes back about six decades, when the Nobel laureate Richard Feynman brought his famous talk “There’s Plenty of Room at the Bottom” in 1959 (225). In his lecture, Feynman envisioned a world in which tiny machines or molecules are tailored to specific needs are produced and used in multiple fields including, information science, biology, chemistry, and medicine (226, 227). Despite this early insight in the world of nanoscale, the term nanotechnology wasn’t actually coined until 1974, when at a conference on production engineering Japanese scientist Norio Taniguchi used the word to describe semiconductor processes exhibiting characteristic control at the nanometer scale (228, 229). At the time, Taniguchi defined nanotechnology as a field where materials are processed, separated, consolidated, and/or deformed at atomic or molecular levels. By 1986, K. Eric Drexler had independently come up with the term nanotechnology in his book *Engines of Creation: The Coming Era of Nanotechnology*, where he outlined the potential of manufacturing of nanomaterials at the molecular level to fundamentally change the world (230). Since then, nanotechnology has become a field of highly multidisciplinary research.

Over the last few decades, the advances in the field of nanotechnology have contributed significantly in the progression of multiple disciplines, including science (biology, chemistry, medicine, and physics) and industry (consumer goods, electronics, and agriculture) (231, 232). Branching off from nanotechnology, nanomedicine has gained significant attention due to its seemingly endless potential. Currently, there are two widely accepted definitions of nanomedicine. One of the more simpler definitions of nanomedicine is described as a technology using molecular tools in the context of the current knowledge of the human body for medical diagnosis and treatment (233). The other definition of nanomedicine expands further on the initial definition by detailing the world of nanoscale and

suggesting the use of nanoscale or nanostructured materials according to their unique structural and associated functional properties for medical purposes.

At the turn of the 19th century, the concept of "magic bullet" was originally proposed by Paul Ehrlich, in which he first formulated the idea of selective targeting and damaging of the diseased or infected tissue/organs. Over the years this concept was elucidated more in various physical and biochemical principles, focusing on the development of systems that could achieve therapeutically acceptable degree of target specificity and selectivity. The contemporary definition of "magical bullet" would undoubtedly include synchronization between the active "bullet", which would be the drug, a targeting moiety such as ligands and receptors (234). This would allow specific delivery of the "bullet" to the target, and a vector, for which the drug may be loaded onto for secure delivery. While the individual components for the "magic bullet" have been available for a while, only with the recent advances in nanotechnology could all three ingredients (bullet, vector, and target) be combined.

3.2 Nanoparticles as Therapeutic Agents

Among the multiple potential uses of nanomaterials in current cancer therapeutic designs, two models stand out above others. The first model focuses in the use of nanomaterials as vectors to carry potential therapeutic molecules at the proximity to the target (235). Organic nanomaterials including but not limited to liposomes, dendrimers, micelles, polymeric conjugates, and even viruses are currently being designed as carriers that deliver and release specific anti-tumor therapeutics at the target of interest, thereby maximizing the treatment effects (235-238). The second model, which is quite discrete from the first one, employs nanoparticles (NPs) themselves as "bullets", in which the NPs are used as direct therapeutic agents against the targeted malignant cells by utilizing electromagnetic radiation at precise wavelengths (235). This includes both the photodynamic and the photo-thermal

therapy. In photodynamic therapy, photosensitizing agents that initiate a specific photochemical or photophysical reaction when absorbing light between the range of 600~800 nm wavelengths are administered (239). Once the NPs reach the target, the target region is stimulated with light at appropriate wavelength using light amplification by stimulated emission of radiation (lasers) and fiber-optic devices. The stimulated photosensitizing agent excites molecular oxygen to its singlet state ($^1O_2$), which is a highly cytotoxic reactive oxygen species, attacking any organic compound it encounters. On the other hand, while photo-thermal therapies also do require light stimulation, they extend from photodynamic therapies in the mode that damage induction is being delivered. Upon excitation by an external source of electromagnetic field such as lasers, certain metals and compounds, such as gold, graphene/carbon, silica, copper, and iron (238) have innate property of absorbing these energy at specific wavelengths and converting them into vibrational energy in the form of heat. Hyperthermia has been used previously to treat cancer patients by raising the temperature of the targeted regions up to 44°C (240-243). At such temperatures, significant and non- reversible damage to cells is exerted by means of DNA damage (242, 244), protein denaturation (243, 245), and disruption of the cellular membrane (246, 247). Expanding on this principle, photo-thermal therapy is being established as a novel therapy to induce local damage at the targeted tumor. Thus, photo-thermal therapy has gained considerable attention in cancer treatment, largely due to its superiority in specificity to the target while being less invasive compared to the currently available surgery, radiotherapy, or chemotherapy (248, 249), by only affecting the targeted region and minimizing potential side effects.

Targeting of the malignant cells by photo-thermal agents is largely achieved through the passive enhanced permeability and retention (EPR) effects or by active targeting of the tumor using specific ligands (250). EPR effects have been widely applied as a simple and efficient method of targeting tumor by exploiting the unique properties of the tumor

microenvironment (**Figure 3.1**). In the article the Hallmarks of Cancer, Hanahan and Weinberg listed "sustained angiogenesis" as a potential mechanism of tumor development (251). In most normal tissues, their blood vessels consist of capillaries that are intact and non-fenestrated, consisting of a single layer of endothelial cells with functional tight junctions (252). On the contrary, tumors inherently have leaky vasculatures due to widening of the inter-endothelial junctions, formations of fenestrations, and irregular formations of basement membranes (252, 253). These "holes" in the tumor vessels are sufficiently large enough, allowing for therapeutic agents to accumulate at the site much more rapidly than at normal cells (**Figure 3.1A**). A dysfunctional lymphatic drainage system is another unique feature of tumor microenvironment. Combined, the presence of leaky vasculatures and lack of lymphatic drainage system promotes the accumulation and retention of therapeutic photo-thermal agents to reach and be retained at the tumor interstitum more readily (234, 250, 252). Nevertheless, a prerequisite for passive targeting by EPR effects is to ensure that the half-life of the photo-thermal agents in circulation is sufficient for them to reach and accumulate at the tumor site. One way to enhance the half-life of the NPs is to attach amphiphilic polymers such as polyethylene glycol (PEG) chain on their surface, a process known as PEGylation (234, 252, 254, 255) (**Figure 3.2**). The PEG shell on the surface of a coated NP would repel plasma proteins such as opsonins from binding, thereby preventing microphage action and allowing the agents to stay in circulation for an extended period (256-258). This extension would then permit sufficient amount of photo-thermal agents to accumulate on the target for potential therapy.

The fundamental principle of the EPR effect is dependent on the passive accumulation of NPs to tumor. Furthermore, the specificity of tumor targeting may be dramatically enhanced by employing a specific recognition mechanism in which moieties such as ligands or receptors specific to the tumor are used. This strategy may include ligand-

or receptor-mediated targeting such as monoclonal antibody-mediated targeting (194, 205, 259), peptide-mediated targeting (260-263), aptamer-mediated targeting (264-266), folate receptor-mediated targeting (267, 268) and more (**Figure 3.1B**). When combined with the EPR effect, this active targeting strategy may be employed to further increase targeting specificity, selectivity and accumulation of the photo-thermal agent while reducing potential cytotoxic side effects by reducing non-specific interactions with non-targeted tissue and cells.

Once the photo-thermal agents successfully accumulate at the tumor site, the next step in photo-thermal therapy is to irradiate the region with electromagnetic radiations using light sources, using laser devices. Upon exposure to the light sources, the free electrons on surface of the agents collectively oscillate in resonance with the incoming light, causing the electrons to resonate and make transitions from the ground state to the excited state (269-271). This resonance, referred to as surface plasmon resonance (SPR), is dependent on the size, shape, and the dielectric constants of both the agent and the surrounding materials (271). The collective oscillation of conduction electrons causes strong plasmonic electromagnetic field on the surface of the excited material, which provides unique optical properties such as optical absorption and surface enhanced Raman scattering (SERS) that may also be used for applications in theranostics/imaging (272). For the purposes of photo-thermal ablation, the excited surface electrons subsequently relax to the ground state through non-radiative decay channels, thereby increasing their kinetic energy to cause the heating of the local environment, which may be directed toward destroying tumor cells.

Many bulk metals exhibit this plasmonic behavior, yet the range in which plasmonic properties are observed is very narrow in the visible spectrum, limiting their potential use in photo-thermal therapy (273). The agents that are used for photo-thermal therapy often include gold, carbon, and iron-based nanomaterials. These materials not only have highly efficient

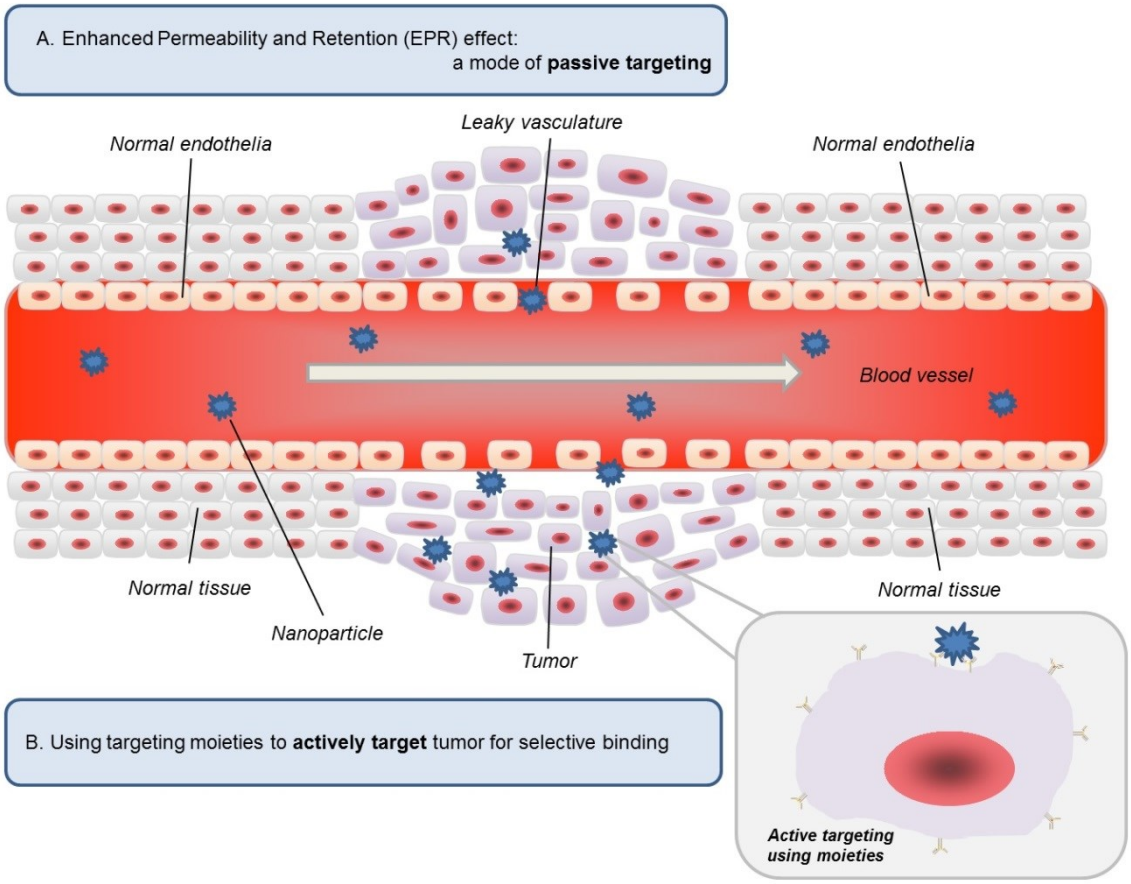

Figure 3.1 EPR effect versus active targeting of the tumor. Unlike normal tissue that have tight endothelia surrounding the vasculature, tumors have are fenestrations along the blood vessels (leaky vasculature), which allow molecules (including therapeutic agents such as nanoparticles) to access at the site of tumor growth more readily in a form of passive targeting (Figure 3.1A). This is known as the enhanced permeability and retention (EPR) effect. In addition, by employing an active targeting strategy in which targeting moieties specific for the tumor mass is added onto the therapeutic agent, a therapeutic effect that is exclusive only to the tumor may be observed (Figure 3.1B).

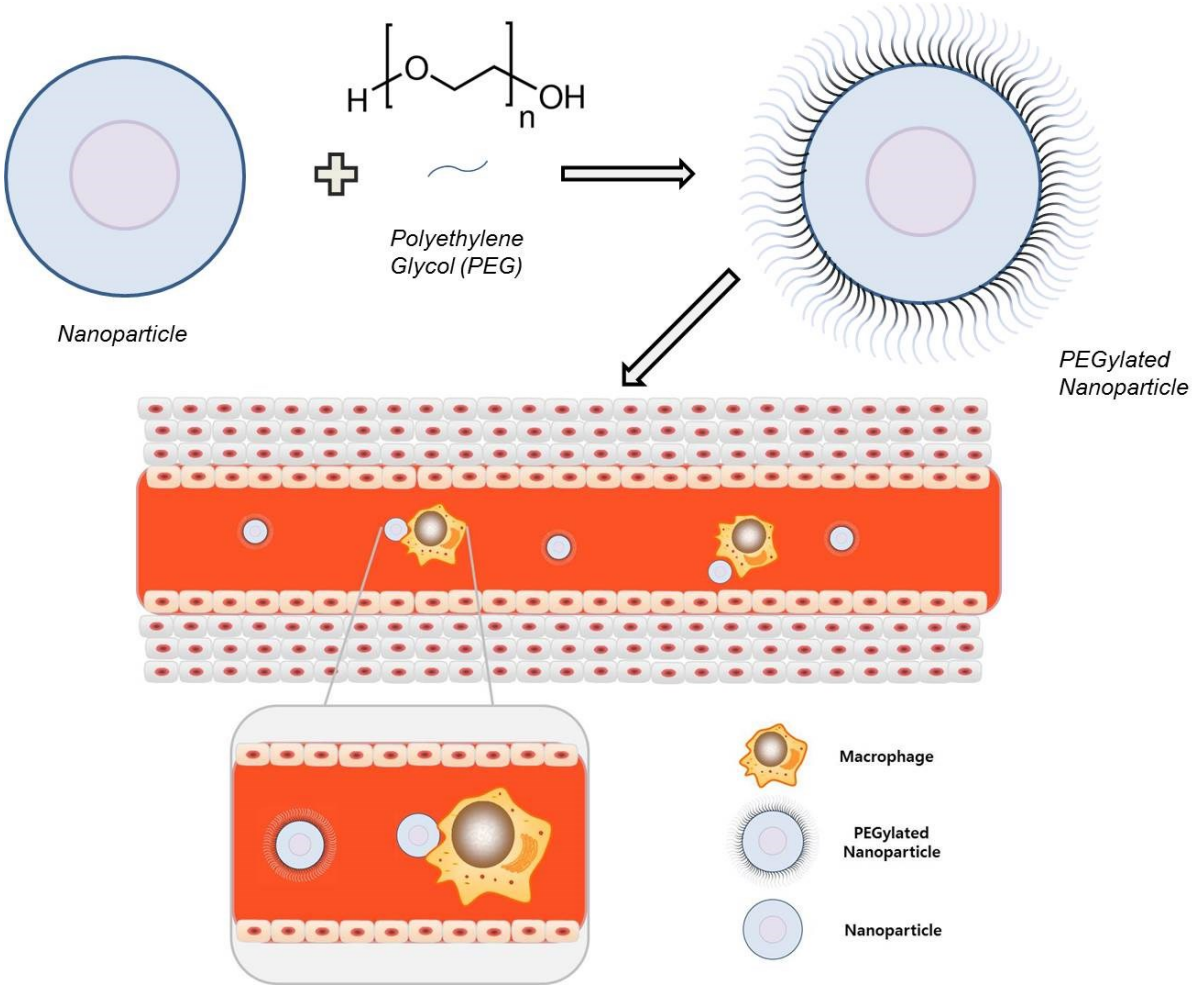

Figure 3.2 PEGylation and improved circulation of nanoparticles. Although nanomaterials that are tested for therapeutic effects are small enough in size (in the range of nanometers up to a micron), these materials often face challenges in *in vivo* environment such as weak solubility, short circulation life, and toxicity. By attaching biologically inert polyethylene glycol chains on the surface of these nanoparticles, the nanoparticles are then "masked" from the immune system, hence reduced immunogenicity and antigenicity, as well as prolonged circulatory time which allows the nanoparticles to reach to the target of interest.

light-to-heat conversion profiles, they also have strong absorption properties in the visible and near infrared (NIR) regions of the light spectrum (269). This becomes a critical condition in the selection of photo-thermal agent in clinical settings when considering the ability of lasers to penetrate tissue and reach the agents to induce therapeutic effects. Light at the NIR spectrum is considered as ideal for photo-thermal therapy, as at this wavelength the light experiences minimal absorption from tissue chromophores and the aqueous environment (274, 275). Additionally, these nanomaterials may be engineered to optimize various optical properties by modifying their size and surface functionalization, further justifying their use in photo-thermal approach (276, 277). Therefore, gold, carbon, and iron-based NPs and their role in nanomedicine will be described in the subsequent sections.

3.3 Carbon-based Materials

Carbon-based materials, including graphenes and carbon nanotubes (CNTs), offer a unique combination of physical and chemical properties that make them an ideal candidate for photo-thermal therapy. While they are very small (ranging from few nanometers up to a micrometer (278)), their primary advantage is that they have extremely large surface area available for chemical functionalization (238, 279, 280). By applying appropriate chemistry such as direct conjugation, linker chemistry, and noncovalent interactions such as pi stacking and hydrophobic interactions, may be used as a platform on which targeting moieties such as antibodies, aptamers, peptides, and small molecules may be conjugated onto (264, 281-285) or may also be used as vectors to load and deliver anticancer agents of interest such as drugs, genes and proteins to the specific site of interest (238). Secondly, these materials are known for their efficient absorption in the NIR regions (286, 287). Once light at the NIR regions is absorbed, the carbon materials readily convert the external irradiation into heat, which may be directed within a specific region for therapeutic effects. Often, covalent functionalization

by PEGylation is performed on the surface of the carbon-based materials, which allows these aromatic NPs to exhibit hydrophilic properties as well (288). The length of the PEG chain has been positively correlated with the circulation time in both graphene and in CNTs (288).

3.3.1 Graphene

Graphene consists of a single layer of sp2-bonded carbon atoms that are packed into a unique two-dimensional honeycomb crystal lattice (280, 289). Graphene oxide (GO), a derivative of graphene, is in particular considered for biomedical applications due to the ease of preparation (290) and its richness in functional groups and extensive surface area availability (279, 291). Before the layers of graphene were discovered and isolated from graphite crystals and shown to have unique electrical, optical, chemical and mechanical properties, it was merely regarded as a part of the graphite's crystal structure (292-294). Nevertheless, in the recent years, the exceptional properties of graphene sheets have begun to threat the dominance of CNTs in the potential biomedical applications. Graphene, especially in the PEGylated forms, are reported to have lower *in vitro* cytotoxicity compared to CNTs (295).

The planar structure, availability of functional groups such as epoxy bridges, hydroxyl and carboxyl groups, and the abundance of delocalized pi electrons in GO sheets endow them with an outstanding ability to immobilize different substances, including drugs, ligands, and fluorophores for theranostics purposes (296, 297). The large surface area of graphene also allow for surplus availability of pi electrons, which can used to form pi stacking interactions available to some aromatic anti-cancer drugs, including doxorubicin and camptothecin (298). Furthermore, while GO generally have hydrophilic edges due to the presence of oxides from oxidation of graphene to enhance solubility, they also have hydrophobic basal plane that may be exploited for hydrophobic effect, thus enhancing

graphene-drug interaction by hydrophobic interactions. The loading capacity and the release of these anti-cancer drugs are found to be dependent on the hydrogen bond formed between the hydroxyl and the carboxyl group of the GO and the amine groups on the drug, as well as the pH of the environment (299, 300). Once administered and delivered to the targeted cell, there are two proposed routes of internalization, of one is energy-dependent endocytosis or phagocytosis, and the other being energy-independent direct penetration into the target cell (288, 301, 302). Some suggest that the GO-based NPs enter cells only through the energy-dependent endocytosis, based on the lower cytotoxicity observed in cells by GO-based NPs compared to the cytotoxicity profiles observed with CNT-based NPs (303). Lastly, targeting moieties specific for the tumors may also be engineered onto the surface of the NPs, promoting further specificity in drug delivery thus minimizing potential cytotoxic side effects on non-cancerous cells.

The potential of GO and its derivatives as a photo-thermal agent has also been evaluated in recent years. Combined with the strong NIR optical absorption capacity, efficient thermal conversion, and potential tumor-targeting specificity, GOs have become a strong candidate for such methods. First *in vivo* study using PEGylated GO-NPs in photo-thermal therapy was performed in 2010 (304). In this study, 4T1 breast tumor xenograft mice were injected with the NPs intravenously via passive targeting (EPR effect) of the tumor. Once the NPs had accumulated at the tumor site, as confirmed by fluorescent labeling, the tumor mass was irradiated with an 808 nm laser for 5 minutes at power of 2 W/cm^2. The investigators found that 100% of xenograft tumors were eliminated post-treatment, indicating the effectiveness of GO NPs as *in vivo* photo-thermal agents. To complement these results, a similar ultra-small reduced nano-GO (nRGO-PEG) were prepared, in which the PEGylated GO NPs were reduced again before being re-coated with PEGylated phospholipid (305, 306). The additional reduction of the GO NPs “cleans” residual functional groups from the surface,

yielding a GO product with higher optical potential and enhanced NIR absorbance (279). These nRGO-PEG were also conjugated with an Arg-Gly-Asp peptide to encourage selective cellular uptake to targeted U87MG glioma cell lines. This improvement in surface modification by reduction methods has undoubtedly improved tumor ablation efficiency *in vivo*, as when compared to the initial experiments; the injection of nRGO-PEG into 4T1 breast cancer xenograft tumors resulted in complete ablation in 5 minutes with an 808 nm laser needed only 0.15 W/cm^2 (versus 2 W/cm^2) of laser power (306). The ability to achieve complete therapeutic effect using a very low optical power is beneficial not only in minimizing nonspecific damage on untargeted tissues, but also in improving treatment efficacy when applied to larger or internal tumors.

3.3.2 Carbon Nanotubes

CNTs are well ordered, hollow, carbon graphitic nanomaterials with cylindrical structures consisting of a single (single-walled) or multiple layers (multi-walled) of graphene sheets rolled at specific and discrete angles (280, 307) (**Figure 3.3**). First discovered in 1991 by Sumio Iijima, CNTs have since then gained a reputation in biomedical fields based on their unique structures and properties, including strength and size (stability, high aspect ratio, and large surface area)(238, 278). Typically, CNTs are available in single-walled (single walled carbon nanotube, SWCNT) or multi-walled (multi-walled carbon nanotubes, MWCNT, consisting of several layers of carbon sheets rolled in concentric layers) forms, depending on the method of synthesis (308, 309). Both forms have been regularly used for biomedical purposes, and although there has not been a conclusive conclusion on which form is better for biomedical purposes, there are indications on which form may be more suitable for specific purposes (310). For example, SWCNTs, consisting of a single layer of rolled graphene sheet, boasts a large spatial surface area (up to 1300 m^2/g in SWCNT versus few hundred m^2/g in

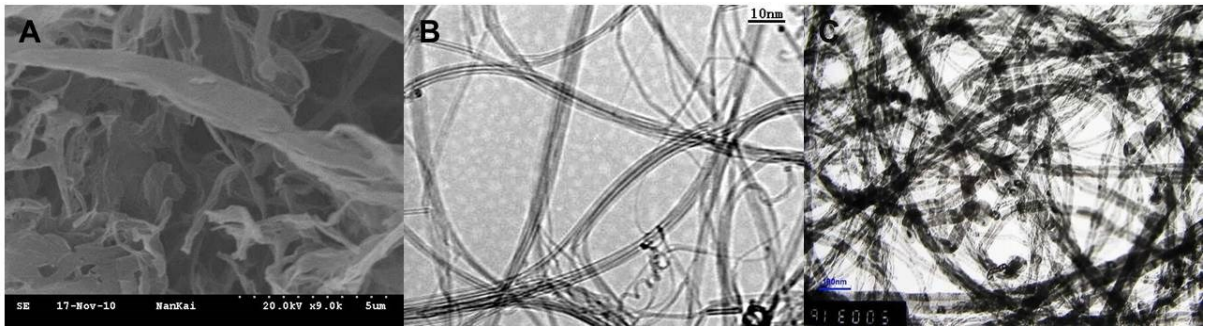

Figure 3.3 Carbon-based nanoparticles. Figure 3.3A displays graphene oxide. Figure 3.3B displays single-walled carbon nanotubes. Figure 3.3C displays multi-walled carbon nanotubes.

The figures are adopted from http://www.cheaptubes.com (311)

MWCNT (312)) for which therapeutic agents may be loaded onto effectively. Furthermore, thanks to the hollow inner structure, drugs may be incorporated into the inner cavities of the CNTs, which allows protection of unstable drugs from the biological environment and controlled drug release depending on the tube diameter (313, 314). On the other hand, MWCNTs have more defects in their structure during synthesis compared to SWCNTs, which ironically would make surface functionalization and modification more accessible (310).

As previously mentioned, the potential CNT cytotoxicity associated with cellular penetration is the one of the biggest challenges in the use of CNTs in clinical settings. Because of their innate hydrophobicity, CNTs regularly aggregate into bundles when suspended in an aqueous environment, and must be dispersed prior to *in vivo* applications. Surface modifications of CNTs by acid oxidation may introduce functional groups such as carboxyl, phenolic, and lactone groups on their surface by weakening the graphenic backbone (315). This allows polarization of the molecule and therefore enhances stability of CNTs in aqueous solution. If functionalized for water-solubility, CNTs have been observed to clear away from circulation within few hours, with no specific organ accumulation. Carboxylated SWCNTs are naturally degraded naturally within 90 days by phagolysosomal simulant fluid, avoiding any long term accumulation in organs (316). Further modification with PEG chains enhances length of stay in circulation. Longer PEG chains on the CNTs grant superior circulation, as less NPs coated with PEG5400 are observed to being removed from circulation by the reticuloendothelial system (RES) compared to the PEG2000-coated ones (317).

The concept of CNT-mediated drug delivery to tumor targets is not so different from graphene-mediated drug delivery. Because both graphene and CNTs are carbon-based materials, they share similar electrical and chemical profiles. The aromatic rings allow both pi stacking and hydrophobic interactions, which are two crucial noncovalent interactions essential for NP-drug binding. Similarly, CNTs can also be used as a scaffold to carry drugs

that often by themselves have narrow therapeutic window due to toxicity or those that may accelerate development of resistance due to non-specificity (238, 285). Classes of anticancer agents that have been loaded onto CNTs for targeted delivery include topoisomerase inhibitors (camptothecin family of drugs) (318, 319), anthracyclines (DNA intercalators such as doxorubicin) (320-322), platinum-based drugs (DNA chelators such as cisplatin and carboplatin) (323, 324), antimetabolites (disrupts metabolic pathways during the formation of nucleic acids in cancer cells, including antifolates methotrexate and purine/pyrimidine antagonists such as 5-fluorouracil and gemcitabine) (325-327), and antimicrotubules (taxane family of drugs) (328, 329). Once the CNT-drug complex reaches the tumor mass via active or passive targeting, the complex is internalized and the drug load is released (285). Several mechanisms have also been proposed for this enhanced cellular uptake of CNTs, including, energy-dependent, receptor-mediated endocytosis (285, 330). On the other hand, internalization of the CNTs may also occur across the cell membrane in an energy-independent, passive manner through diffusion or penetration (287, 331, 332). Based on their small size (sub-1 μm range) and needle-like shape, SWCNTs may penetrate across the membrane without energy expenditure by "piercing" the cell (333). Penetration into the cell membrane via this "piercing" process has been suggested as a mechanism for the cytotoxicity associated with CNTs. However, further investigations are required to fully understand the effects of internalization and cytotoxicity associated with the carbon-based nanomaterial.

Similar to graphene, CNTs also have distinct properties that make them an ideal candidate as photo-thermal agents. First, they efficiently convert NIR radiation into heat (287). It has been reported that exposure of CNTs to high pulse energy laser leads to a dramatic increase in the temperature the degree of few thousand degrees within microseconds (334, 335). Furthermore, unlike many bulk metals, CNTs also possess a very broad electromagnetic absorbance spectrum covering both NIR I and II windows ranging from 650

nm to 1350 nm, which is the ideal range for efficient tissue penetration (274, 275, 336). Therefore, the photo-physical properties of CNTs may be engineered according to the "nano-antenna effect", by tailoring the size (diameter and length) and wall number of the tube yet still retaining their unique wavelength-thermal conversion efficiency required for effective photo-thermal therapy (337). The initial study on photo-thermal ablation of tumors using CNTs was performed in 2005 by targeting the folate receptors in HeLa cells (206). Confocal fluorescence microscopy confirmed that upon reaching the target, the functionalized CNTs were internalized and that 5 minute exposure to an 808 nm laser with power of 3.5 W/cm^2 was sufficient to inflict irreversible damage on the tumor. Since then, different strategies have been employed to further optimize CNTs photo-thermal efficiency. Cancer-specific antibodies such as α-IGFR1 or α-HER2 (210) or cell-specific α-CD22 and α-CD25 targeted antibodies (190) have been used to achieve a more selective cell ablation effect in both *in vitro* and *in vivo*.

3.4 Gold-based Materials

The use of gold (Au) in therapeutic practices have first been reported centuries ago (338). Nevertheless, the therapeutic usage of gold in modern standards was adopted only following the advance of chemistry and nanoscience in the 20th century (338, 339). The unique physical and chemical properties of Au-NPs, including chemical inertness (340-342), electronic (343), optical (343-345), and surface properties (346-348), all point toward their applications in biological and clinical studies. Among multiple types of Au-NPs that are currently studied in the photo-thermal approach of cancer research, Au-nanoshells, Au-nanorods, and Au-nanocages are most actively investigated (**Figure 3.4**). All three of these Au-NPs have been reported to raise temperatures by more than 20°C when irradiated by a 805 nm laser at a power density of 0.8 W/cm^2 for less than 10 minutes (349). The shape and

size of these Au-NPs may be altered to shift the peak absorbance range at the NIR. As mentioned earlier, NIR light has distinctive advantages in potential clinical researches for avoiding *in vivo* autoflourescence and tissue absorbance at the wavelength range of 270~665 nm, allowing efficient penetration through tissues (203, 269, 350, 351).

3.4.1 Gold Nanoshells

First discovered by the Halas group from Rice University in 2003, the Au-nanoshells (GNS) are spherical NPs that consist of a dielectric core (usually silica-based), which are covered by a thin gold shell (352, 353). When irradiated by electromagnetic radiation, the outer gold and the inner core demonstrate plasmon hybridization, where the metal electrons collectively oscillate between the layers, resulting in plasmon resonance (352). Subsequently, once the electrons on the surface relax back to the ground state, heat is released into the surroundings (354). The ratio of the radius of the dielectric core to the thickness of the shell may be optimized, allowing fine-tuning of optical resonances (273, 351).

The first generation of GNS produced did not have a specific target moiety (273). Human breast epithelial carcinoma SK-BR-3 cells were used as the positive control in which these cells were incubated with the GNS and were irradiated with NIR laser at 820 nm wavelength (35 W/cm^2 *in vitro* for 7 minutes, 4 W/cm^2 *in vivo* for up to 6 minutes) to achieve cell ablation effects *in vitro*, or initiate an increase in temperature that may induce irreversible tissue damage *in vivo*. In these xenograft studies, targeting of the tumor by the nanoshells was entirely dependent on the passive EPR effect. To elaborate on tumor targeting, an active approach was utilized by using specific ligands such as antibodies against cell lines that express tumor marker receptors. The Halas group was able to improve on their original

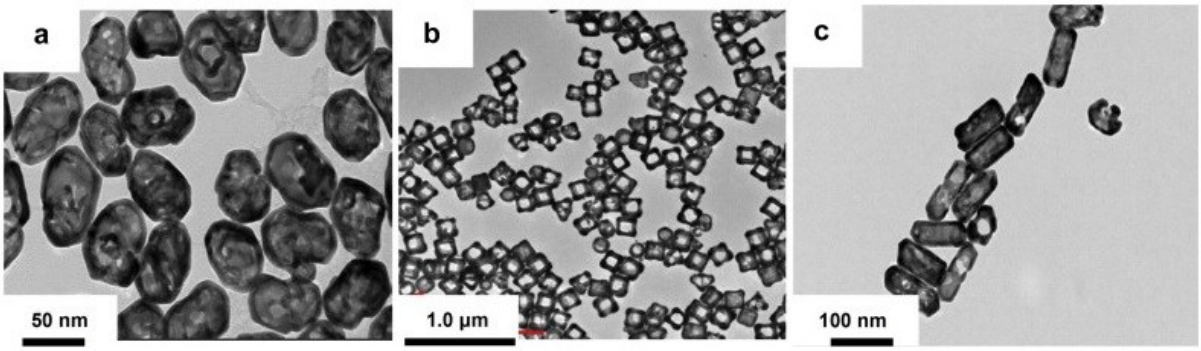

Figure 3.4 Gold-based nanoparticles. Figure 3.4A displays gold nanoparticles-in-shell. Figure 3.4B displays gold nanocages. Figure 3.4C displays gold nanorods-in-shell.

The figures are adopted from "Gold nanoshells-mediated bimodal photodynamic and photothermal cancer treatment using ultra-low doses of near infra-red light" (355)

design of GNS by using a heterobifunctional PEG linker (OPSS-PEG-NHS), in which α-HER2 was attached to the linker through the NHS group, and the thiol group present in OPSS was conjugated onto the surface of the GNS (196). The viability of HER2-expressing SKBr3 cells after GNS treatment and laser irradiation was evaluated using calcein staining, with cytotoxic effects only observed in α-HER2-treated cells that and not in any other conditions. In other studies, epidermoid carcinoma A431 cell lines that overexpress EGFR were also targeted using monoclonal α-EGFR[C225] and tested for photo-thermal efficiency *in vitro* (194). In the same study, the antibody-labeled GNS were also injected into mouse models and the biodistribution patterns of the GNS were evaluated. These studies confirmed death of targeted tumor cells using laser powers and wavelength comparable to abovementioned experiments. Other groups have used other targeting moieties such as adenovirus vectors (356), folate receptors (357, 358), aptamers (359, 360), peptides (260), and others for theranostic/imaging purposes. Lastly, GNS have been used as carriers to deliver anti-cancer agents such as doxorubicin (361, 362), camptothecin (363), taxol agents (260, 364), and others to achieve simultaneous chemotherapeutic and photo-thermal effects and further improving therapeutic outcomes.

3.4.2 Gold Nanorods

Unlike other gold NPs, the synthesis of gold nanorods (GNR) is unique in that it requires the use of cetyl-trimethylammonium bromide (CTAB) as a surfactant (365, 366). Surfactants such as CTAB are employed to maintain the shape of the nanorods and to prevent aggregation (367). However, as CTAB has potential cytotoxic effects it must be removed from the GNR solution to also for functionalization the nanorods and enhance its biological capabilities (352, 367, 368). Most often, free CTAB in the colloidal GNR solution is washed away and the nanorods are functionalized on the surface with thiol-PEG (PEG-SH) (365).

PEGylation of the GNR improves their biocompatibility and circulation time. GNRs behave similar to other Au-NPs, except their modified size optimizes their peak absorption and scattering characteristics (352). Furthermore, GNRs are reported to be more efficient than GNSs due to their polarization properties (367). Following standard seed-mediated growth protocols for the synthesis, GNRs in the size range of 10-100nm are synthesized, which are generally smaller than the larger Au-coated GNS (100~150 nm) (369-371). While smaller particles such as GNRs could produce the highest transduction efficiencies, larger particles such as the GNS may satisfy the thermal requirements required for photo-thermal ablation in smaller quantities(370). Therefore, according to the specific conditions and requirements, different Au-NPs may be employed. Since replacing citrate with CTAB during the GNR synthesis, El-Sayed group has engineered multiple types of GNRs according to size, optical properties, and surface functionalization to optimize photo-thermal ablation. The strategy of active targeting of the tumor was employed by conjugating α-EGFR on the nanorods, allowed them to bind to the targeted tumor surface with high affinity (372). Excitation by 10 W/cm^2 laser at 800 nm for 4 minutes was sufficient to ablate targeted tumor cells, while twice the power (20 W/cm^2) was required to illicit any damage to untargeted control cells (372). Another group injected GNRs directly in a mouse sarcoma model and confirmed tumor ablation *in vivo* (373). The mice were injected with PEGylated GNRs, and did not show any signs of distress or toxicity. Subsequently, the mice also received electromagnetic radiation at the power of 1.6 W/cm^2 for ten minutes, and observed internal tumor temperature was raised up to 46.3°C; more than sufficient temperature rise to inflict damage on the tumor and cause cell hemorrhage.

Recently, instead of washing away the residual CTAB, some groups have attempted to develop polymersomes to modify GNR surface by electrostatic absorption (374). These polymersomes are formed by the self-assembly of amphiphilic block copolymers according

to their appropriate hydrophilic/hydrophobic ratios(375). Based on the hydrophobic interactions, hydrophobic molecules may be integrated within the layer of the polymersome (376, 377). Within this layer, antitumor drugs such as doxorubicin may be released from the polymersome by temperature changes induced by irradiated GNRs. This would allow targeted delivery of the drug, greatly improving drug release efficiency as lower drug doses would then be required to achieve similar therapeutic effects. Applying these principles to mouse models, doxorubicin-conjugated polymersome coated GNRs were injected into the xenografts and were exposed to laser treatment for 5 minutes at 2.5 W/cm^2. As expected, in the mice that received the combined drug-photo-thermal treatment, the tumor was completely removed at the xenografted location (374). Furthermore, some of the mice in the control groups that either received doxorubicin or the GNR alone showed tumor recurrence, which advocates the effectiveness of the combined chemo- and photo-thermal strategy in approaching cancer treatment when compared to the stand-alone approaches.

3.4.3 Gold Nanocages

Gold nanocages (GNC) are another class of Au-based NPs with relatively small size (~45 nm in edge length) that are actively being studied for the use in photo-thermal ablation and drug delivery (352, 378, 379). They were first synthesized in 2005, with the main challenge of overcoming the shortcomings inherent with GNS and GNR (379). The GNS first developed by the Halas group had a core diameter around 110 nm with the surrounding gold shell around 10 nm thick, which is large when compared to GNC. On the other hand, while GNRs have smaller size in the sub-100nm range, the large dependence on surfactants such as CTAB during the particle synthesis remains a major challenge as these surfactants are toxic and must be removed if to be used *in vivo*. GNCs are characterized by their hollow interior structures and porous holes, which may be exploited during encapsulating processes for

targeted drug delivery (272, 378, 380). Furthermore, similar to GNSs and GNRs, GNCs can be tailored to exhibit localized surface plasmon resonance (LCPR) peaks in the NIR region, allowing efficient photo-thermal conversion based on strong optical absorption and high Raman enhancement (272, 379). Currently, several GNCs targeting surface receptors of breast cancer cells (379) or transmembrane proteins of cancer stem cells (381) have been formulated. Similar to previous methods, the GNCs need to be PEGylated to extend circulation time, and can also be conjugated with different targeting ligands to selectively target tumor cells. Unlike GNS and GNRs that required stronger power intensity in the range of 10s of W/cm^2 at ~800 nm, which is far beyond the tolerable laser power intensity to be used on skin at this wavelength (382), photo-thermal ablation with GNCs only require electromagnetic radiation of 1.5 W/cm^2 over 5 minutes to accomplish efficient cell ablation (379). Since then, other groups have improved on the use of GNCs in photo-thermal therapy by making modifications to the initial GNC synthesis protocols. A combinatorial approach was designed in which cationic mammalian-membrane-disruptive peptide cTL (CFVQWFSKFLGRIL-NH2)-GNC hybrid was prepared and administered into mouse models to achieve dual photo-thermal- and cytotoxic effects (261). Compared to the stand-alone treatment of cTL peptide, the use of cTL-GNC hybrid photo-thermal therapy at 0.4 W/cm^2 850 nm wavelength laser exposure for 5 minutes resulted in a dramatic improvement in tumor ablation efficiency, with 61% cell ablation using irradiated cTL-GNC versus 20% cell ablation in cTL alone trials. Similarly, double-walled GNC/silica nanorattles were prepared to enhance stability, biocompatibility, and drug-loading capacity of GNCs by creating a more extensive surface area in which molecules of interest may be conjugated onto, including ligands such as Tat peptide to promote cell internalization or antitumor drugs such as doxorubicin (272). These modifications permit even further reduction of laser power in achieving comparable ablation effects. When combined with doxorubicin, these double-

walled GNC/silica “nanorattles” required 10 minute exposure to laser at power of only 0.12 W/cm^2 to achieve up to 80% cell ablation. Lastly, another model was arranged in which aptamers against prostate specific membrane antigen (PSMA) were prepared as a targeting ligand to a GNC-single walled carbon nanotube (SWCNT) hybrid (265). Once incubated with the tumor cells, the GNC-SWCNT complex was excited with 1064 nm wavelength laser at 1.5 W/cm^2 for 10 minutes. Compared to standalone GNRs functionalized with PSMA aptamers against LNCaPs (2% cell ablation), the GNC-SWCNT complex showed superior cell ablation efficiency under the same conditions (95% cell ablation).

3.5 Iron-based Nanoparticles

Compared to the previous nanomaterials, iron NPs (Fe-NPs) open up a new window in cancer therapeutics. While the discussion of carbon- and gold-based materials have focused on their ability to load drugs and produce efficient photo-thermal conversion upon irradiation, Fe-based NPs also exhibit what is known as superparamagnetic properties that could be exploited for biomedical applications (383, 384). One of the most common uses for the superparamagnetic properties of Fe-NPs is as contrast agents in magnetic resonance imaging (MRI) (385, 386). It has been reported that approximately 35% of clinical MRI scans require contrast agents to improve the sensitivity and accuracy of the imaging (387), and as such contrast agents based on iron oxides such as magnetite, maghemite, or hermatite have been widely used to aid imaging and diagnosis of lesions during MRI(388, 389).

Furthermore, the use of iron oxides is not limited to imaging purposes. Iron oxides make up the core in iron oxide NP (IONP) formation, which are known to be used for photo-thermal therapy, drug delivery, and hyperthermia therapy (383, 390). Although the light absorbance of IONPs in the NIR region is not as profound as other plasmonic NPs such as carbon or gold, appropriate surface modifications may make up for this (391). Using IONPs

that were modified with carboxymethyl chitosan (392), PEG (393), or were transformed into Prussian blue NPs by reacting with potassium ferrocyanide (394), resulted in efficient cell ablation after irradiating them with laser at power up to 5 W/cm^2 (exact cell ablation numbers not reported in the articles). Furthermore, by combining the photo-thermal capabilities of IONPs with their magnetic properties, a cumulative and potentially synergistic effect was observed, where cell viability of the dual photo-thermal and magnetic hyperthermia resulted in cell viability of 14±7%, compared to only 74±15% with just magnetic hyperthermia and 36±3% with laser treatment only (391). In such scenario, the power of electromagnetic radiation required was also reduced dramatically from the abovementioned ranges to 300 mW/cm^2 at 808 nm wavelength, which is within the guideline suggested by the Laser Institute of America, is safe use of a laser against cutaneous tissues (395).

IONPs have also been used as nanocarriers in targeted drug delivery systems. Similar to other NP-based drug delivery, anti-tumor agents such as doxorubicin have been loaded onto the surface of the particles. They are also often PEGylated to enhance *in vivo* biocompatibility and stability (396). What makes IONPs unique from other nanovectors is the application of magnetic field on the target site to guide them toward the tumor region (397). In addition to the EPR effect, the magnetic-field-directed targeting of tumor further improves therapeutic efficiency. Simultaneously, during these transfers, MRI may be used to track the movement of the NP complexes in circulation.

Lastly, hyperthermia therapy with IONPs is distinct from the photo-thermal therapies for the use of oscillating magnetic fields to stimulate IONPs, which would then subsequently leads to generation of heat. The heat generation of superparamagnetic IONPs depends on the strength of the magnetic field, magnetic properties and size of the NPs (384, 396). If the diameter of IONP applied is smaller than 100 nm, heat is produced due to the friction induced from oscillating IONPs according to the magnetic field gradient. On the other hand, for larger

IONPs, heat is rather generated by the rotation of the magnetic moment at each field oscillation (398-400). Comparing magnetic hyperthermia therapy with photo-thermal approach, the magnetic field that is used to excite IONPs may penetrate tissue more efficiently than light in NIR range used for photo-thermal ablation (286, 401). On the other hand, due to slower heating rate, hyperthermia treatment in general requires longer and repeated exposure with magnetic field compared to the length of laser irradiation required for photo-thermal ablation. This extended treatment results in a significant thermal diffusion from the area of exposure, which may induce non-specific damage onto nearby normal tissues (402). Furthermore, because of the strong magnetic field applied, metallic materials around the region of treatment must be removed or avoided from the magnetic exposure. Despite this room for improvement, hyperthermia therapies using iron-based NPs have been extensively studied and have undergone/are undergoing human clinical trials for safety and efficacy evaluations (403-406).

3.6 Potential Translation of Nanoparticle Therapeutics into the Clinic

Up to now, the basic therapeutic applications and research potentials of nanomaterials in *in vitro* and pre-clinical *in vivo* settings were discussed. Nevertheless, medical researches aim to translate the potential pre-clinical innovations into clinical settings, with the ultimate objective of providing patients with essential care. Over the last few years, the unique plasmonic properties of the abovementioned NPs were applied for theranostic purposes. By labeling the NPs with contrasting agents, the use of NPs open up possibilities in imaging modality by allowing physicians to identify clearly and obtain better understanding of the treatment region. However, cancer is a heterogeneous disease. Tumor heterogeneity encompasses more than distinct morphology and phenotype, but also includes variabilities in gene expression, metabolism, motility, proliferation, and metastatic potential (407-409).

These variations may occur between different tumor masses (inter-tumoral) and/or within the single tumor mass (intra-tumoral). The heterogeneitic nature of cancer, including both inter-tumoral (410-412) and intra-tumoral (411-416), has been well described in the literature. Nevertheless, as a result of next generation sequencing technology the extensiveness of somatic DNA alterations being reported in tumors, in numbers much higher than what was originally anticipated (156, 417-419). Thus, the heterogeneitic nature of tumors still remains to be the principal challenge in cancer treatment as individual tumor cells may develop distinctive, yet functionally critical features that promote cancer progression and adopt a unique pathophysiology (413). This, in turn, would lead to a "tug of war", where development of a unique, comprehensive treatment regime would be required to address the malignant expansion of new tumors. Another potential challenge in cancer treatment is the presence of shared traits and mutations between tumor foci and tissue samples that are histologically "normal". Multifocal tumors, such as CaP, by definition, are often identified to be genetically distinct from each other. Nevertheless, this intra-patient heterogeneity of non-driving somatic mutations common in both malignant and normal tissue samples complicate the use of biological targeted treatments, as the difficulty in characterizing the dominant biology of patient's cancer is multiplied. This is especially critical for the use of NPs as precision focal therapy agents in delivering therapeutic effects to the targeted area and preventing damaging nearby tissue.

Currently, there are number of ongoing clinical trials using iron oxide contrast agents to improve the quality of MRI (ClinicalTrials.gov Identifier: NCT01895829, NCT02744248, NCT02511028, NCT01815333). It remains to be seen whether these NPs are approved, as previously available iron oxide contrast agents such as ferumoxides (Feridex) and ferumoxsil (Gastromark) has been discontinued from clinical use in the U.S. due to regulatory and marketing concerns (420-422).

The concept of improving the therapeutic index by delivering the drug molecule near the tumor mass, especially in regards to clinical environment, has been formulated for a while. This idea was impaired by the method of delivery, where the presence of the immune system restricts extended stay of foreign molecules in circulation as well as the limitations in selective targeting of the tumor mass. Both challenges were approached by the use of nanomaterials. One example of nanomaterial-mediated chemotherapy is ABI-007, where the protein albumin as a delivery vehicle for paclitaxel (423). Paclitaxel, along with doxorubicin, belongs to the taxane family of anti-cancer drugs that interfere with the breakdown of microtubules during mitotic cell division (424). While paclitaxel itself is a highly proficient anti-cancer agent, its poor solubility in water due to its structural hydrophobicity, initially required the use of solvents such as Cremophor EL and ethanol for clinical uses despite the severe allergic reactions associated with them (423, 425, 426). Therefore, albumin was selected as an alternative means to carry the water-insoluble paclitaxel in circulation. Numerous clinical trials using these albumin-bound paclitaxel (Abraxane) formulations were performed to confirm the superior therapeutic efficacy (427, 428). In addition to the success of ABI-007, more nanoparticle-drug formulations such as CRLX101 (cyclodextrin-based polymer carrying camptothecin; ClinicalTrials.gov Identifier: NCT02010567) (429) and BIND-014 (polymeric nanoparticle targeting PSMA, containing doxorubicin as the therapeutic agent; ClinicalTrials.gov Identifier: NCT02010567) (430) are currently undergoing clinical trials, and it remains to be seen whether the use of nanomaterials in drug delivery can become a common practice.

On the other hand, clinical development in photo-thermal therapy using plasmonic NPs has rather been slow. Although the concept of temperature-induced cell death has been recognized for few decades (431), the method of generating heat at the region of interest had been limited (432). Furthermore, electromagnetic irradiation had been used to ablate tumors,

yet not only the results were unsatisfactory (evaluated by tumor recurrence and metastasis), without the use of efficient photo-thermal agents these methods required a considerable amount of laser power which was also detrimental to normal cells (433, 434). It has only been about ten years since the first reports of photo-thermal therapy in current format became available in pre-clinical settings (353). Therefore, while the field is rapidly advancing, it is still experimental and the translation of photo-thermal therapy into clinics would require more time. Currently, only one clinical trial has been performed in regards to photo-thermal therapy. A non-randomized pilot study regarding safety and efficacy was performed on 11 patients using Aurolase™, which is a therapy based on the gold nanoshells produced from the Halas group. (ClinicalTrials.gov Identifier: NCT01679470) (435). Based on the unreleased results from the pilot study, phase 1 clinical trial targeting prostate cancer patients are currently under way.

3.7 Conclusion

Modern methods in medicine have revolutionized the way diseases are being managed. However, although our increasing understanding of the underlying mechanisms of cancer has shown advancements, we have also seen the limitations of our current approach toward treatment. Perhaps the single biggest challenge in the management of cancer is the inevitable development of resistance against currently available therapeutic regimes. The biological and chemical interventions undoubtedly exert selective pressure on the tumor, which then would contribute to progression of tumor by promoting survival of the resistant-phenotype (185). Therefore, in addition to the traditional biological and chemical interventions, novel approaches across different fields of science, including the application of nanomaterials and the use of nanotechnology, have been employed in cancer research and treatment. The small size and the unique properties of these NPs allow them to be utilized not

only as vectors to carry drugs, but also to be used as an immediate agent to deliver physical energy at the site of tumor, thereby leaving an irreversible damage. In particular, the photo-thermal approach in which the abovementioned NPs convert light into heat is gaining attention as a potential therapeutic option in tumor ablation therapy, with *in vitro* and pre-clinical animal models results showing promising results, can be translated to successful clinical trials.

REFERENCES

1. Adams J. The case of scirrhous of the prostate gland with corresponding affliction of the lymphatic glands in the lumbar region and in the pelvis. Lancet. 1853;1(1547):393-4.
2. Carlsson S, Vickers A. Spotlight on prostate cancer: the latest evidence and current controversies. BMC Med. 2015;13:60.
3. Denmeade SR, Isaacs JT. A history of prostate cancer treatment. Nat Rev Cancer. 2002;2(5):389-96.
4. Siegel RL, Miller KD, Jemal A. Cancer statistics, 2016. CA Cancer J Clin. 2016;66(1):7-30.
5. Society CC. Canadian Cancer Society's Advisory Committee on Cancer Statistics. Canadian Cancer Statistics 2015. Toronto, ON2015.
6. Statistics OfN. Cancer Registration Statistics: England Statistical Bulletins. 2015.
7. Rebbeck TR, Haas GP. Temporal trends and racial disparities in global prostate cancer prevalence. Can J Urol. 2014;21(5):7496-506.
8. Zhu Y, Wang HK, Qu YY, Ye DW. Prostate cancer in East Asia: evolving trend over the last decade. Asian J Androl. 2015;17(1):48-57.
9. Odedina FT, Akinremi TO, Chinegwundoh F, Roberts R, Yu D, Reams RR, et al. Prostate cancer disparities in Black men of African descent: a comparative literature review of prostate cancer burden among Black men in the United States, Caribbean, United Kingdom, and West Africa. Infect Agent Cancer. 2009;4 Suppl 1:S2.
10. Jones AL, Chinegwundoh F. Update on prostate cancer in black men within the UK. Ecancermedicalscience. 2014;8:455.
11. Ito K. Prostate cancer in Asian men. Nat Rev Urol. 2014;11(4):197-212.
12. WHO. World Cancer Report 2014. 150 cours Albert Thomas, 69372 Lyon Cedex 08, France: International Agency for Research on Cancer; 2014.
13. Packer JR, Maitland NJ. The molecular and cellular origin of human prostate cancer. Biochim Biophys Acta. 2016;1863(6 Pt A):1238-60.
14. Cooper CS, Eeles R, Wedge DC, Van Loo P, Gundem G, Alexandrov LB, et al. Analysis of the genetic phylogeny of multifocal prostate cancer identifies multiple independent clonal expansions in neoplastic and morphologically normal prostate tissue. Nat Genet. 2015;47(4):367-72.
15. Tindall D. Prostate cancer : biochemistry, molecular biology and genetics. New York: Springer; 2013. xii, 522 pages p.
16. Attard G, Parker C, Eeles RA, Schroder F, Tomlins SA, Tannock I, et al. Prostate cancer. Lancet. 2016;387(10013):70-82.
17. Goldgar DE, Easton DF, Cannon-Albright LA, Skolnick MH. Systematic population-based assessment of cancer risk in first-degree relatives of cancer probands. J Natl Cancer Inst. 1994;86(21):1600-8.
18. Leslie NR, Longy M. Inherited PTEN mutations and the prediction of phenotype. Semin Cell Dev Biol. 2016;52:30-8.
19. Castro E, Goh CL, Eeles RA. Prostate cancer screening in BRCA and Lynch syndrome mutation carriers. Am Soc Clin Oncol Educ Book. 2013.
20. Foulkes WD. Inherited susceptibility to common cancers. N Engl J Med. 2008;359(20):2143-53.
21. Isaacs WB. Inherited susceptibility for aggressive prostate cancer. Asian J Androl. 2012;14(3):415-8.
22. Eeles R, Goh C, Castro E, Bancroft E, Guy M, Al Olama AA, et al. The genetic

epidemiology of prostate cancer and its clinical implications. Nat Rev Urol. 2014;11(1):18-31.
23. Lee J, Demissie K, Lu SE, Rhoads GG. Cancer incidence among Korean-American immigrants in the United States and native Koreans in South Korea. Cancer Control. 2007;14(1):78-85.
24. Sun JH, Lee SA. Association between CAG repeat polymorphisms and the risk of prostate cancer: a meta-analysis by race, study design and the number of (CAG)n repeat polymorphisms. Int J Mol Med. 2013;32(5):1195-203.
25. Gu M, Dong X, Zhang X, Niu W. The CAG repeat polymorphism of androgen receptor gene and prostate cancer: a meta-analysis. Mol Biol Rep. 2012;39(3):2615-24.
26. Cheng L, Song SY, Pretlow TG, Abdul-Karim FW, Kung HJ, Dawson DV, et al. Evidence of independent origin of multiple tumors from patients with prostate cancer. J Natl Cancer Inst. 1998;90(3):233-7.
27. Djavan B, Susani M, Bursa B, Basharkhah A, Simak R, Marberger M. Predictability and significance of multifocal prostate cancer in the radical prostatectomy specimen. Tech Urol. 1999;5(3):139-42.
28. Wise AM, Stamey TA, McNeal JE, Clayton JL. Morphologic and clinical significance of multifocal prostate cancers in radical prostatectomy specimens. Urology. 2002;60(2):264-9.
29. Matoso A, Epstein JI. Grading of Prostate Cancer: Past, Present, and Future. Curr Urol Rep. 2016;17(3):25.
30. Shier D, Butler J, Lewis R. Hole's essentials of human anatomy & physiology. Twelfth edition. ed. New York, NY: McGraw-Hill Education; 2015. xxiii, 632 pages p.
31. Martini F, Timmons MJ, Tallitsch RB. Human anatomy. 7th ed. Boston: Pearson Benjamin Cummings; 2012. xxxiv, 870 p. p.
32. Myers RP. Structure of the adult prostate from a clinician's standpoint. Clin Anat. 2000;13(3):214-5.
33. McNeal JE. The zonal anatomy of the prostate. Prostate. 1981;2(1):35-49.
34. Shaikhibrahim Z, Lindstrot A, Ellinger J, Rogenhofer S, Buettner R, Perner S, et al. The peripheral zone of the prostate is more prone to tumor development than the transitional zone: is the ETS family the key? Mol Med Rep. 2012;5(2):313-6.
35. Liverman CT, Blazer, D. G. Testosterone and Health Outcomes. In: Liverman CT, Blazer DG, editors. Testosterone and Aging: Clinical Research Directions. Washington (DC)2004.
36. Aaron L, Franco OE, Hayward SW. Review of Prostate Anatomy and Embryology and the Etiology of Benign Prostatic Hyperplasia. Urol Clin North Am. 2016;43(3):279-88.
37. Orsted DD, Bojesen SE. The link between benign prostatic hyperplasia and prostate cancer. Nat Rev Urol. 2013;10(1):49-54.
38. Chang RT, Kirby R, Challacombe BJ. Is there a link between BPH and prostate cancer? Practitioner. 2012;256(1750):13-6, 2.
39. Montironi R, Mazzucchelli R, Lopez-Beltran A, Cheng L, Scarpelli M. Mechanisms of disease: high-grade prostatic intraepithelial neoplasia and other proposed preneoplastic lesions in the prostate. Nat Clin Pract Urol. 2007;4(6):321-32.
40. Montironi R, Mazzucchelli R, Lopez-Beltran A, Scarpelli M, Cheng L. Prostatic intraepithelial neoplasia: its morphological and molecular diagnosis and clinical significance. BJU Int. 2011;108(9):1394-401.
41. De Marzo AM, Nelson WG, Bieberich CJ, Yegnasubramanian S. Prostate cancer: New answers prompt new questions regarding cell of origin. Nat Rev Urol. 2010;7(12):650-2.
42. Cheng L, Paterson RF, Beck SD, Parks J. Prostatic intraepithelial neoplasia: an update. Clin Prostate Cancer. 2004;3(1):26-30.

43. Calabrese P, Tavare S, Shibata D. Pretumor progression: clonal evolution of human stem cell populations. The American journal of pathology. 2004;164(4):1337-46.
44. Xie W, Wong YC, Tsao SW. Correlation of increased apoptosis and proliferation with development of prostatic intraepithelial neoplasia (PIN) in ventral prostate of the Noble rat. Prostate. 2000;44(1):31-9.
45. Gomella LG, Liu XS, Trabulsi EJ, Kelly WK, Myers R, Showalter T, et al. Screening for prostate cancer: the current evidence and guidelines controversy. Can J Urol. 2011;18(5):5875-83.
46. van Royen ME, van Cappellen WA, de Vos C, Houtsmuller AB, Trapman J. Stepwise androgen receptor dimerization. Journal of cell science. 2012;125(8):1970-9.
47. Punnen S, Cooperberg MR, D'Amico AV, Karakiewicz PI, Moul JW, Scher HI, et al. Management of biochemical recurrence after primary treatment of prostate cancer: a systematic review of the literature. Eur Urol. 2013;64(6):905-15.
48. Moul JW. Hormone naive prostate cancer: predicting and maximizing response intervals. Asian J Androl. 2015;17(6):929-35; discussion 33.
49. Crawford ED, Bennett CL, Andriole GL, Garnick MB, Petrylak DP. The utility of prostate-specific antigen in the management of advanced prostate cancer. BJU Int. 2013;112(5):548-60.
50. Quero L, Rozet F, Beuzeboc P, Hennequin C. The androgen receptor for the radiation oncologist. Cancer/Radiothérapie. 2015;19(3):220-7.
51. Karantanos T, Corn PG, Thompson TC. Prostate cancer progression after androgen deprivation therapy: mechanisms of castrate-resistance and novel therapeutic approaches. Oncogene. 2013;32(49):5501-11.
52. van der Steen T, Tindall DJ, Huang H. Posttranslational Modification of the Androgen Receptor in Prostate Cancer. International Journal of Molecular Sciences. 2013;14(7):14833-59.
53. Singh M, Jha R, Melamed J, Shapiro E, Hayward SW, Lee P. Stromal androgen receptor in prostate development and cancer. The American journal of pathology. 2014;184(10):2598-607.
54. Wen S, Chang HC, Tian J, Shang Z, Niu Y, Chang C. Stromal androgen receptor roles in the development of normal prostate, benign prostate hyperplasia, and prostate cancer. The American journal of pathology. 2015;185(2):293-301.
55. Howlader N NA, Krapcho M, Miller D, Bishop K, Altekruse SF, Kosary CL, Yu M, Ruhl J, Tatalovich Z, Mariotto A, Lewis DR, Chen HS, Feuer EJ, Cronin KA (eds). SEER Cancer Statistics Review, 1975-2013 National Cancer Institute. Bethesda, MD: National Cancer Institute; 2015 [updated September 12, 2016. Available from: https://seer.cancer.gov/statfacts/html/prost.html.
56. Alfaqih MA, Allott EH, Hamilton RJ, Freeman MR, Freedland SJ. The current evidence on statin use and prostate cancer prevention: are we there yet? Nat Rev Urol. 2017;14(2):107-19.
57. Miller DC, Hafez KS, Stewart A, Montie JE, Wei JT. Prostate carcinoma presentation, diagnosis, and staging: an update form the National Cancer Data Base. Cancer. 2003;98(6):1169-78.
58. Marta GN, Hanna SA, Fernandes da Silva JL, Carvalho Hde A. Screening for prostate cancer: an updated review. Expert review of anticancer therapy. 2013;13(1):101-8.
59. Kang BJ, Jeun M, Jang GH, Song SH, Jeong IG, Kim CS, et al. Diagnosis of prostate cancer via nanotechnological approach. Int J Nanomedicine. 2015;10:6555-69.
60. Hanahan D, Weinberg RA. Hallmarks of cancer: the next generation. Cell. 2011;144(5):646-74.

61. Biomarkers Definitions Working G. Biomarkers and surrogate endpoints: preferred definitions and conceptual framework. Clin Pharmacol Ther. 2001;69(3):89-95.
62. Pentyala S, Whyard T, Pentyala S, Muller J, Pfail J, Parmar S, et al. Prostate cancer markers: An update. Biomed Rep. 2016;4(3):263-8.
63. Balk SP, Ko YJ, Bubley GJ. Biology of prostate-specific antigen. J Clin Oncol. 2003;21(2):383-91.
64. Wang MC, Valenzuela LA, Murphy GP, Chu TM. Purification of a human prostate specific antigen. Invest Urol. 1979;17(2):159-63.
65. Papsidero LD, Wang MC, Valenzuela LA, Murphy GP, Chu TM. A prostate antigen in sera of prostatic cancer patients. Cancer Res. 1980;40(7):2428-32.
66. Kim J, Coetzee GA. Prostate specific antigen gene regulation by androgen receptor. Journal of cellular biochemistry. 2004;93(2):233-41.
67. Catalona WJ, Smith DS, Ratliff TL, Dodds KM, Coplen DE, Yuan JJ, et al. Measurement of prostate-specific antigen in serum as a screening test for prostate cancer. N Engl J Med. 1991;324(17):1156-61.
68. Stephan C, Ralla B, Jung K. Prostate-specific antigen and other serum and urine markers in prostate cancer. Biochim Biophys Acta. 2014;1846(1):99-112.
69. Gambert SR. Screening for prostate cancer. Int Urol Nephrol. 2001;33(2):249-57.
70. Ilic D, Neuberger MM, Djulbegovic M, Dahm P. Screening for prostate cancer. Cochrane Database Syst Rev. 2013(1):CD004720.
71. Catalona WJ, Richie JP, deKernion JB, Ahmann FR, Ratliff TL, Dalkin BL, et al. Comparison of prostate specific antigen concentration versus prostate specific antigen density in the early detection of prostate cancer: receiver operating characteristic curves. J Urol. 1994;152(6 Pt 1):2031-6.
72. Thompson IM, Pauler DK, Goodman PJ, Tangen CM, Lucia MS, Parnes HL, et al. Prevalence of prostate cancer among men with a prostate-specific antigen level < or =4.0 ng per milliliter. N Engl J Med. 2004;350(22):2239-46.
73. Hayes JH, Barry MJ. Screening for prostate cancer with the prostate-specific antigen test: a review of current evidence. JAMA. 2014;311(11):1143-9.
74. Bussemakers MJ, van Bokhoven A, Verhaegh GW, Smit FP, Karthaus HF, Schalken JA, et al. DD3: a new prostate-specific gene, highly overexpressed in prostate cancer. Cancer research. 1999;59(23):5975-9.
75. Hessels D, Schalken JA. The use of PCA3 in the diagnosis of prostate cancer. Nat Rev Urol. 2009;6(5):255-61.
76. Hessels D, Klein Gunnewiek JM, van Oort I, Karthaus HF, van Leenders GJ, van Balken B, et al. DD3(PCA3)-based molecular urine analysis for the diagnosis of prostate cancer. Eur Urol. 2003;44(1):8-15; discussion -6.
77. Ferreira LB, Palumbo A, de Mello KD, Sternberg C, Caetano MS, de Oliveira FL, et al. PCA3 noncoding RNA is involved in the control of prostate-cancer cell survival and modulates androgen receptor signaling. BMC Cancer. 2012;12:507.
78. Romero Otero J, Garcia Gomez B, Campos Juanatey F, Touijer KA. Prostate cancer biomarkers: an update. Urol Oncol. 2014;32(3):252-60.
79. Kumar-Sinha C, Tomlins SA, Chinnaiyan AM. Recurrent gene fusions in prostate cancer. Nat Rev Cancer. 2008;8(7):497-511.
80. Wei JT. Urinary biomarkers for prostate cancer. Curr Opin Urol. 2015;25(1):77-82.
81. Tomlins SA, Rhodes DR, Perner S, Dhanasekaran SM, Mehra R, Sun XW, et al. Recurrent fusion of TMPRSS2 and ETS transcription factor genes in prostate cancer. Science. 2005;310(5748):644-8.
82. Perner S, Demichelis F, Beroukhim R, Schmidt FH, Mosquera JM, Setlur S, et al.

TMPRSS2:ERG fusion-associated deletions provide insight into the heterogeneity of prostate cancer. Cancer research. 2006;66(17):8337-41.
83. Narod SA, Seth A, Nam R. Fusion in the ETS gene family and prostate cancer. Br J Cancer. 2008;99(6):847-51.
84. Tomlins SA, Laxman B, Varambally S, Cao X, Yu J, Helgeson BE, et al. Role of the TMPRSS2-ERG gene fusion in prostate cancer. Neoplasia. 2008;10(2):177-88.
85. Demichelis F, Fall K, Perner S, Andren O, Schmidt F, Setlur SR, et al. TMPRSS2:ERG gene fusion associated with lethal prostate cancer in a watchful waiting cohort. Oncogene. 2007;26(31):4596-9.
86. Mehra R, Han B, Tomlins SA, Wang L, Menon A, Wasco MJ, et al. Heterogeneity of TMPRSS2 gene rearrangements in multifocal prostate adenocarcinoma: molecular evidence for an independent group of diseases. Cancer Res. 2007;67(17):7991-5.
87. Robert G, Jannink S, Smit F, Aalders T, Hessels D, Cremers R, et al. Rational basis for the combination of PCA3 and TMPRSS2:ERG gene fusion for prostate cancer diagnosis. Prostate. 2013;73(2):113-20.
88. Sanguedolce F, Cormio A, Brunelli M, D'Amuri A, Carrieri G, Bufo P, et al. Urine TMPRSS2: ERG Fusion Transcript as a Biomarker for Prostate Cancer: Literature Review. Clin Genitourin Cancer. 2016;14(2):117-21.
89. Hossain D, Bostwick DG. Significance of the TMPRSS2:ERG gene fusion in prostate cancer. BJU Int. 2013;111(5):834-5.
90. Clark JP, Cooper CS. ETS gene fusions in prostate cancer. Nat Rev Urol. 2009;6(8):429-39.
91. Chang SS. Overview of prostate-specific membrane antigen. Rev Urol. 2004;6 Suppl 10:S13-8.
92. Barve A, Jin W, Cheng K. Prostate cancer relevant antigens and enzymes for targeted drug delivery. J Control Release. 2014;187:118-32.
93. Ghosh A, Heston WD. Tumor target prostate specific membrane antigen (PSMA) and its regulation in prostate cancer. J Cell Biochem. 2004;91(3):528-39.
94. O'Keefe DS, Bacich DJ, Heston WD. Comparative analysis of prostate-specific membrane antigen (PSMA) versus a prostate-specific membrane antigen-like gene. Prostate. 2004;58(2):200-10.
95. Maurer T, Eiber M, Schwaiger M, Gschwend JE. Current use of PSMA-PET in prostate cancer management. Nat Rev Urol. 2016;13(4):226-35.
96. Gregorakis AK, Holmes EH, Murphy GP. Prostate-specific membrane antigen: current and future utility. Semin Urol Oncol. 1998;16(1):2-12.
97. Ross JS, Sheehan CE, Fisher HA, Kaufman RP, Jr., Kaur P, Gray K, et al. Correlation of primary tumor prostate-specific membrane antigen expression with disease recurrence in prostate cancer. Clin Cancer Res. 2003;9(17):6357-62.
98. Sokoloff RL, Norton KC, Gasior CL, Marker KM, Grauer LS. A dual-monoclonal sandwich assay for prostate-specific membrane antigen: levels in tissues, seminal fluid and urine. Prostate. 2000;43(2):150-7.
99. Schmidt B, Anastasiadis AG, Seifert HH, Franke KH, Oya M, Ackermann R. Detection of circulating prostate cells during radical prostatectomy by standardized PSMA RT-PCR: association with positive lymph nodes and high malignant grade. Anticancer Res. 2003;23(5A):3991-9.
100. Bouchelouche K, Choyke PL. Prostate-specific membrane antigen positron emission tomography in prostate cancer: a step toward personalized medicine. Curr Opin Oncol. 2016;28(3):216-21.
101. Tosoian JJ, Carter HB, Lepor A, Loeb S. Active surveillance for prostate cancer:

current evidence and contemporary state of practice. Nat Rev Urol. 2016;13(4):205-15.
102. Bill-Axelson A, Holmberg L, Garmo H, Rider JR, Taari K, Busch C, et al. Radical prostatectomy or watchful waiting in early prostate cancer. N Engl J Med. 2014;370(10):932-42.
103. Parker C. Active surveillance: towards a new paradigm in the management of early prostate cancer. Lancet Oncol. 2004;5(2):101-6.
104. Wilt TJ, Brawer MK, Jones KM, Barry MJ, Aronson WJ, Fox S, et al. Radical prostatectomy versus observation for localized prostate cancer. N Engl J Med. 2012;367(3):203-13.
105. Perera M, Krishnananthan N, Lindner U, Lawrentschuk N. An update on focal therapy for prostate cancer. Nat Rev Urol. 2016.
106. Coates J, Souhami L, El Naqa I. Big Data Analytics for Prostate Radiotherapy. Front Oncol. 2016;6:149.
107. Nomiya T, Tsuji H, Toyama S, Maruyama K, Nemoto K, Tsujii H, et al. Management of high-risk prostate cancer: radiation therapy and hormonal therapy. Cancer Treat Rev. 2013;39(8):872-8.
108. Zaorsky NG, Harrison AS, Trabulsi EJ, Gomella LG, Showalter TN, Hurwitz MD, et al. Evolution of advanced technologies in prostate cancer radiotherapy. Nat Rev Urol. 2013;10(10):565-79.
109. Lumen N, Ost P, Van Praet C, De Meerleer G, Villeirs G, Fonteyne V. Developments in external beam radiotherapy for prostate cancer. Urology. 2013;82(1):5-10.
110. Lee WR. Reducing biochemical recurrence rates in EBRT-treated prostate cancer patients: the influence of dose and dose per fraction. Future Oncol. 2007;3(6):649-54.
111. Vicini F, Vargas C, Gustafson G, Edmundson G, Martinez A. High dose rate brachytherapy in the treatment of prostate cancer. World J Urol. 2003;21(4):220-8.
112. Gerbaulet A, European Society for Therapeutic R, Oncology. The GEC ESTRO handbook of brachytherapy. Brussel: ESTRO; 2002.
113. Skowronek J. Low-dose-rate or high-dose-rate brachytherapy in treatment of prostate cancer - between options. J Contemp Brachytherapy. 2013;5(1):33-41.
114. Skowronek J. Brachytherapy in the therapy of prostate cancer - an interesting choice. Contemp Oncol (Pozn). 2013;17(5):407-12.
115. Capogrosso P, Salonia A, Briganti A, Montorsi F. Postprostatectomy Erectile Dysfunction: A Review. World J Mens Health. 2016;34(2):73-88.
116. Canalichio K, Jaber Y, Wang R. Surgery and hormonal treatment for prostate cancer and sexual function. Transl Androl Urol. 2015;4(2):103-9.
117. Sopko NA, Burnett AL. Erection rehabilitation following prostatectomy--current strategies and future directions. Nat Rev Urol. 2016;13(4):216-25.
118. Kojima Y, Takahashi N, Haga N, Nomiya M, Yanagida T, Ishibashi K, et al. Urinary incontinence after robot-assisted radical prostatectomy: pathophysiology and intraoperative techniques to improve surgical outcome. Int J Urol. 2013;20(11):1052-63.
119. Sriprasad S, Feneley MR, Thompson PM. History of prostate cancer treatment. Surg Oncol. 2009;18(3):185-91.
120. Wolf DA, Herzinger T, Hermeking H, Blaschke D, Horz W. Transcriptional and posttranscriptional regulation of human androgen receptor expression by androgen. Molecular endocrinology (Baltimore, Md. 1993;7(7):924-36.
121. Spratt DE, Zumsteg ZS, Feng FY, Tomlins SA. Translational and clinical implications of the genetic landscape of prostate cancer. Nature reviews Clinical oncology. 2016;13(10):597-610.
122. Merson S, Yang ZH, Brewer D, Olmos D, Eichholz A, McCarthy F, et al. Focal

amplification of the androgen receptor gene in hormone-naive human prostate cancer. Br J Cancer. 2014;110(6):1655-62.
123. Wilson S, Qi J, Filipp FV. Refinement of the androgen response element based on ChIP-Seq in androgen-insensitive and androgen-responsive prostate cancer cell lines. Sci Rep. 2016;6:32611.
124. Crona DJ, Milowsky MI, Whang YE. Androgen receptor targeting drugs in castration-resistant prostate cancer and mechanisms of resistance. Clin Pharmacol Ther. 2015;98(6):582-9.
125. Chandrasekar T, Yang JC, Gao AC, Evans CP. Targeting molecular resistance in castration-resistant prostate cancer. BMC Med. 2015;13:206.
126. Beer TM, Armstrong AJ, Rathkopf DE, Loriot Y, Sternberg CN, Higano CS, et al. Enzalutamide in metastatic prostate cancer before chemotherapy. N Engl J Med. 2014;371(5):424-33.
127. Scher HI, Fizazi K, Saad F, Taplin ME, Sternberg CN, Miller K, et al. Increased survival with enzalutamide in prostate cancer after chemotherapy. The New England journal of medicine. 2012;367(13):1187-97.
128. de Bono JS, Logothetis CJ, Molina A, Fizazi K, North S, Chu L, et al. Abiraterone and increased survival in metastatic prostate cancer. N Engl J Med. 2011;364(21):1995-2005.
129. Ryan CJ, Smith MR, de Bono JS, Molina A, Logothetis CJ, de Souza P, et al. Abiraterone in metastatic prostate cancer without previous chemotherapy. N Engl J Med. 2013;368(2):138-48.
130. Tran C, Ouk S, Clegg NJ, Chen Y, Watson PA, Arora V, et al. Development of a second-generation antiandrogen for treatment of advanced prostate cancer. Science. 2009;324(5928):787-90.
131. Clegg NJ, Wongvipat J, Joseph JD, Tran C, Ouk S, Dilhas A, et al. ARN-509: a novel antiandrogen for prostate cancer treatment. Cancer Res. 2012;72(6):1494-503.
132. Attard G, Antonarakis ES. Prostate cancer: AR aberrations and resistance to abiraterone or enzalutamide. Nat Rev Urol. 2016.
133. Giacinti S, Bassanelli M, Aschelter AM, Milano A, Roberto M, Marchetti P. Resistance to abiraterone in castration-resistant prostate cancer: a review of the literature. Anticancer Res. 2014;34(11):6265-9.
134. Giacinti S, Carlini P, Roberto M, Bassanelli M, Strigari L, Pavese F, et al. Duration of response to first androgen deprivation therapy, time to castration resistance prostate cancer, and outcome of metastatic castration resistance prostate cancer patients treated with abiraterone acetate. Anticancer Drugs. 2016.
135. Zhao J, Zhao Y, Wang L, Zhang J, Karnes RJ, Kohli M, et al. Alterations of androgen receptor-regulated enhancer RNAs (eRNAs) contribute to enzalutamide resistance in castration-resistant prostate cancer. Oncotarget. 2016;7(25):38551-65.
136. Claessens F, Helsen C, Prekovic S, Van den Broeck T, Spans L, Van Poppel H, et al. Emerging mechanisms of enzalutamide resistance in prostate cancer. Nat Rev Urol. 2014;11(12):712-6.
137. Korpal M, Korn JM, Gao X, Rakiec DP, Ruddy DA, Doshi S, et al. An F876L mutation in androgen receptor confers genetic and phenotypic resistance to MDV3100 (enzalutamide). Cancer discovery. 2013;3(9):1030-43.
138. Attard G, Sydes MR, Mason MD, Clarke NW, Aebersold D, de Bono JS, et al. Combining enzalutamide with abiraterone, prednisone, and androgen deprivation therapy in the STAMPEDE trial. Eur Urol. 2014;66(5):799-802.
139. Bambury RM, Rathkopf DE. Novel and next-generation androgen receptor-directed therapies for prostate cancer: Beyond abiraterone and enzalutamide. Urol Oncol.

2016;34(8):348-55.
140. Sternberg CN, Petrylak DP, Madan RA, Parker C. Progress in the treatment of advanced prostate cancer. American Society of Clinical Oncology educational book / ASCO American Society of Clinical Oncology Meeting. 2014:117-31.
141. Shiota M, Yokomizo A, Eto M. Taxane Chemotherapy for Hormone-Naive Prostate Cancer with Its Expanding Role as Breakthrough Strategy. Front Oncol. 2015;5:304.
142. Schweizer MT, Antonarakis ES. Chemotherapy and its evolving role in the management of advanced prostate cancer. Asian J Androl. 2014;16(3):334-40.
143. Cheetham P, Petrylak DP. Tubulin-targeted agents including docetaxel and cabazitaxel. Cancer J. 2013;19(1):59-65.
144. Zhu ML, Horbinski CM, Garzotto M, Qian DZ, Beer TM, Kyprianou N. Tubulin-targeting chemotherapy impairs androgen receptor activity in prostate cancer. Cancer Res. 2010;70(20):7992-8002.
145. Knavel EM, Brace CL. Tumor ablation: common modalities and general practices. Tech Vasc Interv Radiol. 2013;16(4):192-200.
146. Magnuson WJ, Mahal A, Yu JB. Emerging Technologies and Techniques in Radiation Therapy. Semin Radiat Oncol. 2017;27(1):34-42.
147. King CR, Freeman D, Kaplan I, Fuller D, Bolzicco G, Collins S, et al. Stereotactic body radiotherapy for localized prostate cancer: pooled analysis from a multi-institutional consortium of prospective phase II trials. Radiother Oncol. 2013;109(2):217-21.
148. Datta NR, Rogers S, Ordonez SG, Puric E, Bodis S. Hyperthermia and radiotherapy in the management of head and neck cancers: A systematic review and meta-analysis. Int J Hyperthermia. 2016;32(1):31-40.
149. Uchida T, Tomonaga T, Kim H, Nakano M, Shoji S, Nagata Y, et al. Improved outcomes with advancements in high intensity focused ultrasound devices for the treatment of localized prostate cancer. J Urol. 2015;193(1):103-10.
150. Cho S, Kang SH. Current status of cryotherapy for prostate and kidney cancer. Korean J Urol. 2014;55(12):780-8.
151. Shah TT, Ahmed H, Kanthabalan A, Lau B, Ghei M, Maraj B, et al. Focal cryotherapy of localized prostate cancer: a systematic review of the literature. Expert Rev Anticancer Ther. 2014;14(11):1337-47.
152. Sadar MD, Hussain M, Bruchovsky N. Prostate cancer: molecular biology of early progression to androgen independence. Endocrine-related cancer. 1999;6(4):487-502.
153. Anderson K, Lutz C, van Delft FW, Bateman CM, Guo Y, Colman SM, et al. Genetic variegation of clonal architecture and propagating cells in leukaemia. Nature. 2011;469(7330):356-61.
154. Berger MF, Lawrence MS, Demichelis F, Drier Y, Cibulskis K, Sivachenko AY, et al. The genomic complexity of primary human prostate cancer. Nature. 2011;470(7333):214-20.
155. Lee W, Jiang Z, Liu J, Haverty PM, Guan Y, Stinson J, et al. The mutation spectrum revealed by paired genome sequences from a lung cancer patient. Nature. 2010;465(7297):473-7.
156. Pleasance ED, Cheetham RK, Stephens PJ, McBride DJ, Humphray SJ, Greenman CD, et al. A comprehensive catalogue of somatic mutations from a human cancer genome. Nature. 2010;463(7278):191-6.
157. Puente XS, Pinyol M, Quesada V, Conde L, Ordonez GR, Villamor N, et al. Whole-genome sequencing identifies recurrent mutations in chronic lymphocytic leukaemia. Nature. 2011;475(7354):101-5.
158. Yu YP, Song C, Tseng G, Ren BG, LaFramboise W, Michalopoulos G, et al. Genome abnormalities precede prostate cancer and predict clinical relapse. The American journal of

pathology. 2012;180(6):2240-8.
159. Baca SC, Garraway LA. The genomic landscape of prostate cancer. Frontiers in endocrinology. 2012;3:69.
160. Xu X, Zhu K, Liu F, Wang Y, Shen J, Jin J, et al. Identification of somatic mutations in human prostate cancer by RNA-Seq. Gene. 2013.
161. Wu C, Wyatt AW, Lapuk AV, McPherson A, McConeghy BJ, Bell RH, et al. Integrated genome and transcriptome sequencing identifies a novel form of hybrid and aggressive prostate cancer. J Pathol. 2012;227(1):53-61.
162. Grasso CS, Wu YM, Robinson DR, Cao X, Dhanasekaran SM, Khan AP, et al. The mutational landscape of lethal castration-resistant prostate cancer. Nature. 2012;487(7406):239-43.
163. Hieronymus H, Sawyers CL. Traversing the genomic landscape of prostate cancer from diagnosis to death. Nature genetics. 2012;44(6):613-4.
164. Gelet A, Chapelon JY, Margonari J, Theillere Y, Gorry F, Cathignol D, et al. Prostatic tissue destruction by high-intensity focused ultrasound: experimentation on canine prostate. J Endourol. 1993;7(3):249-53.
165. Hashida Y, Tanaka H, Zhou S, Kawakami S, Yamashita F, Murakami T, et al. Photothermal ablation of tumor cells using a single-walled carbon nanotube-peptide composite. J Control Release. 2014;173:59-66.
166. Panchapakesan B, Lu S, Sivakumar K, Teker K, Cesarone G, Wickstrom E. Single-Wall Carbon Nanotube Nanobomb Agents for Killing Breast Cancer Cells. NanoBiothchnology. 2005;1:7.
167. Burke A, Ding X, Singh R, Kraft RA, Levi-Polyachenko N, Rylander MN, et al. Long-term survival following a single treatment of kidney tumors with multiwalled carbon nanotubes and near-infrared radiation. Proc Natl Acad Sci U S A. 2009;106(31):12897-902.
168. Burlaka A, Lukin S, Prylutska S, Remeniak O, Prylutskyy Y, Shuba M, et al. Hyperthermic effect of multi-walled carbon nanotubes stimulated with near infrared irradiation for anticancer therapy: in vitro studies. Exp Oncol. 2010;32(1):48-50.
169. Avetisyan YA, Yakunin AN, Tuchin VV. Thermal energy transfer by plasmon-resonant composite nanoparticles at pulse laser irradiation. Applied optics. 2012;51(10):C88-94.
170. Pattani VP, Tunnell JW. Nanoparticle-mediated photothermal therapy: a comparative study of heating for different particle types. Lasers Surg Med. 2012;44(8):675-84.
171. Dotan I, Roche PJ, Paliouras M, Mitmaker EJ, Trifiro MA. Engineering Multi-Walled Carbon Nanotube Therapeutic Bionanofluids to Selectively Target Papillary Thyroid Cancer Cells. PLoS One. 2016;11(2):e0149723.
172. Huang YYTEM. Dispersion of Carbon Nanotubes: Mixing, Sonication, Stabilization, and Composite Properties. Polymers. 2012;4:275-95.
173. Hashim U.; Farehanim MAA, N.; Norhafiezah, S.; Fatin, M.F.; Rahim Ruslinda A.; Ayub, R.M., editor Opitical Properties of MWCNTs Dispersed in Various Solutions. 2nd International Conference on Biomedical Enginnering (ICoBE); 2015; Penang.
174. Chen CH, Wu YJ, Chen JJ. Gold nanotheranostics: photothermal therapy and imaging of Mucin 7 conjugated antibody nanoparticles for urothelial cancer. BioMed research international. 2015;2015:813632.
175. Fekrazad R, Hakimiha N, Farokhi E, Rasaee MJ, Ardestani MS, Kalhori KA, et al. Treatment of oral squamous cell carcinoma using anti-HER2 immunonanoshells. Int J Nanomedicine. 2011;6:2749-55.
176. Yang K, Yang G, Chen L, Cheng L, Wang L, Ge C, et al. FeS nanoplates as a multifunctional nano-theranostic for magnetic resonance imaging guided photothermal

therapy. Biomaterials. 2015;38:1-9.
177. Mhawech-Fauceglia P, Zhang S, Terracciano L, Sauter G, Chadhuri A, Herrmann FR, et al. Prostate-specific membrane antigen (PSMA) protein expression in normal and neoplastic tissues and its sensitivity and specificity in prostate adenocarcinoma: an immunohistochemical study using mutiple tumour tissue microarray technique. Histopathology. 2007;50(4):472-83.
178. Perner S, Hofer MD, Kim R, Shah RB, Li H, Moller P, et al. Prostate-specific membrane antigen expression as a predictor of prostate cancer progression. Hum Pathol. 2007;38(5):696-701.
179. Marchal C, Redondo M, Padilla M, Caballero J, Rodrigo I, Garcia J, et al. Expression of prostate specific membrane antigen (PSMA) in prostatic adenocarcinoma and prostatic intraepithelial neoplasia. Histol Histopathol. 2004;19(3):715-8.
180. Sweat SD, Pacelli A, Murphy GP, Bostwick DG. Prostate-specific membrane antigen expression is greatest in prostate adenocarcinoma and lymph node metastases. Urology. 1998;52(4):637-40.
181. Anti-PSMA antibody [EPR6253] (ab133579): abcam; [Available from: http://www.abcam.com/psma-antibody-epr6253-ab133579.html.
182. Weyne E, Castiglione F, Van der Aa F, Bivalacqua TJ, Albersen M. Landmarks in erectile function recovery after radical prostatectomy. Nat Rev Urol. 2015;12(5):289-97.
183. Incrocci L. Radiotherapy for prostate cancer and sexual health. Transl Androl Urol. 2015;4(2):124-30.
184. Ficarra V, Novara G, Rosen RC, Artibani W, Carroll PR, Costello A, et al. Systematic review and meta-analysis of studies reporting urinary continence recovery after robot-assisted radical prostatectomy. Eur Urol. 2012;62(3):405-17.
185. Chandrasekar T, Yang JC, Gao AC, Evans CP. Mechanisms of resistance in castration-resistant prostate cancer (CRPC). Transl Androl Urol. 2015;4(3):365-80.
186. Sun X, Zhang G, Patel D, Stephens D, Gobin AM. Targeted cancer therapy by immunoconjugated gold-gold sulfide nanoparticles using Protein G as a cofactor. Ann Biomed Eng. 2012;40(10):2131-9.
187. Yang TD, Choi W, Yoon TH, Lee KJ, Lee JS, Han SH, et al. Real-time phase-contrast imaging of photothermal treatment of head and neck squamous cell carcinoma: an in vitro study of macrophages as a vector for the delivery of gold nanoshells. J Biomed Opt. 2012;17(12):128003.
188. Schwartz JA, Price RE, Gill-Sharp KL, Sang KL, Khorchani J, Goodwin BS, et al. Selective nanoparticle-directed ablation of the canine prostate. Lasers Surg Med. 2011;43(3):213-20.
189. Mendoza-Nava H, Ferro-Flores G, Ocampo-Garcia B, Serment-Guerrero J, Santos-Cuevas C, Jimenez-Mancilla N, et al. Laser heating of gold nanospheres functionalized with octreotide: in vitro effect on HeLa cell viability. Photomedicine and laser surgery. 2013;31(1):17-22.
190. Chakravarty P, Marches R, Zimmerman NS, Swafford AD, Bajaj P, Musselman IH, et al. Thermal ablation of tumor cells with antibody-functionalized single-walled carbon nanotubes. Proc Natl Acad Sci U S A. 2008;105(25):8697-702.
191. Marches R, Chakravarty P, Musselman IH, Bajaj P, Azad RN, Pantano P, et al. Specific thermal ablation of tumor cells using single-walled carbon nanotubes targeted by covalently-coupled monoclonal antibodies. International journal of cancer. 2009;125(12):2970-7.
192. Xiao Y, Gao X, Taratula O, Treado S, Urbas A, Holbrook RD, et al. Anti-HER2 IgY antibody-functionalized single-walled carbon nanotubes for detection and selective

destruction of breast cancer cells. BMC Cancer. 2009;9:351.
193. Lapotko D, Lukianova E, Potapnev M, Aleinikova O, Oraevsky A. Method of laser activated nano-thermolysis for elimination of tumor cells. Cancer letters. 2006;239(1):36-45.
194. Melancon MP, Lu W, Yang Z, Zhang R, Cheng Z, Elliot AM, et al. In vitro and in vivo targeting of hollow gold nanoshells directed at epidermal growth factor receptor for photothermal ablation therapy. Mol Cancer Ther. 2008;7(6):1730-9.
195. Boca SC, Potara M, Gabudean AM, Juhem A, Baldeck PL, Astilean S. Chitosan-coated triangular silver nanoparticles as a novel class of biocompatible, highly effective photothermal transducers for in vitro cancer cell therapy. Cancer letters. 2011;311(2):131-40.
196. Loo C, Lowery A, Halas N, West J, Drezek R. Immunotargeted nanoshells for integrated cancer imaging and therapy. Nano Lett. 2005;5(4):709-11.
197. McDevitt MR, Barendswaard E, Ma D, Lai L, Curcio MJ, Sgouros G, et al. An alpha-particle emitting antibody ([213Bi]J591) for radioimmunotherapy of prostate cancer. Cancer research. 2000;60(21):6095-100.
198. Heister E, Brunner EW, Dieckmann GR, Jurewicz I, Dalton AB. Are carbon nanotubes a natural solution? Applications in biology and medicine. ACS Appl Mater Interfaces. 2013;5(6):1870-91.
199. Qin Z, Wang Y, Randrianalisoa J, Raeesi V, Chan WC, Lipinski W, et al. Quantitative Comparison of Photothermal Heat Generation between Gold Nanospheres and Nanorods. Sci Rep. 2016;6:29836.
200. Huang HC, Rege K, Heys JJ. Spatiotemporal temperature distribution and cancer cell death in response to extracellular hyperthermia induced by gold nanorods. ACS Nano. 2010;4(5):2892-900.
201. Popp MK, Oubou I, Shepherd C, Nager Z, Anderson C, Pagliaro L. Photothermal Therapy Using Gold Nanorods and Near-Infrared Light in a Murine Melanoma Model Increases Survival and Decreases Tumor Volume. Journal of Nanomaterials. 2014;2014:8.
202. Eldridge BN, Bernish BW, Fahrenholtz CD, Singh R. Photothermal Therapy of Glioblastoma Multiforme Using Multiwalled Carbon Nanotubes Optimized for Diffusion in Extracellular Space. ACS Biomaterials Science & Engineering. 2016;2(6):963-76.
203. Hudson DE, Hudson DO, Wininger JM, Richardson BD. Penetration of laser light at 808 and 980 nm in bovine tissue samples. Photomed Laser Surg. 2013;31(4):163-8.
204. Hartung T, Daston G. Are In Vitro Tests Suitable for Regulatory Use? Toxicological Sciences. 2009;111(2):233-7.
205. Dotan I, Roche PJR, Paliouras M, Mitmaker EJ, Trifiro MA. Engineering Multi-Walled Carbon Nanotube Therapeutic Bionanofluids to Selectively Target Papillary Thyroid Cancer Cells. PLoS ONE. 2016;11(2):e0149723.
206. Kam NW, O'Connell M, Wisdom JA, Dai H. Carbon nanotubes as multifunctional biological transporters and near-infrared agents for selective cancer cell destruction. Proc Natl Acad Sci U S A. 2005;102(33):11600-5.
207. Hashida Y, Tanaka H, Zhou S, Kawakami S, Yamashita F, Murakami T, et al. Photothermal ablation of tumor cells using a single-walled carbon nanotube-peptide composite. J Control Release. 2014;173:59-66.
208. Burlaka A, Lukin S, Prylutska S, Remeniak O, Prylutskyy Y, Shuba M, et al. Hyperthermic effect of multi-walled carbon nanotubes stimulated with near infrared irradiation for anticancer therapy: in vitro studies. Exp Oncol. 2010;32(1):48-50.
209. El-Sayed IH, Huang X, El-Sayed MA. Selective laser photo-thermal therapy of epithelial carcinoma using anti-EGFR antibody conjugated gold nanoparticles. Cancer letters. 2006;239(1):129-35.
210. Ning S, Shaoxin L, Eric W, Balaji P. Integrated molecular targeting of IGF1R and

HER2 surface receptors and destruction of breast cancer cells using single wall carbon nanotubes. Nanotechnology. 2007;18(31):315101.
211. Abo-Elfadl MT, Gamal-Eldeen AM, Elshafey MM, Abdalla GM, Ali SS, Ali MR, et al. Photothermal therapeutic effect of PEGylated gold nano-semicubes in chemically-induced skin cancer in mice. J Photochem Photobiol B. 2016;164:21-9.
212. Chen J, Wang D, Xi J, Au L, Siekkinen A, Warsen A, et al. Immuno gold nanocages with tailored optical properties for targeted photothermal destruction of cancer cells. Nano letters. 2007;7(5):1318-22.
213. Liang X, Shang W, Chi C, Zeng C, Wang K, Fang C, et al. Dye-conjugated single-walled carbon nanotubes induce photothermal therapy under the guidance of near-infrared imaging. Cancer letters. 2016;383(2):243-9.
214. Song J, Wang F, Yang X, Ning B, Harp MG, Culp SH, et al. Gold Nanoparticle Coated Carbon Nanotube Ring with Enhanced Raman Scattering and Photothermal Conversion Property for Theranostic Applications. Journal of the American Chemical Society. 2016;138(22):7005-15.
215. Liu Z, Chan L, Chen L, Bai Y, Chen T. Facile Fabrication of Near-Infrared-Responsive and Chitosan-Functionalized Cu2 Se Nanoparticles for Cancer Photothermal Therapy. Chem Asian J. 2016.
216. Paholak HJ, Stevers NO, Chen H, Burnett JP, He M, Korkaya H, et al. Elimination of epithelial-like and mesenchymal-like breast cancer stem cells to inhibit metastasis following nanoparticle-mediated photothermal therapy. Biomaterials. 2016;104:145-57.
217. Zhao Q, Yi X, Li M, Zhong X, Shi Q, Yang K. High near-infrared absorbing Cu5FeS4 nanoparticles for dual-modal imaging and photothermal therapy. Nanoscale. 2016;8(27):13368-76.
218. Chen W, Zhang X, Ai F, Yang X, Zhu G, Wang F. Graphitic Carbon Nanocubes Derived from ZIF-8 for Photothermal Therapy. Inorg Chem. 2016;55(12):5750-2.
219. Wu M, Guo Q, Xu F, Liu S, Lu X, Wang J, et al. Engineering phosphopeptide-decorated magnetic nanoparticles as efficient photothermal agents for solid tumor therapy. J Colloid Interface Sci. 2016;476:158-66.
220. Jorgensen JT, Norregaard K, Tian P, Bendix PM, Kjaer A, Oddershede LB. Single Particle and PET-based Platform for Identifying Optimal Plasmonic Nano-Heaters for Photothermal Cancer Therapy. Sci Rep. 2016;6:30076.
221. Li KC, Chu HC, Lin Y, Tuan HY, Hu YC. PEGylated Copper Nanowires as a Novel Photothermal Therapy Agent. ACS Appl Mater Interfaces. 2016;8(19):12082-90.
222. Kalluru P, Vankayala R, Chiang CS, Hwang KC. Nano-graphene oxide-mediated In vivo fluorescence imaging and bimodal photodynamic and photothermal destruction of tumors. Biomaterials. 2016;95:1-10.
223. Biffi S, Petrizza L, Garrovo C, Rampazzo E, Andolfi L, Giustetto P, et al. Multimodal near-infrared-emitting PluS Silica nanoparticles with fluorescent, photoacoustic, and photothermal capabilities. Int J Nanomedicine. 2016;11:4865-74.
224. Chen H, Wang L, Yeh J, Wu X, Cao Z, Wang YA, et al. Reducing non-specific binding and uptake of nanoparticles and improving cell targeting with an antifouling PEO-b-PgammaMPS copolymer coating. Biomaterials. 2010;31(20):5397-407.
225. Feynman RP. There's Plenty of Room at the Bottom. American Physical Society; Pasedena, CA1959.
226. Feynman RP. There's Plenty of Room at the Bottom. Engineering and Science (Caltech). 1960;23(5):22-36.
227. Krukemeyer MG KV, Huebner F, Wagner W, Resch R. History and Possible Uses of Nanomedicine Based on Nanoparticles and Nanotechnological Progress. J Nanomed

Nanotechnol. 2015;6(336).
228. Taniguchi N, editor On the Basic Concept of 'Nano-Technology'. International Conference on Production Engineering; 1974; Tokyo: Japan Society of Precision Engineering.
229. Guston DH. Encyclopedia of nanoscience and society. Thousand Oaks, Calif.: SAGE; 2010.
230. Drexler KE. Engines of creation. 1st ed. Garden City, N.Y.: Anchor Press/Doubleday; 1986. xii, 298 p. p.
231. Kaehler T. Nanotechnology: basic concepts and definitions. Clin Chem. 1994;40(9):1797-9.
232. Whatmore RW. Nanotechnology--what is it? Should we be worried? Occup Med (Lond). 2006;56(5):295-9.
233. Wagner V, Dullaart A, Bock AK, Zweck A. The emerging nanomedicine landscape. Nat Biotechnol. 2006;24(10):1211-7.
234. Arias JL. Drug targeting strategies in cancer treatment: an overview. Mini Rev Med Chem. 2011;11(1):1-17.
235. Bregoli L, Movia D, Gavigan-Imedio JD, Lysaght J, Reynolds J, Prina-Mello A. Nanomedicine applied to translational oncology: A future perspective on cancer treatment. Nanomedicine. 2016;12(1):81-103.
236. Brown PD, Patel PR. Nanomedicine: a pharma perspective. Wiley Interdiscip Rev Nanomed Nanobiotechnol. 2015;7(2):125-30.
237. Hare JI, Lammers T, Ashford MB, Puri S, Storm G, Barry ST. Challenges and strategies in anti-cancer nanomedicine development: An industry perspective. Adv Drug Deliv Rev. 2016.
238. Son KH, Hong JH, Lee JW. Carbon nanotubes as cancer therapeutic carriers and mediators. International journal of nanomedicine. 2016;11:5163-85.
239. Agostinis P, Berg K, Cengel KA, Foster TH, Girotti AW, Gollnick SO, et al. Photodynamic therapy of cancer: an update. CA Cancer J Clin. 2011;61(4):250-81.
240. van der Zee J. Heating the patient: a promising approach? Ann Oncol. 2002;13(8):1173-84.
241. Hildebrandt B, Wust P, Ahlers O, Dieing A, Sreenivasa G, Kerner T, et al. The cellular and molecular basis of hyperthermia. Crit Rev Oncol Hematol. 2002;43(1):33-56.
242. Turner T, Caspari T. When heat casts a spell on the DNA damage checkpoints. Open Biol. 2014;4:140008.
243. Murphy MJ, Torstensson PA. Thermal relaxation times: an outdated concept in photothermal treatments. Lasers Med Sci. 2014;29(3):973-8.
244. Armour EP, Raaphorst GP. Long duration mild temperature hyperthermia and brachytherapy. Int J Hyperthermia. 2004;20(2):175-89.
245. Qu X, Yao C, Wang J, Li Z, Zhang Z. Anti-CD30-targeted gold nanoparticles for photothermal therapy of L-428 Hodgkin's cell. Int J Nanomedicine. 2012;7:6095-103.
246. Lapotko D. Plasmonic nanoparticle-generated photothermal bubbles and their biomedical applications. Nanomedicine (Lond). 2009;4(7):813-45.
247. Staels B, Rubenstrunk A, Noel B, Rigou G, Delataille P, Millatt LJ, et al. Hepatoprotective effects of the dual peroxisome proliferator-activated receptor alpha/delta agonist, GFT505, in rodent models of nonalcoholic fatty liver disease/nonalcoholic steatohepatitis. Hepatology. 2013;58(6):1941-52.
248. Zou L, Wang H, He B, Zeng L, Tan T, Cao H, et al. Current Approaches of Photothermal Therapy in Treating Cancer Metastasis with Nanotherapeutics. Theranostics. 2016;6(6):762-72.
249. Chen Q, Wen J, Li H, Xu Y, Liu F, Sun S. Recent advances in different modal

imaging-guided photothermal therapy. Biomaterials. 2016;106:144-66.
250. Torchilin VP. Passive and active drug targeting: drug delivery to tumors as an example. Handb Exp Pharmacol. 2010(197):3-53.
251. Hanahan D, Weinberg RA. The hallmarks of cancer. Cell. 2000;100(1):57-70.
252. Maruyama K. Intracellular targeting delivery of liposomal drugs to solid tumors based on EPR effects. Adv Drug Deliv Rev. 2011;63(3):161-9.
253. Danhier F, Feron O, Preat V. To exploit the tumor microenvironment: Passive and active tumor targeting of nanocarriers for anti-cancer drug delivery. J Control Release. 2010;148(2):135-46.
254. Veronese FM, Harris JM. Introduction and overview of peptide and protein pegylation. Adv Drug Deliv Rev. 2002;54(4):453-6.
255. Klibanov AL, Maruyama K, Torchilin VP, Huang L. Amphipathic polyethyleneglycols effectively prolong the circulation time of liposomes. FEBS Lett. 1990;268(1):235-7.
256. Cho K, Wang X, Nie S, Chen ZG, Shin DM. Therapeutic nanoparticles for drug delivery in cancer. Clin Cancer Res. 2008;14(5):1310-6.
257. Decuzzi P, Pasqualini R, Arap W, Ferrari M. Intravascular delivery of particulate systems: does geometry really matter? Pharm Res. 2009;26(1):235-43.
258. Allen TM, Hansen C, Martin F, Redemann C, Yau-Young A. Liposomes containing synthetic lipid derivatives of poly(ethylene glycol) show prolonged circulation half-lives in vivo. Biochim Biophys Acta. 1991;1066(1):29-36.
259. Park JW, Kirpotin DB, Hong K, Shalaby R, Shao Y, Nielsen UB, et al. Tumor targeting using anti-her2 immunoliposomes. J Control Release. 2001;74(1-3):95-113.
260. Hao Y, Zhang B, Zheng C, Ji R, Ren X, Guo F, et al. The tumor-targeting core-shell structured DTX-loaded PLGA@Au nanoparticles for chemo-photothermal therapy and X-ray imaging. J Control Release. 2015;220(Pt A):545-55.
261. Piao JG, Liu D, Hu K, Wang L, Gao F, Xiong Y, et al. Cooperative Nanoparticle System for Photothermal Tumor Treatment without Skin Damage. ACS Appl Mater Interfaces. 2016;8(4):2847-56.
262. Schiffelers RM, Koning GA, ten Hagen TL, Fens MH, Schraa AJ, Janssen AP, et al. Anti-tumor efficacy of tumor vasculature-targeted liposomal doxorubicin. J Control Release. 2003;91(1-2):115-22.
263. Janssen AP, Schiffelers RM, ten Hagen TL, Koning GA, Schraa AJ, Kok RJ, et al. Peptide-targeted PEG-liposomes in anti-angiogenic therapy. Int J Pharm. 2003;254(1):55-8.
264. Farokhzad OC, Jon S, Khademhosseini A, Tran TN, Lavan DA, Langer R. Nanoparticle-aptamer bioconjugates: a new approach for targeting prostate cancer cells. Cancer Res. 2004;64(21):7668-72.
265. Khan SA, Kanchanapally R, Fan Z, Beqa L, Singh AK, Senapati D, et al. A gold nanocage-CNT hybrid for targeted imaging and photothermal destruction of cancer cells. Chem Commun (Camb). 2012;48(53):6711-3.
266. Farokhzad OC, Cheng J, Teply BA, Sherifi I, Jon S, Kantoff PW, et al. Targeted nanoparticle-aptamer bioconjugates for cancer chemotherapy in vivo. Proc Natl Acad Sci U S A. 2006;103(16):6315-20.
267. Gabizon A, Shmeeda H, Horowitz AT, Zalipsky S. Tumor cell targeting of liposome-entrapped drugs with phospholipid-anchored folic acid-PEG conjugates. Adv Drug Deliv Rev. 2004;56(8):1177-92.
268. Shmeeda H, Mak L, Tzemach D, Astrahan P, Tarshish M, Gabizon A. Intracellular uptake and intracavitary targeting of folate-conjugated liposomes in a mouse lymphoma model with up-regulated folate receptors. Mol Cancer Ther. 2006;5(4):818-24.

269. Huang X, Jain PK, El-Sayed IH, El-Sayed MA. Plasmonic photothermal therapy (PPTT) using gold nanoparticles. Lasers Med Sci. 2008;23(3):217-28.
270. Ding X, Liow CH, Zhang M, Huang R, Li C, Shen H, et al. Surface plasmon resonance enhanced light absorption and photothermal therapy in the second near-infrared window. J Am Chem Soc. 2014;136(44):15684-93.
271. Eustis S, el-Sayed MA. Why gold nanoparticles are more precious than pretty gold: noble metal surface plasmon resonance and its enhancement of the radiative and nonradiative properties of nanocrystals of different shapes. Chem Soc Rev. 2006;35(3):209-17.
272. Hu F, Zhang Y, Chen G, Li C, Wang Q. Double-walled Au nanocage/SiO2 nanorattles: integrating SERS imaging, drug delivery and photothermal therapy. Small. 2015;11(8):985-93.
273. Hirsch LR, Stafford RJ, Bankson JA, Sershen SR, Rivera B, Price RE, et al. Nanoshell-mediated near-infrared thermal therapy of tumors under magnetic resonance guidance. Proc Natl Acad Sci U S A. 2003;100(23):13549-54.
274. Pansare V, Hejazi S, Faenza W, Prud'homme RK. Review of Long-Wavelength Optical and NIR Imaging Materials: Contrast Agents, Fluorophores and Multifunctional Nano Carriers. Chem Mater. 2012;24(5):812-27.
275. Weissleder R. A clearer vision for in vivo imaging. Nat Biotechnol. 2001;19(4):316-7.
276. Tsai MF, Chang SH, Cheng FY, Shanmugam V, Cheng YS, Su CH, et al. Au nanorod design as light-absorber in the first and second biological near-infrared windows for in vivo photothermal therapy. ACS Nano. 2013;7(6):5330-42.
277. Chen O, Yang Y, Wang T, Wu H, Niu C, Yang J, et al. Surface-functionalization-dependent optical properties of II-VI semiconductor nanocrystals. J Am Chem Soc. 2011;133(43):17504-12.
278. Iijima S. Helical microtubules of graphitic carbon. Nature. 1991;354(6348):56-8.
279. Yang K, Feng L, Shi X, Liu Z. Nano-graphene in biomedicine: theranostic applications. Chem Soc Rev. 2013;42(2):530-47.
280. Markovic ZM, Harhaji-Trajkovic LM, Todorovic-Markovic BM, Kepic DP, Arsikin KM, Jovanovic SP, et al. In vitro comparison of the photothermal anticancer activity of graphene nanoparticles and carbon nanotubes. Biomaterials. 2011;32(4):1121-9.
281. Steichen SD, Caldorera-Moore M, Peppas NA. A review of current nanoparticle and targeting moieties for the delivery of cancer therapeutics. Eur J Pharm Sci. 2013;48(3):416-27.
282. Adams GP, Weiner LM. Monoclonal antibody therapy of cancer. Nat Biotechnol. 2005;23(9):1147-57.
283. Yu MK, Park J, Jon S. Targeting strategies for multifunctional nanoparticles in cancer imaging and therapy. Theranostics. 2012;2(1):3-44.
284. McCarthy JR, Bhaumik J, Karver MR, Sibel Erdem S, Weissleder R. Targeted nanoagents for the detection of cancers. Mol Oncol. 2010;4(6):511-28.
285. Wong BS, Yoong SL, Jagusiak A, Panczyk T, Ho HK, Ang WH, et al. Carbon nanotubes for delivery of small molecule drugs. Adv Drug Deliv Rev. 2013;65(15):1964-2015.
286. Singh R, Torti SV. Carbon nanotubes in hyperthermia therapy. Adv Drug Deliv Rev. 2013;65(15):2045-60.
287. Iancu C, Mocan L. Advances in cancer therapy through the use of carbon nanotube-mediated targeted hyperthermia. International journal of nanomedicine. 2011;6:1675-84.
288. Liu Z, Robinson JT, Sun X, Dai H. PEGylated nanographene oxide for delivery of water-insoluble cancer drugs. J Am Chem Soc. 2008;130(33):10876-7.
289. Novoselov KS, Jiang D, Schedin F, Booth TJ, Khotkevich VV, Morozov SV, et al.

Two-dimensional atomic crystals. Proc Natl Acad Sci U S A. 2005;102(30):10451-3.
290. Dikin DA, Stankovich S, Zimney EJ, Piner RD, Dommett GH, Evmenenko G, et al. Preparation and characterization of graphene oxide paper. Nature. 2007;448(7152):457-60.
291. Li JL, Hou XL, Bao HC, Sun L, Tang B, Wang JF, et al. Graphene oxide nanoparticles for enhanced photothermal cancer cell therapy under the irradiation of a femtosecond laser beam. J Biomed Mater Res A. 2014;102(7):2181-8.
292. Novoselov KS, Geim AK, Morozov SV, Jiang D, Zhang Y, Dubonos SV, et al. Electric field effect in atomically thin carbon films. Science. 2004;306(5696):666-9.
293. Geim AK, Novoselov KS. The rise of graphene. Nat Mater. 2007;6(3):183-91.
294. Zhang Y, Nayak TR, Hong H, Cai W. Graphene: a versatile nanoplatform for biomedical applications. Nanoscale. 2012;4(13):3833-42.
295. Zhang Y, Ali SF, Dervishi E, Xu Y, Li Z, Casciano D, et al. Cytotoxicity effects of graphene and single-wall carbon nanotubes in neural phaeochromocytoma-derived PC12 cells. ACS Nano. 2010;4(6):3181-6.
296. Wang C, Li J, Amatore C, Chen Y, Jiang H, Wang XM. Gold nanoclusters and graphene nanocomposites for drug delivery and imaging of cancer cells. Angew Chem Int Ed Engl. 2011;50(49):11644-8.
297. Shi S, Chen F, Ehlerding EB, Cai W. Surface engineering of graphene-based nanomaterials for biomedical applications. Bioconjug Chem. 2014;25(9):1609-19.
298. Pan Y, Sahoo NG, Li L. The application of graphene oxide in drug delivery. Expert Opin Drug Deliv. 2012;9(11):1365-76.
299. Yang X, Zhang X, Liu Z, Ma Y, Huang Y, Chen Y. High-Efficiency Loading and Controlled Release of Doxorubicin Hydrochloride on Graphene Oxide. The Journal of Physical Chemistry C. 2008;112(45):17554-8.
300. Depan D, Shah, J., Misra, R.D.K. Controlled release of drug from folate-decorated and graphene mediated drug delivery system: Synthesis, loading efficiency, and drug release response. Materials Science and Engineering: C. 2011;31(7):1305–12.
301. Zheng XT, Ma XQ, Li CM. Highly efficient nuclear delivery of anti-cancer drugs using a bio-functionalized reduced graphene oxide. J Colloid Interface Sci. 2016;467:35-42.
302. Zhang L, Xia J, Zhao Q, Liu L, Zhang Z. Functional graphene oxide as a nanocarrier for controlled loading and targeted delivery of mixed anticancer drugs. Small. 2010;6(4):537-44.
303. Sahoo NG, Bao H, Pan Y, Pal M, Kakran M, Cheng HK, et al. Functionalized carbon nanomaterials as nanocarriers for loading and delivery of a poorly water-soluble anticancer drug: a comparative study. Chem Commun (Camb). 2011;47(18):5235-7.
304. Yang K, Zhang S, Zhang G, Sun X, Lee ST, Liu Z. Graphene in mice: ultrahigh in vivo tumor uptake and efficient photothermal therapy. Nano Lett. 2010;10(9):3318-23.
305. Robinson JT, Tabakman SM, Liang Y, Wang H, Casalongue HS, Vinh D, et al. Ultrasmall reduced graphene oxide with high near-infrared absorbance for photothermal therapy. J Am Chem Soc. 2011;133(17):6825-31.
306. Yang K, Wan J, Zhang S, Tian B, Zhang Y, Liu Z. The influence of surface chemistry and size of nanoscale graphene oxide on photothermal therapy of cancer using ultra-low laser power. Biomaterials. 2012;33(7):2206-14.
307. Madani SY, Naderi N, Dissanayake O, Tan A, Seifalian AM. A new era of cancer treatment: carbon nanotubes as drug delivery tools. Int J Nanomedicine. 2011;6:2963-79.
308. Danailov D, Keblinski P, Nayak S, Ajayan PM. Bending properties of carbon nanotubes encapsulating solid nanowires. J Nanosci Nanotechnol. 2002;2(5):503-7.
309. Bekyarova E, Ni Y, Malarkey EB, Montana V, McWilliams JL, Haddon RC, et al. Applications of Carbon Nanotubes in Biotechnology and Biomedicine. J Biomed

Nanotechnol. 2005;1(1):3-17.
310. Zhang W, Zhang Z, Zhang Y. The application of carbon nanotubes in target drug delivery systems for cancer therapies. Nanoscale Research Letters. 2011;6(1):555-.
311. Cheaptubes.com 2017 [Available from: https://www.cheaptubes.com/.
312. Peigney A, Laurent, Ch., Flahaut, E., Bacsa, R.R., Rousset, A. Specific surface area of carbon nanotubes and bundles of carbon nanotubes. Carbon. 2001;39(4):507-14.
313. Wu L, Man C, Wang H, Lu X, Ma Q, Cai Y, et al. PEGylated multi-walled carbon nanotubes for encapsulation and sustained release of oxaliplatin. Pharm Res. 2013;30(2):412-23.
314. Heister E, Brunner EW, Dieckmann GR, Jurewicz I, Dalton AB. Are Carbon Nanotubes a Natural Solution? Applications in Biology and Medicine. ACS Applied Materials & Interfaces. 2013;5(6):1870-91.
315. Shaffer MSP, Fan, X., Windle, A.H. Dispersion and packing of carbon nanotubes. Carbon. 1998;36(11):1603-12.
316. Liu X, Hurt RH, Kane AB. Biodurability of Single-Walled Carbon Nanotubes Depends on Surface Functionalization. Carbon N Y. 2010;48(7):1961-9.
317. Liu Z, Cai W, He L, Nakayama N, Chen K, Sun X, et al. In vivo biodistribution and highly efficient tumour targeting of carbon nanotubes in mice. Nat Nanotechnol. 2007;2(1):47-52.
318. Wu W, Li R, Bian X, Zhu Z, Ding D, Li X, et al. Covalently combining carbon nanotubes with anticancer agent: preparation and antitumor activity. ACS Nano. 2009;3(9):2740-50.
319. Tian Z, Yin M, Ma H, Zhu L, Shen H, Jia N. Supramolecular assembly and antitumor activity of multiwalled carbon nanotube-camptothecin complexes. J Nanosci Nanotechnol. 2011;11(2):953-8.
320. Ali-Boucetta H, Al-Jamal KT, McCarthy D, Prato M, Bianco A, Kostarelos K. Multiwalled carbon nanotube-doxorubicin supramolecular complexes for cancer therapeutics. Chem Commun (Camb). 2008(4):459-61.
321. Rungnim C, Rungrotmongkol T, Poo-Arporn RP. pH-controlled doxorubicin anticancer loading and release from carbon nanotube noncovalently modified by chitosan: MD simulations. J Mol Graph Model. 2016;70:70-6.
322. Ji J, Liu M, Meng Y, Liu R, Yan Y, Dong J, et al. Experimental Study of Magnetic Multi-Walled Carbon Nanotube-Doxorubicin Conjugate in a Lymph Node Metastatic Model of Breast Cancer. Med Sci Monit. 2016;22:2363-73.
323. Decatris MP, Sundar S, O'Byrne KJ. Platinum-based chemotherapy in metastatic breast cancer: current status. Cancer Treat Rev. 2004;30(1):53-81.
324. Feazell RP, Nakayama-Ratchford N, Dai H, Lippard SJ. Soluble Single-Walled Carbon Nanotubes as Longboat Delivery Systems for Platinum(IV) Anticancer Drug Design. Journal of the American Chemical Society. 2007;129(27):8438-9.
325. Prato M, Kostarelos K, Bianco A. Functionalized carbon nanotubes in drug design and discovery. Acc Chem Res. 2008;41(1):60-8.
326. Yang D, Yang F, Hu J, Long J, Wang C, Fu D, et al. Hydrophilic multi-walled carbon nanotubes decorated with magnetite nanoparticles as lymphatic targeted drug delivery vehicles. Chem Commun (Camb). 2009(29):4447-9.
327. Yang F, Jin C, Yang D, Jiang Y, Li J, Di Y, et al. Magnetic functionalised carbon nanotubes as drug vehicles for cancer lymph node metastasis treatment. Eur J Cancer. 2011;47(12):1873-82.
328. Lay CL, Liu HQ, Tan HR, Liu Y. Delivery of paclitaxel by physically loading onto poly(ethylene glycol) (PEG)-graft-carbon nanotubes for potent cancer therapeutics.

Nanotechnology. 2010;21(6):065101.
329. Arya N, Arora A, Vasu KS, Sood AK, Katti DS. Combination of single walled carbon nanotubes/graphene oxide with paclitaxel: a reactive oxygen species mediated synergism for treatment of lung cancer. Nanoscale. 2013;5(7):2818-29.
330. Kam NW, Dai H. Carbon nanotubes as intracellular protein transporters: generality and biological functionality. J Am Chem Soc. 2005;127(16):6021-6.
331. Pantarotto D, Briand JP, Prato M, Bianco A. Translocation of bioactive peptides across cell membranes by carbon nanotubes. Chem Commun (Camb). 2004(1):16-7.
332. Caoduro C, Hervouet E, Girard-Thernier C, Gharbi T, Boulahdour H, Delage-Mourroux R, et al. Carbon nanotubes as gene carriers: Focus on internalization pathways related to functionalization and properties. Acta Biomater. 2016.
333. Raffa V, Ciofani G, Vittorio O, Riggio C, Cuschieri A. Physicochemical properties affecting cellular uptake of carbon nanotubes. Nanomedicine (Lond). 2010;5(1):89-97.
334. Li JL, Bao HC, Hou XL, Sun L, Wang XG, Gu M. Graphene oxide nanoparticles as a nonbleaching optical probe for two-photon luminescence imaging and cell therapy. Angew Chem Int Ed Engl. 2012;51(8):1830-4.
335. Yang H, Feng X, Wang Q, Huang H, Chen W, Wee AT, et al. Giant two-photon absorption in bilayer graphene. Nano Lett. 2011;11(7):2622-7.
336. Robinson JT, Welsher K, Tabakman SM, Sherlock SP, Wang H, Luong R, et al. High Performance In Vivo Near-IR (>1 mum) Imaging and Photothermal Cancer Therapy with Carbon Nanotubes. Nano Res. 2010;3(11):779-93.
337. Torti SV, Byrne F, Whelan O, Levi N, Ucer B, Schmid M, et al. Thermal ablation therapeutics based on CN(x) multi-walled nanotubes. Int J Nanomedicine. 2007;2(4):707-14.
338. Cao-Milan R, Liz-Marzan LM. Gold nanoparticle conjugates: recent advances toward clinical applications. Expert Opin Drug Deliv. 2014;11(5):741-52.
339. Guerrero AR, Hassan N, Escobar CA, Albericio F, Kogan MJ, Araya E. Gold nanoparticles for photothermally controlled drug release. Nanomedicine (Lond). 2014;9(13):2023-39.
340. Khlebtsov N, Dykman L. Biodistribution and toxicity of engineered gold nanoparticles: a review of in vitro and in vivo studies. Chem Soc Rev. 2011;40(3):1647-71.
341. Xia Y, Li W, Cobley CM, Chen J, Xia X, Zhang Q, et al. Gold nanocages: from synthesis to theranostic applications. Acc Chem Res. 2011;44(10):914-24.
342. Manohar S, Ungureanu C, Van Leeuwen TG. Gold nanorods as molecular contrast agents in photoacoustic imaging: the promises and the caveats. Contrast Media Mol Imaging. 2011;6(5):389-400.
343. Sardar R, Funston AM, Mulvaney P, Murray RW. Gold nanoparticles: past, present, and future. Langmuir. 2009;25(24):13840-51.
344. Dykman L, Khlebtsov N. Gold nanoparticles in biomedical applications: recent advances and perspectives. Chem Soc Rev. 2012;41(6):2256-82.
345. Almeida JP, Figueroa ER, Drezek RA. Gold nanoparticle mediated cancer immunotherapy. Nanomedicine. 2014;10(3):503-14.
346. Moyano DF, Rotello VM. Nano meets biology: structure and function at the nanoparticle interface. Langmuir. 2011;27(17):10376-85.
347. Mieszawska AJ, Mulder WJ, Fayad ZA, Cormode DP. Multifunctional gold nanoparticles for diagnosis and therapy of disease. Mol Pharm. 2013;10(3):831-47.
348. Zhou W, Gao X, Liu D, Chen X. Gold Nanoparticles for In Vitro Diagnostics. Chemical reviews. 2015;115(19):10575-636.
349. Wang Y, Black KCL, Luehmann H, Li W, Zhang Y, Cai X, et al. Comparison Study of Gold Nanohexapods, Nanorods, and Nanocages for Photothermal Cancer Treatment. ACS

Nano. 2013;7(3):2068-77.
350. Kim H, Chung K, Lee S, Kim DH, Lee H. Near-infrared light-responsive nanomaterials for cancer theranostics. Wiley Interdisciplinary Reviews: Nanomedicine and Nanobiotechnology. 2016;8(1):23-45.
351. Pissuwan D, Valenzuela SM, Cortie MB. Therapeutic possibilities of plasmonically heated gold nanoparticles. Trends Biotechnol. 2006;24(2):62-7.
352. Hwang S, Nam J, Jung S, Song J, Doh H, Kim S. Gold nanoparticle-mediated photothermal therapy: current status and future perspective. Nanomedicine. 2014;9(13):2003-22.
353. Loo C, Lin A, Hirsch L, Lee MH, Barton J, Halas N, et al. Nanoshell-enabled photonics-based imaging and therapy of cancer. Technol Cancer Res Treat. 2004;3(1):33-40.
354. Maddox M, Liu J, Mandava SH, Callaghan C, John V, Lee BR. Nanotechnology applications in urology: a review. BJU International. 2014;114(5):653-60.
355. Vankayala R, Lin CC, Kalluru P, Chiang CS, Hwang KC. Gold nanoshells-mediated bimodal photodynamic and photothermal cancer treatment using ultra-low doses of near infra-red light. Biomaterials. 2014;35(21):5527-38.
356. Everts M, Saini V, Leddon JL, Kok RJ, Stoff-Khalili M, Preuss MA, et al. Covalently linked Au nanoparticles to a viral vector: potential for combined photothermal and gene cancer therapy. Nano Lett. 2006;6(4):587-91.
357. Topete A, Alatorre-Meda M, Villar-Alvarez EM, Carregal-Romero S, Barbosa S, Parak WJ, et al. Polymeric-gold nanohybrids for combined imaging and cancer therapy. Adv Healthc Mater. 2014;3(8):1309-25.
358. Topete A, Alatorre-Meda M, Iglesias P, Villar-Alvarez EM, Barbosa S, Costoya JA, et al. Fluorescent drug-loaded, polymeric-based, branched gold nanoshells for localized multimodal therapy and imaging of tumoral cells. ACS Nano. 2014;8(3):2725-38.
359. Gan J, Wei X, Li Y, Wu J, Qian K, Liu B. Designer SiO(2)@Au nanoshells towards sensitive and selective detection of small molecules in laser desorption ionization mass spectrometry. Nanomedicine. 2015;11(7):1715-23.
360. Yan W, Yang L, Zhuang H, Wu H, Zhang J. Engineered "hot" core-shell nanostructures for patterned detection of chloramphenicol. Biosens Bioelectron. 2016;78:67-72.
361. Liang Z, Li X, Xie Y, Liu S. 'Smart' gold nanoshells for combined cancer chemotherapy and hyperthermia. Biomed Mater. 2014;9(2):025012.
362. Wu C, Yu C, Chu M. A gold nanoshell with a silica inner shell synthesized using liposome templates for doxorubicin loading and near-infrared photothermal therapy. Int J Nanomedicine. 2011;6:807-13.
363. Li W, Zhang X, Zhou M, Tian B, Yu C, Jie J, et al. Functional core/shell drug nanoparticles for highly effective synergistic cancer therapy. Adv Healthc Mater. 2014;3(9):1475-85.
364. Singhana B, Slattery P, Chen A, Wallace M, Melancon MP. Light-activatable gold nanoshells for drug delivery applications. AAPS PharmSciTech. 2014;15(3):741-52.
365. Liao H, Hafner JH. Gold Nanorod Bioconjugates. Chemistry of Materials. 2005;17(18):4636-41.
366. Nikoobakht B, El-Sayed MA. Preparation and Growth Mechanism of Gold Nanorods (NRs) Using Seed-Mediated Growth Method. Chemistry of Materials. 2003;15(10):1957-62.
367. Jabeen F, Najam-ul-Haq M, Javeed R, Huck CW, Bonn GK. Au-nanomaterials as a superior choice for near-infrared photothermal therapy. Molecules. 2014;19(12):20580-93.
368. Scarabelli L, Sánchez-Iglesias A, Pérez-Juste J, Liz-Marzán LM. A “Tips and Tricks” Practical Guide to the Synthesis of Gold Nanorods. The Journal of Physical Chemistry

Letters. 2015;6(21):4270-9.
369. Kessentini S, Barchiesi D. Quantitative comparison of optimized nanorods, nanoshells and hollow nanospheres for photothermal therapy. Biomed Opt Express. 2012;3(3):590-604.
370. Cole JR, Mirin NA, Knight MW, Goodrich GP, Halas NJ. Photothermal Efficiencies of Nanoshells and Nanorods for Clinical Therapeutic Applications. The Journal of Physical Chemistry C. 2009;113(28):12090-4.
371. Mackey MA, Ali MRK, Austin LA, Near RD, El-Sayed MA. The Most Effective Gold Nanorod Size for Plasmonic Photothermal Therapy: Theory and In Vitro Experiments. The Journal of Physical Chemistry B. 2014;118(5):1319-26.
372. Huang X, El-Sayed IH, Qian W, El-Sayed MA. Cancer Cell Imaging and Photothermal Therapy in the Near-Infrared Region by Using Gold Nanorods. Journal of the American Chemical Society. 2006;128(6):2115-20.
373. Gormley AJ, Greish K, Ray A, Robinson R, Gustafson JA, Ghandehari H. Gold nanorod mediated plasmonic photothermal therapy: A tool to enhance macromolecular delivery. International journal of pharmaceutics. 2011;415(1-2):315-8.
374. Liao J, Li W, Peng J, Yang Q, Li H, Wei Y, et al. Combined cancer photothermal-chemotherapy based on doxorubicin/gold nanorod-loaded polymersomes. Theranostics. 2015;5(4):345-56.
375. Katarzyna Kita-Tokarczyk JG, Thomas Haefele, Wolfgang Meier. Block copolymer vesicles—using concepts from polymer chemistry to mimic biomembranes. Polymer. 2005;46(11):3540-63.
376. Christian DA, Cai S, Bowen DM, Kim Y, Pajerowski JD, Discher DE. Polymersome carriers: from self-assembly to siRNA and protein therapeutics. Eur J Pharm Biopharm. 2009;71(3):463-74.
377. Levine DH, Ghoroghchian PP, Freudenberg J, Zhang G, Therien MJ, Greene MI, et al. Polymersomes: a new multi-functional tool for cancer diagnosis and therapy. Methods. 2008;46(1):25-32.
378. Sun Y, Mayers BT, Xia Y. Template-Engaged Replacement Reaction: A One-Step Approach to the Large-Scale Synthesis of Metal Nanostructures with Hollow Interiors. Nano Letters. 2002;2(5):481-5.
379. Chen J, Wang D, Xi J, Au L, Siekkinen A, Warsen A, et al. Immuno Gold Nanocages with Tailored Optical Properties for Targeted Photothermal Destruction of Cancer Cells. Nano Letters. 2007;7(5):1318-22.
380. Skrabalak SE, Chen J, Sun Y, Lu X, Au L, Cobley LM, et al. Gold Nanocages: Synthesis, Properties, and Applications. Accounts of chemical research. 2008;41(12):1587-95.
381. Sun T, Wang Y, Wang Y, Xu J, Zhao X, Vangveravong S, et al. Using SV119-gold nanocage conjugates to eradicate cancer stem cells through a combination of photothermal and chemo therapies. Adv Healthc Mater. 2014;3(8):1283-91.
382. Wang SH, Wei CW, Jee SH, Li PC. Quantitative Thermal Imaging for Plasmonic Photothermal Therapy. J Med Biol Eng. 2011;31(6):387-93.
383. Valdiglesias V, Fernandez-Bertolez N, Kilic G, Costa C, Costa S, Fraga S, et al. Are iron oxide nanoparticles safe? Current knowledge and future perspectives. J Trace Elem Med Biol. 2016;38:53-63.
384. Gupta AK, Gupta M. Synthesis and surface engineering of iron oxide nanoparticles for biomedical applications. Biomaterials. 2005;26(18):3995-4021.
385. Wang YX. Superparamagnetic iron oxide based MRI contrast agents: Current status of clinical application. Quant Imaging Med Surg. 2011;1(1):35-40.
386. Wang YX, Hussain SM, Krestin GP. Superparamagnetic iron oxide contrast agents:

physicochemical characteristics and applications in MR imaging. Eur Radiol. 2001;11(11):2319-31.
387. Major JL, Meade TJ. Bioresponsive, cell-penetrating, and multimeric MR contrast agents. Acc Chem Res. 2009;42(7):893-903.
388. Bulte JW, Kraitchman DL. Iron oxide MR contrast agents for molecular and cellular imaging. NMR Biomed. 2004;17(7):484-99.
389. Gao J, Gu H, Xu B. Multifunctional magnetic nanoparticles: design, synthesis, and biomedical applications. Acc Chem Res. 2009;42(8):1097-107.
390. Siddiqi KS, Ur Rahman A, Tajuddin, Husen A. Biogenic Fabrication of Iron/Iron Oxide Nanoparticles and Their Application. Nanoscale Res Lett. 2016;11(1):498.
391. Espinosa A, Di Corato R, Kolosnjaj-Tabi J, Flaud P, Pellegrino T, Wilhelm C. Duality of Iron Oxide Nanoparticles in Cancer Therapy: Amplification of Heating Efficiency by Magnetic Hyperthermia and Photothermal Bimodal Treatment. ACS Nano. 2016;10(2):2436-46.
392. Shen S, Kong F, Guo X, Wu L, Shen H, Xie M, et al. CMCTS stabilized Fe3O4 particles with extremely low toxicity as highly efficient near-infrared photothermal agents for in vivo tumor ablation. Nanoscale. 2013;5(17):8056-66.
393. Chu M, Shao Y, Peng J, Dai X, Li H, Wu Q, et al. Near-infrared laser light mediated cancer therapy by photothermal effect of Fe3O4 magnetic nanoparticles. Biomaterials. 2013;34(16):4078-88.
394. Fu G, Sanjay ST, Dou M, Li X. Nanoparticle-mediated photothermal effect enables a new method for quantitative biochemical analysis using a thermometer. Nanoscale. 2016;8(10):5422-7.
395. America LIo. ANSI Z136.1 - American National Standard for Safe Use of Lasers2014.
396. Yen SK, Padmanabhan P, Selvan ST. Multifunctional iron oxide nanoparticles for diagnostics, therapy and macromolecule delivery. Theranostics. 2013;3(12):986-1003.
397. Laurent S, Saei AA, Behzadi S, Panahifar A, Mahmoudi M. Superparamagnetic iron oxide nanoparticles for delivery of therapeutic agents: opportunities and challenges. Expert Opin Drug Deliv. 2014;11(9):1449-70.
398. Cherukuri P, Glazer ES, Curley SA. Targeted hyperthermia using metal nanoparticles. Adv Drug Deliv Rev. 2010;62(3):339-45.
399. Hilger I, Kaiser WA. Iron oxide-based nanostructures for MRI and magnetic hyperthermia. Nanomedicine (Lond). 2012;7(9):1443-59.
400. Laurent S, Dutz S, Hafeli UO, Mahmoudi M. Magnetic fluid hyperthermia: focus on superparamagnetic iron oxide nanoparticles. Adv Colloid Interface Sci. 2011;166(1-2):8-23.
401. Giustini AJ, Petryk AA, Cassim SM, Tate JA, Baker I, Hoopes PJ. Magnetic Nanoparticle Hyperthermia in Cancer Treatment. Nano Life. 2010;1(1n02).
402. Muller S. Magnetic fluid hyperthermia therapy for malignant brain tumors--an ethical discussion. Nanomedicine. 2009;5(4):387-93.
403. Gneveckow U, Jordan A, Scholz R, Bruss V, Waldofner N, Ricke J, et al. Description and characterization of the novel hyperthermia- and thermoablation-system MFH 300F for clinical magnetic fluid hyperthermia. Med Phys. 2004;31(6):1444-51.
404. Maier-Hauff K, Rothe R, Scholz R, Gneveckow U, Wust P, Thiesen B, et al. Intracranial thermotherapy using magnetic nanoparticles combined with external beam radiotherapy: results of a feasibility study on patients with glioblastoma multiforme. J Neurooncol. 2007;81(1):53-60.
405. Wust P, Gneveckow U, Johannsen M, Bohmer D, Henkel T, Kahmann F, et al. Magnetic nanoparticles for interstitial thermotherapy--feasibility, tolerance and achieved

temperatures. Int J Hyperthermia. 2006;22(8):673-85.
406. Johannsen M, Gneveckow U, Eckelt L, Feussner A, Waldofner N, Scholz R, et al. Clinical hyperthermia of prostate cancer using magnetic nanoparticles: presentation of a new interstitial technique. Int J Hyperthermia. 2005;21(7):637-47.
407. Nicolson GL. Generation of phenotypic diversity and progression in metastatic tumor cells. Cancer metastasis reviews. 1984;3(1):25-42.
408. Fidler IJ, Hart IR. Biological diversity in metastatic neoplasms: origins and implications. Science. 1982;217(4564):998-1003.
409. Marusyk A, Polyak K. Tumor heterogeneity: causes and consequences. Biochim Biophys Acta. 2010;1805(1):105-17.
410. Gottlieb B, Alvarado C, Wang C, Gharizadeh B, Babrzadeh F, Richards B, et al. Making sense of intratumor genetic heterogeneity: altered frequency of androgen receptor CAG repeat length variants in breast cancer tissues. Human mutation. 2013;34(4):610-8.
411. Swanton C. Intratumor heterogeneity: evolution through space and time. Cancer Res. 2012;72(19):4875-82.
412. Burrell RA, McGranahan N, Bartek J, Swanton C. The causes and consequences of genetic heterogeneity in cancer evolution. Nature. 2013;501(7467):338-45.
413. Marusyk A, Almendro V, Polyak K. Intra-tumour heterogeneity: a looking glass for cancer? Nat Rev Cancer. 2012;12(5):323-34.
414. Allison KH, Sledge GW. Heterogeneity and cancer. Oncology (Williston Park). 2014;28(9):772-8.
415. Carreira S, Romanel A, Goodall J, Grist E, Ferraldeschi R, Miranda S, et al. Tumor clone dynamics in lethal prostate cancer. Sci Transl Med. 2014;6(254):254ra125.
416. Wei L, Wang J, Lampert E, Schlanger S, DePriest AD, Hu Q, et al. Intratumoral and Intertumoral Genomic Heterogeneity of Multifocal Localized Prostate Cancer Impacts Molecular Classifications and Genomic Prognosticators. European urology. 2016.
417. Nishant KT, Singh ND, Alani E. Genomic mutation rates: what high-throughput methods can tell us. BioEssays : news and reviews in molecular, cellular and developmental biology. 2009;31(9):912-20.
418. Korneliussen TS, Albrechtsen A, Nielsen R. ANGSD: Analysis of Next Generation Sequencing Data. BMC bioinformatics. 2014;15:356.
419. Lawrence MS, Stojanov P, Mermel CH, Robinson JT, Garraway LA, Golub TR, et al. Discovery and saturation analysis of cancer genes across 21 tumour types. Nature. 2014;505(7484):495-501.
420. Kiessling F, Mertens ME, Grimm J, Lammers T. Nanoparticles for imaging: top or flop? Radiology. 2014;273(1):10-28.
421. Banda NK, Mehta G, Chao Y, Wang G, Inturi S, Fossati-Jimack L, et al. Mechanisms of complement activation by dextran-coated superparamagnetic iron oxide (SPIO) nanoworms in mouse versus human serum. Part Fibre Toxicol. 2014;11:64.
422. FDA. Drugs@FDA: FDA Approved Drug Products [Available from: http://www.accessdata.fda.gov/scripts/cder/daf/index.cfm?event=overview.process&ApplNo=020410.
423. Blair HA, Deeks ED. Albumin-Bound Paclitaxel: A Review in Non-Small Cell Lung Cancer. Drugs. 2015;75(17):2017-24.
424. Ng VG, Mena C, Pietras C, Lansky AJ. Local delivery of paclitaxel in the treatment of peripheral arterial disease. Eur J Clin Invest. 2015;45(3):333-45.
425. Cecco S, Aliberti M, Baldo P, Giacomin E, Leone R. Safety and efficacy evaluation of albumin-bound paclitaxel. Expert Opin Drug Saf. 2014;13(4):511-20.
426. Gelderblom H, Verweij J, Nooter K, Sparreboom A. Cremophor EL - the drawbacks

and advantages of vehicle selection for drug formulation. European Journal of Cancer. 2001;37(13):1590-8.
427. Gradishar WJ, Tjulandin S, Davidson N, Shaw H, Desai N, Bhar P, et al. Phase III trial of nanoparticle albumin-bound paclitaxel compared with polyethylated castor oil-based paclitaxel in women with breast cancer. J Clin Oncol. 2005;23(31):7794-803.
428. Socinski MA, Manikhas GM, Stroyakovsky DL, Makhson AN, Cheporov SV, Orlov SV, et al. A dose finding study of weekly and every-3-week nab-Paclitaxel followed by carboplatin as first-line therapy in patients with advanced non-small cell lung cancer. J Thorac Oncol. 2010;5(6):852-61.
429. Keefe SM, Hoffman-Censits J, Cohen RB, Mamtani R, Heitjan D, Eliasof S, et al. Efficacy of the nanoparticle-drug conjugate CRLX101 in combination with bevacizumab in metastatic renal cell carcinoma: results of an investigator-initiated phase I-IIa clinical trial. Ann Oncol. 2016;27(8):1579-85.
430. Von Hoff DD, Mita MM, Ramanathan RK, Weiss GJ, Mita AC, LoRusso PM, et al. Phase I Study of PSMA-Targeted Docetaxel-Containing Nanoparticle BIND-014 in Patients with Advanced Solid Tumors. Clin Cancer Res. 2016;22(13):3157-63.
431. Gilchrist RK, Medal R, Shorey WD, Hanselman RC, Parrott JC, Taylor CB. Selective inductive heating of lymph nodes. Ann Surg. 1957;146(4):596-606.
432. Roizin-Towle L, Pirro JP. The response of human and rodent cells to hyperthermia. Int J Radiat Oncol Biol Phys. 1991;20(4):751-6.
433. Chen WR, Adams RL, Higgins AK, Bartels KE, Nordquist RE. Photothermal effects on murine mammary tumors using indocyanine green and an 808-nm diode laser: an in vivo efficacy study. Cancer Lett. 1996;98(2):169-73.
434. Feyh J, Gutmann R, Leunig A, Jager L, Reiser M, Saxton RE, et al. MRI-guided laser interstitial thermal therapy (LITT) of head and neck tumors: progress with a new method. J Clin Laser Med Surg. 1996;14(6):361-6.
435. Nanospectra Biosciences I. Efficacy Study of AuroLase Therapy in Subjects With Primary and/or Metastatic Lung Tumors 2014 [Available from: https://clinicaltrials.gov/.